

6-18-2008

Oligomerization of Levoglucosan in Proxies of Biomass Burning Aerosols

Bryan J. Holmes
University of Vermont

Follow this and additional works at: <http://scholarworks.uvm.edu/graddis>

Recommended Citation

Holmes, Bryan J., "Oligomerization of Levoglucosan in Proxies of Biomass Burning Aerosols" (2008). *Graduate College Dissertations and Theses*. Paper 111.

This Dissertation is brought to you for free and open access by the Dissertations and Theses at ScholarWorks @ UVM. It has been accepted for inclusion in Graduate College Dissertations and Theses by an authorized administrator of ScholarWorks @ UVM. For more information, please contact donna.omalley@uvm.edu.

OLIGOMERIZATION OF LEVOGLUCOSAN IN PROXIES OF BIOMASS BURNING
AEROSOLS

A Dissertation Presented

by

Bryan J. Holmes

to

The Faculty of the Graduate College

of

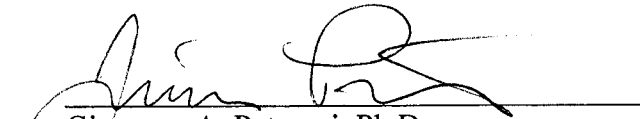
The University of Vermont

In Partial Fulfillment of the Requirements
for the Degree of Doctor of Philosophy
Specializing in Chemistry

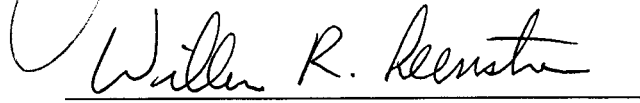
February, 2008

Accepted by the Faculty of the Graduate College, The University of Vermont, in partial fulfillment of the requirements for the degree of Doctor of Philosophy, specializing in Chemistry.


Thesis Examination Committee:




Giuseppe A. Petrucci, Ph.D. **Advisor**



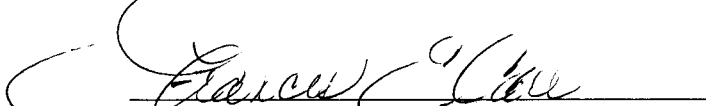
Willem R. Leenstra, Ph.D.



Joel M. Goldberg, Ph.D.



William B. Bowden, Ph. D. **Chairperson**



Frances E. Carr, Ph. D. **Vice President for Research
and Dean of Graduate Studies**

Date: October 26, 2007

ABSTRACT

Biomass burning aerosols play an important role in the chemistry and physics of the atmosphere and therefore, affect global climate. Biomass burning aerosols are generally aqueous and have a strong saccharidic component due to the combustion and pyrolysis of cellulose, a major component of foliar fuel. This class of aerosol is known to affect both the absorption and scatter of solar radiation. Also, biomass burning aerosols contribute to cloud formation through their action as cloud-condensation nuclei. Many questions exist about the chemical speciation and chemical aging of biomass burning aerosols and how this affects their atmospheric properties and ultimately, global climate. Also, knowledge of the chemical components of these aerosols is important in the search for chemical tracers that can give information about the point or regional source, fuel type, and age of a biomass burning aerosol parcel.

Levogluconan was chosen for these studies as a model compound for biomass burning aerosols because of its high measured concentrations in aerosol samples. Levogluconan often dominates the aerosol composition by mass. In this dissertation, laboratory proxy systems were developed to study the solution-phase chemistry of levogluconan with common atmospheric reactants found in biomass burning aerosols (i.e. H^+ , $\cdot OH$). To mimic these natural conditions, acid chemistry was studied using sulfuric acid in water (pH=4.5). The hydroxyl radical ($\cdot OH$) was produced by the Fenton reaction which consists of iron, hydrogen peroxide and acid (H_2SO_4) in aqueous solvent.

For studies in aqueous sulfuric acid, oligomers of levogluconan were measured by matrix-assisted laser desorption and ionization time-of-flight mass spectrometry (MALDI-TOF-MS). A rational mechanism is proposed based on both the acid-catalyzed cationic ring-opening of levogluconan and nucleophilic attack of ROH from levogluconan on the hemi-acetal carbon to produce pyranose oligomers through the formation of glycosidic bonds. Oligomer formation is further supported by attenuated total reflectance Fourier transform infrared spectroscopy (ATR-FTIR). Reactions of levogluconan with $\cdot OH$ produced from Fenton chemistry were studied in solution. Two modes of oligomerization (2000 u) were observed for reaction times between 1 and 7 days using MALDI-TOF-MS and laser desorption ionization (LDI) TOF-MS. Single-mass unit continuum mass distributions with dominant -2 u patterns were measured and superimposed by a +176/+162 u oligomer series. This latter oligomer pattern was attributed to a Criegee rearrangement (+14 u) of levogluconan, initiated by $\cdot OH$, forming a lactone (176 u). The acid-catalyzed reaction of any ROH from levogluconan (+162 u) forms an ester through transesterification of the lactone functionality, whereupon propagation forms polyesters. Proposed products and chemical mechanisms are suggested as sources and precursors of humic-like substances (HULIS), which are known to possess a large saccharic component and are possibly formed from biomass burning aerosols. These products could also serve as secondary tracers, giving further information on the source and age of the aerosol.

CITATIONS

Material from this dissertation has been published in the following form:

Holmes, B. J.; Petrucci, G. A.. (2006) Water-soluble oligomer formation from acid-catalyzed reactions of levoglucosan in proxies of atmospheric aqueous aerosols. *Environmental Science & Technology* 40, (16), 4983-4989.

Holmes, B. J.; Petrucci, G. A., (2007) Oligomerization of levoglucosan by Fenton chemistry in proxies of biomass burning aerosols. *Journal of Atmospheric Chemistry* 58, (2), 151-166.

ACKNOWLEDGEMENTS

The years that I spent working toward this degree had many challenges above the scientific context that brought me close with a number of people whose friendships I will always appreciate. I started at UVM in a new research group headed by Giuseppe “Joe” Petrucci and had many great times that included getting to know my advisor as well as the three other group members. I first became friends with Brian LaFanchi. We connected through our mutual passion for skiing and had many great powder days at variety of resorts and backcountry spots over the years. Through him, I learned to appreciate baseball as I got to see the Boston Red Sox win the World Series after watching Brian work through many painful seasons. Many great times were spent with Brian and Hilary along with their entire social network of friends.

I also got to know Adam Hunt, a Yankees fan, yet somehow friends with Brian. I watched the two on many days after games between the two rival teams, sometimes taunting each other and sometimes just giving the other space after a traumatic game or series. Adam was a great companion for all these years in this research group and I’ll always remember Mark Knights “particles” and “crazy mechanisms” that we both witnessed. I’d like to recognize Jim Zahardis, the fifth member of the Petrucci group, who started with us after we were in our fourth year. You could always count on Jim’s uncanny wit, broad understanding of math and science, animal stories and shout-outs to Thor. I’ll have especially great memories of “The Lord of the Rings” and all its intonations on which we connected. Every time we all could take some time-off to go for coffee, sit on the green and just commiserate on the dysfunctional nuances of our program was great, especially looking back.

Along with these group members, Sandy Wurthmann was always there for the powder days and hang-out times when we were avoiding the work we had ahead. He was an integral part of my experience at UVM and in Vermont as a whole. His wife, Elizabeth and son, Rowan, are important parts of my experience here in Vermont. Having them, Brett, Tobbs, and my old friend Kris around made this time in graduate school special. Thank you all.

I especially want to thank my girlfriend, Julie, for all her support during the years I was in school. While we were both in graduate school, I will always remember the support we both gave each other. Your tolerance and compassion during this time, especially during the last days of my program, was incredible.

Lastly I’d like to thank my family for all there support over these years. I would also like to thank my advisor, Joe Petrucci for being a significant part of my development as a scientist. My experience in this research group will always be valued.

TABLE OF CONTENTS

	Page
CITATIONS	ii
ACKNOWLEDGEMENTS	iii
GLOSSARY	viii
LIST OF TABLES	ix
LIST OF FIGURES	x
1. INTRODUCTION	1
1.1. INTRODUCTION TO ATMOSPHERIC AEROSOLS	1
1.1.1. <i>Definitions and Terms</i>	1
1.1.2. <i>Characterization of Atmospheric Aerosols</i>	1
1.1.3. <i>Cloud Formation by Atmospheric Aerosols</i>	3
1.1.4. <i>Atmospheric Aerosol Emissions: Climate Effects</i>	3
1.1.4.1. <i>The Aerosol Direct Effect</i>	5
1.1.4.2. <i>The Aerosol Indirect Effect</i>	6
1.2. <i>Biomass Burning Emissions</i>	6
1.2.1. <i>Introduction</i>	6
1.2.2. <i>Characterization of Biomass Burning Aerosols</i>	9
1.2.3. <i>The Climate Forcing of Biomass Burning Aerosols</i>	9
1.2.4. <i>Cloud Condensation Properties of Biomass Burning Aerosols</i>	10
1.3. CARBONACEOUS AEROSOL FORMED FROM BIOMASS BURNING.....	11

1.3.1. Introduction.....	11
1.3.2. Water Soluble Organic Compounds in Biomass Burning Aerosols.....	13
1.3.3. Organic Tracers for Biomass Burning Aerosols	14
1.3.4. Levoglucosan	16
2. LEVOGLUCOSAN PROXY EXPERIMENTAL METHODOLOGY.....	20
2.1. MODEL REACTION SYSTEM	20
2.1.1. INTRODUCTION	20
2.1.2. General Experimental Setup.....	21
2.1.3. Model Chemical Reaction Systems.....	21
2.2. Development of Analytical Methodology.....	22
2.2.1. Proxy Reaction Conditions	22
2.2.2. Time-of-Flight Mass Spectrometry.....	22
2.2.3. Matrix-Assisted Laser Desorption and Ionization Time-of-Flight Mass Spectrometry.....	23
2.2.4. MALDI-TOF-MS Sample Preparation and Instrument Settings	25
2.2.5. Laser Desorption and Ionization Time-of-Flight Mass Spectrometry.....	27
2.2.6. Electrospray Ionization Mass Spectrometry.....	28
2.2.7. Attenuated Total Reflectance Fourier-Transform Infrared Spectroscopy....	29
3. WATER SOLUBLE OLIGOMER FORMATION FROM ACID-CATALYZED REACTIONS OF LEVOGLUCOSAN IN PROXIES OF ATMOSPHERIC AQUEOUS AEROSOLS⁸¹	30

3.1. INTRODUCTION	30
3.2. EXPERIMENTAL.....	32
3.2.1. <i>Experimental Design</i>	32
3.2.2. <i>Sample Preparation for Analytical Analysis</i>	32
3.3. RESULTS AND DISCUSSION.....	33
3.3.1. <i>Experimental Description and Background Control Experiments</i>	33
3.3.2. <i>The Fenton Reaction</i>	34
3.3.3. <i>Identification of Chemical Mechanism</i>	38
3.3.4. <i>Potential Role of Iron in Reaction Systems</i>	42
3.3.5. <i>Proposed Chemical Mechanism for Oligomers Pattern</i>	43
3.3.6. <i>Oligomer Polydispersity and Reaction Kinetic Analysis</i>	46
3.3.7. <i>ATR-FTIR Supporting Data for Saccharidic Oligomer Formation</i>	54
7.2. CONCLUSIONS.....	55
4. OLIGOMERIZATION OF LEVOGLUCOSAN BY FENTON CHEMISTRY IN PROXIES OF BIOMASS BURNING AEROSOLS ⁹⁸	58
4.1. INTRODUCTION	58
4.2. EXPERIMENTAL DESIGN.....	59
4.2.1. <i>Biomass Burning Aerosol Proxy Reactions</i>	59
4.2.2. <i>Sample Preparation and Analysis</i>	59
4.3. RESULTS AND DISCUSSION.....	61
4.3.1. <i>•OH Production by the Fenton Reaction</i>	61
4.3.2. <i>•OH Reactions of Levoglucosan</i>	62

4.3.3.	<i>Oligomerization Mass Patterns: MALDI-TOF-MS</i>	70
4.3.4.	<i>MALDI-TOF-MS Matrix Background</i>	73
4.3.5.	<i>Studies Supporting Solution-Phase Chemistry</i>	74
4.3.6.	<i>MALDI-TOF-MS: Lithium Cationization</i>	78
4.4.	CONCLUSIONS	83
5.	COMPREHENSIVE CONCLUSIONS	85
5.1.	<i>Summary of Experimental Findings</i>	85
5.2.	GENERAL IMPLICATIONS OF EXPERIMENTAL RESULTS ON CLIMATE SCIENCE ...	86
5.2.1.	<i>Application of Experimental Results to Formation Mechanisms of Humic-Like Substances (HULIS)</i>	87
5.2.2.	<i>Broad Scientific Implications of Chemical Research in Biomass Burning Aerosols</i>	89
5.3.	SUGGESTED RESEARCH DIRECTIONS	90
6.	APPENDIX A	92
6.1.	DEVELOPMENT AND OPTIMIZATION OF THE MALDI-TOF-MS METHODOLOGY	92
7.	REFERENCES	96

GLOSSARY

ATR-FTIR: Attenuated Total Reflectance Infrared Spectroscopy

BC: Black Carbon

CCN: Cloud Condensation Nuclei

CHCA: α -Cyano-4-hydroxycinnamic acid

DHB: 2,5-dihydroxybenzoic acid

EC: Elemental Carbon

GHG: Green House Gases

HULIS: Humic-Like Substances

IPCC: International Panel on Climate Change

LDI-TOF-MS: Laser Desorption and Ionization Time-of-Flight Mass Spectrometry

MALDI-TOF-MS: Matrix Assisted Laser Desorption and Ionization Mass

Spectrometry

OC: Organic Carbon

\cdot OH: Hydroxyl Radical

PAH: Polycyclic Aromatic Hydrocarbons

PM: Particulate Matter

SA: Sinapic Acid

SOA: Secondary Organic Aerosols

VOC: Volatile Organic Compounds

WIOC: Water Insoluble Organic Compounds

WSOC: Water Soluble Organic Compounds

LIST OF TABLES

Table	Page
Table 3-1 Summary of the five experimental conditions used to investigate the aqueous-phase chemistry of levoglucosan in bulk. Reactant concentrations: Levoglucosan: 1×10^{-3} M, $\text{FeCl}_3 \cdot 6\text{H}_2\text{O}$: 5×10^{-6} M, H_2O_2 : 1×10^{-4} M, H_2SO_4 : pH = 4.5.	34

LIST OF FIGURES

Figure	Page
Figure 1 Estimated radiative forcing of atmospheric components, IPCC, 2001. ³⁸	10
Figure 2-1 Diagram of MALDI process. www.chm.bris.ac.uk/ms/theory/maldi-ionisation.html	24
Figure 2-2 MALDI-TOF-MS schematic. www.cbsu.tc.cornell.edu/vanwijk/mass_spec.htm	26
Figure 3-1a MALDI-TOF-MS of Reaction A (levoglucosan, H ₂ O ₂ , H ₂ SO ₄ , Fe ³⁺), day 0.5, using DHB/NaCl matrix in positive ion, reflectron mode. Spectra are normalized to the 185 Da (levoglucosan + Na ⁺) peak. (* - indicates relevant product peaks).....	35
Figure 3-1b MALDI-TOF-MS of Reaction A (levoglucosan, H ₂ O ₂ , H ₂ SO ₄ , Fe ³⁺), day 1, using DHB/NaCl matrix in positive ion, reflectron mode. Spectra are normalized to the 185 U (levoglucosan + Na ⁺) peak. (* - indicates relevant product peaks).....	36
Figure 3-1c MALDI-TOF-MS of Reaction A (levoglucosan, H ₂ O ₂ , H ₂ SO ₄ , Fe ³⁺), day 3, using DHB/NaCl matrix in positive ion, reflectron mode. Spectra are normalized to the 185 U (levoglucosan + Na ⁺) peak. (* - indicates relevant product peaks).....	37
Figure 3-1d MALDI-TOF-MS of Reaction A (levoglucosan, H ₂ O ₂ , H ₂ SO ₄ , Fe ³⁺), day 7, using DHB/NaCl matrix in positive ion, reflectron mode. Spectra are normalized to the 185 U (levoglucosan + Na ⁺) peak. (* - indicates relevant product peaks).....	38
Figure 3-2 Electrospray ionization mass spectrometry (ESI-MS) of the dried day 1 sample for reaction B. (*- indicates relevant product peaks).....	40

Figure 3-3 MALDI-TOF-MS of Reaction B (levoglucosan, H ₂ SO ₄), day 1 using DHB/NaCl matrix in positive ion, reflectron mode. Spectrum is normalized to the 185 U (levoglucosan + Na ⁺) peak. (* - indicates relevant product peaks).	42
Figure 3-4 Proposed acid-catalyzed mechanism for the oligomerization of levoglucosan (I).....	45
Figure 3-5 Mass peak intensity data normalized to day 0.5 for the [x-mer] ⁺ products for Reaction A. (●) 2-mer; (▲) 3-mer; (▼) 4-mer; (Δ) 5-mer; (□) 6-mer; (◄) 7-mer. Lines are drawn to aid the eye. Error bars represent 1 standard deviation on 1000 laser shots.....	47
Figure 3-6a Number (Mn) and weight (Mw) averaged molar mass distributions for the [x-mer] ⁺ mass peaks from reaction A. (■) Mn, (●) Mw. Error bars represent 1 standard deviation on 1000 laser shots.....	48
Figure 3-6b Number (Mn) and weight (Mw) averaged molar mass distributions for the [x-mer+18] ⁺ mass peaks from reaction A. (■) Mn, (●) Mw. Error bars represent 1 standard deviation on 1000 laser shots.	49
Figure 3-7a Mass peak intensity data normalized to day 0.5 for the [x-mer] ⁺ products for Reaction B. (■)1-mer; (●) 2-mer; (▲) 3-mer; (▼) 4-mer; (Δ) 5-mer; (□) 6-mer, (◄) 7-mer. Lines are drawn to aid the eye. Error bars represent 1 standard deviation on 1000 laser shots.....	50
Figure 3-7b Mass peak intensity data normalized to day 0.5 for the [x-mer + 18] ⁺ products for Reaction B. (■)1-mer; (●) 2-mer; (▲) 3-mer; (▼) 4-mer; (Δ) 5-mer;	

(□) 6-mer, (◀) 7-mer. Lines are drawn to aid the eye. Error bars represent 1 standard deviation on 1000 laser shots.	51
Figure 3-8a Number (Mn) and weight (Mw) averaged molar mass distributions for the [x-mer] ⁺ mass peaks from Reaction B. (■) Mn, (●) Mw. Error bars represent 1 standard deviation on 1000 laser shots.	53
Figure 3-8b Number (Mn) and weight (Mw) averaged molar mass distributions for the [x-mer+18] ⁺ mass peaks from Reaction B. (■) Mn, (●) Mw. Error bars represent 1 standard deviation on 1000 laser shots.	54
Figure 3-9 ATR-FTIR spectra of dry, lyophilized chemical products from (A) Reaction A and (B) Reaction B, in addition to the reference compounds (1) cellulose, (2) α-cyclodextrin, (3) levoglucosan and (4) α-D-glucose.	55
Figure 4-1a MALDI-TOF mass spectra of the sodiated products from the reaction of levoglucosan in the Fenton system; day 1, 1x10 ⁻³ M H ₂ O ₂ using DHB/NaCl matrix in positive ion, reflectron mode. Spectrum is normalized to the 185 u (levoglucosan + Na ⁺) ion peak. (* - indicates emphasized oligomer mass peak pattern).....	64
Figure 4-1b MALDI-TOF mass spectra of the sodiated products from the reaction of levoglucosan in the Fenton system; day 3, 1x10 ⁻³ M H ₂ O ₂ using DHB/NaCl matrix in positive ion, reflectron mode. Spectrum is normalized to the 185 u (levoglucosan + Na ⁺) ion peak. (* - indicates emphasized oligomer mass peak pattern).....	65
Figure 4-1c MALDI-TOF mass spectra of the sodiated products from the reaction of levoglucosan in the Fenton system; day 7, 1x10 ⁻³ M H ₂ O ₂ using DHB/NaCl matrix	

in positive ion, reflectron mode. Spectrum is normalized to the 185 u (levoglucosan + Na ⁺) ion peak. (* - indicates emphasized oligomer mass peak pattern).....	66
Figure 4-2 LDI-TOF mass spectra of the sodiated products from the reaction of levoglucosan in the Fenton system; day 3, using DHB/NaCl matrix in positive ion, reflectron mode. The spectrum is normalized to the 185 u (levoglucosan + Na ⁺) ion peak.....	68
Figure 4-3 Proposed mechanism for the formation of a glucosone by reaction of a disaccharide with [•] OH.....	69
Figure 4-4 Proposed mechanism for the formation of a ring-expanded lactone from levoglucosan (Cmpd II) by hydroperoxyl formation initiated by OH [•] followed by a Criegee rearrangement.....	71
Figure 4-5 Proposed mechanism for the formation of ester-containing oligomeric products from the Fenton system through the acid-catalyzed transesterification reactions of levoglucosan and the monomeric Criegee lactone product (Cmpd II, Scheme 3-2).....	72
Figure 4-6 Comparison of the normalized 537 u mass peak ion signal. Error bars represent 1 standard deviation on 3000 laser shots.....	76
Figure 4-7 Comparison of the normalized 537 u ion signal for days 1, 3, and 7 using 10 ⁻³ M H ₂ O ₂ . Error bars represent 1 standard deviation on 3000 laser shots.....	77
Figure 4-8 ATR-FTIR of the lyophilized, dried products of (A) the Fenton reaction of levoglucosan (10 ⁻³ M H ₂ O ₂), day 3 and (B) the aqueous reaction of levoglucosan, H ₂ SO ₄ , and Fe ³⁺ in the absence of H ₂ O ₂ on day 3.....	78

Figure 4-9 MALDI-TOF mass spectra of the sodiated products from the reaction of levoglucosan in the Fenton system; day 7, 1×10^{-3} M H_2O_2 using DHB/LiCl matrix in positive ion, reflectron mode. Spectrum is normalized to the 169 u (levoglucosan + Li^+) ion peak. Peak in parenthesis indicate significant mass peaks observed in the background measurements. (* - indicates emphasized oligomer mass peak pattern)80

Figure 4-10 Proposed mechanism for the dehydration (-18 u) of compound IIIa through nucleophilic intramolecular cyclization by ROH with the terminal gem-diol carbon to produce compound IIIc (+Li = 327 u). 81

1. INTRODUCTION

1.1. Introduction to Atmospheric Aerosols

1.1.1. Definitions and Terms

An aerosol is defined as a collection of solid or liquid particles suspended in a gas. While, by definition, an aerosol includes the solid/liquid and gas components, in the literature the term aerosol usually refers only to the condensed-phase component(s). As is common in the literature, the terms aerosol and particulate will be used interchangeably in this dissertation. Common examples of aerosols found in the Earth's atmosphere are smoke, smog, fog, and dust. Atmospheric aerosols are known to have significant impact on atmospheric chemistry, climate forcing and human health. Both the size distribution and chemical composition of the aerosol are important in the potential impact of atmospheric aerosols. Important aerosol composition characteristics include: size, shape, chemical reactivity, and optical properties.^{1,2}

1.1.2. Characterization of Atmospheric Aerosols

Particulate matter (PM) found in the atmosphere ranges in size from ~ 0.002 to ~ 100 μm in diameter. Over this wide range of particle sizes, several discrete size modes arise from a variety of sources rather than a broad continuum of sizes. Particles found in the atmosphere are generally grouped into two broad categories

based on size: fine aerosols, which have a diameter less than 2.5 μm and coarse aerosols which have a diameter greater than 2.5 μm . Fine aerosols are typically formed through combustion or nucleation events, followed by growth via coagulation or condensation. An example of this growth process is the condensation of low volatility gas-phase chemicals on a molecular cluster.³ Fine mode aerosols, due to their relatively small size, have atmospheric residence times averaging about 3 to 5 days and are affected mainly by dry deposition to the landscape and rainout. They often have high concentrations of organics and soluble inorganic species such as nitrate, sulfate, and ammonium. Coarse aerosols, on the other hand, are much larger and more affected by gravitational sedimentation, lending to them a shorter atmospheric residence time (seconds to hours). Sources include volcanic emissions, sea spray and dust storms, all of which are generally driven by mechanical or abrasive processes. Chemically, coarse particles are generally dominated by inorganic species such as minerals, and black carbon (soot), while fine particles have high concentrations of organics and soluble inorganic ions such as sulfate, nitrate, and ammonium.^{1,2}

When considering the sources of aerosols in the atmosphere, it is useful to categorize aerosol sources as either primary or secondary. Primary aerosols are emitted directly from their source into the atmosphere in the particle phase. Examples of primary aerosols include sea spray, windborne dust, and soot. Secondary aerosols are emitted as volatile gas-phase compounds and are converted to the particle phase in the atmosphere, often as a result of some type of chemical transformation.

Oxidation of a number of atmospheric gases can result in secondary sources of aerosols, including SO₂, NO_x, and a wide range of volatile organic compounds (VOCs). As a result, secondary aerosol sources include, but are not limited to, combustion processes, foliage emissions, marine emission, and volcanoes. Primary aerosols are usually in the coarse size fraction while secondary aerosols tend to be in the fine size fraction, though some exceptions exist (e.g., primary soot emissions from combustion processes are mainly fine particles).^{1,2}

1.1.3. Cloud Formation by Atmospheric Aerosols

Some types of aerosol have the ability to develop into cloud droplets, thereby acting as cloud condensation nuclei (CCN). In order to produce a cloud droplet under atmospheric conditions, water vapor needs the solid or liquid surface of an aerosol to transition to a liquid in the aerosol phase under supersaturated conditions. Although many types of aerosol act as CCN, generally, biomass burning aerosols are known to have a high capacity for cloud nucleation. A given aerosol source will affect both the number concentration, size distribution, and the chemical components of the cloud droplet as they develop with age.⁴⁻⁶

1.1.4. Atmospheric Aerosol Emissions: Climate Effects

Globally, aerosols are emitted into the atmosphere at a rate of about 3600 teragrams (Tg) per year.² Both anthropogenic and biogenic sources are significant contributors to the total atmospheric particulate load. Biogenic emissions total around

3100 Tg/year and anthropogenic emissions are estimated to be about 500 Tg/yr.² Assessment of the total global aerosol mass flux shows that ~80% of that emitted from both anthropogenic and natural sources is soil dust and sea salt particles that are in the coarse size range. Fine aerosols, therefore, compose ~20% of the total aerosol mass. This class of aerosol consists of individual particles that have between 10^{-3} - 10^{-9} of the mass of individual coarse particles. This relationship between fine and coarse aerosols results in the fact that, of the total number of atmospheric aerosols, almost all (~100%) are in the fine size fraction.

Often, the impact of aerosols is determined by the number concentration rather than the mass. This is observed in phenomena such as cloud condensation where the number of cloud condensation nuclei/aerosol determines the hydrology and reflective properties of clouds. Cloud measurements have shown that competition for gas-phase water (humidity) by high numbers of aerosol can suppress cloud droplet growth because of the high surface area present. By increasing the aerosol numbers and, therefore, the surface area available for condensation of water within an aerosol parcel, there is not enough water to grow the aerosols to the critical size for rainout.⁷ A result of this is suppression of rainout which increases the aerosol/cloud-droplet atmospheric residence time. By affecting the cloud-droplet size and aerosol/cloud-droplet atmospheric residence time, changes to the clouds' albedo (reflectivity) occur, therefore affecting the radiation budget of the Earth.

1.1.4.1. The Aerosol Direct Effect

Research over the past decade has shown that atmospheric aerosols, a majority of which are formed from anthropogenic sources, possess the ability to affect the radiation budget of the Earth in both positive and negative directions. This means that atmospheric aerosols can have a warming or cooling effect on the Earth, which depends on both particle sizes and chemical composition. Specifically, warming is caused by absorption of radiation by the aerosol, whereas cooling is due to scattering of radiation back into space. Early climate models were unable to account for the measured temperature increase, from 0.3 to 0.6 K, since the industrial age based only on the increase in green house gas (GHG) emissions over that time.² The addition of the aerosol effect into climate models provided significantly better agreement with the observed temperature increases.⁸⁻¹²

The capacity for aerosols to absorb or scatter radiation is known as the aerosol *direct* effect, which has been shown to influence Earth's radiation budget significantly, as aerosols can absorb or scatter solar radiation^{13, 14} as well as infrared radiation emitted from Earth's surface. The magnitude of the aerosol direct effect on climate forcing is influenced by the aerosol's number concentration, size, chemical composition, and optical properties.^{1,2} There is a significant complexity in quantifying the aerosol direct effect that arises from the uncertainty of the mixing state of absorbing materials (e.g., soot) and reflecting materials (e.g., ammonium sulfate) in an aerosol parcel. The climate forcing for a given aerosol population is strongly dependent on whether materials with different optical properties are evenly

distributed over all aerosols, separated into discrete types of aerosol, absorbing or scattering, or, the most likely scenario, somewhere in between (e.g., soot core with an aqueous ammonium sulfate outer layer).

1.1.4.2. The Aerosol Indirect Effect

Many aerosol *indirect* effects exist where atmospherically processed aerosols (e.g., cloud formation from nucleation by aerosols) can affect atmospheric processes, thereby changing Earth's radiation budget. The growth of cloud droplets by CCN is an example of this effect and can cause significant scattering of solar radiation back to space, thereby cooling the Earth. Additionally, the Twomey effect^{15, 16} is a phenomenon which can increase cloud lifetimes, also providing a mechanism which cools the Earth. Aerosol indirect effects are hypothesized to, in some cases, have a more significant impact than direct effects.¹⁷ The aerosol indirect effects, however, are very difficult to quantify because of the complex physical and chemical pathways that affect climate forcing.

1.2. Biomass Burning Emissions

1.2.1. Introduction

Biomass burning, a major source of organic carbon, soot and particulates^{18, 19} in the atmosphere, is a global phenomenon with over 80% of the burning occurring in tropical regions such as the Amazon basin.²⁰ Emissions of biomass burning include

both chemically and radiatively active trace gases and particulates that are in quantities that affect climate on a local, regional, and even a global scale. The global effects of biomass burning can be attributed to the high convective nature of the equatorial regions where much of the world's burning occurs, transporting the gases and aerosols long distances.

Vegetation is the main source of fuel consumed in biomass burning and contains mainly the polymeric structures which are found in the cell walls. The composition of wood is dominated by fibers of cellulose (40-50%) and also lesser amounts of hemicellulose (15-25%) and lignin (15-30%). Cellulose is a linear, crystalline material consisting of glucose monomers ($n = 7,000 - 15,000$) linked by β 1-4 bonds. Hemicellulose is an amorphous, branched polymer which contains sugar monomers such as xylose, mannose, galactose, rhamnose, and arabinose. It is much shorter in length than cellulose, possessing typically around 200 sugar monomers. Finally, lignin is a large, racemic, cross-linked polymer which is hydrophobic and aromatic in nature. Its molecular weight is in excess of 10,000 u. There are three general monomers (*p*-coumaryl alcohol, coniferyl alcohol, and sinapyl alcohol), which are all methoxylated to various degrees. Together, these three polymeric materials account for greater than 90% of the dry weight of most vascular plants.²¹ The remaining mass is composed of various lipids, proteins, and other metabolites, as well as water and minerals. The combustion of the organic material in vegetation is a complex sequence of chemical reactions and physical transformations including pyrolysis, combustion, depolymerization, water elimination, oxidation, fragmentation, char formation and

volatilization.²²

Qualitatively, smoke particles are composed of ~ 50-60 % organic carbon and ~5-10 % elemental carbon (black soot), and trace inorganic species (e.g., K⁺). They can be solid, liquid, or a combination. Smoke particles are generally known to have an aqueous component as they are formed from combustion processes. From a global perspective, one estimate reports the total contribution of biomass burning to the global particulate load to be about 7% (104 Tg/yr). Further, compared to global emissions, the particulate organic carbon is 39% (69 Tg/yr), and elemental carbon (black soot) is >86% (~108 Tg/yr).²⁰ Aerosol particles (smoke) emitted from biomass burning sources have 80-90% of their volume in the fine mode and therefore have significant atmospheric lifetimes.^{23, 24}

Studies to characterize the organic composition of biomass burning aerosols are mainly motivated by the climate²⁵ and human health effects^{26, 27, 28} of this aerosol class. Currently, only a small percentage of the organic compounds within these aerosols have been identified. Also, little is known about the chemistry of these types of primary aerosols, especially with aerosol age, as only a few studies have characterized ambient biomass fires.^{29, 30} In order to add to the body of knowledge of the chemistry of primary aerosols emitted from biomass fires, this dissertation has focused on fundamental chemistry that may occur in this type of aerosol, specifically as it applies to the anhydrosaccharide, levoglucosan (c.f. Section 1.3.4.)

1.2.2. Characterization of Biomass Burning Aerosols

The organic components of biomass burning aerosols are often composed of a highly complex mixture of compounds with a diversity of chemical structures and reactivities, as well as physical properties.³¹ The complexity of these aerosols makes comprehensive characterization on the molecular level difficult. To this end, many laboratory studies have characterized biomass aerosol compounds by burning, for example, individual components of vegetation such as cellulose^{22, 32, 33} and vegetation in its complete form^{34, 35} yielding information of the chemical speciation of these systems. Additionally, many field campaigns have been carried out to characterize real biomass burning aerosols.^{36, 37} The major observation of these investigations is that sugar derivatives are a major component of cellulose and hemi-cellulose pyrolysis.^{22, 35}

1.2.3. The Climate Forcing of Biomass Burning Aerosols

The direct effect of biomass burning emissions on the Earth's radiation budget was estimated in 2001 by the International Panel on Climate Change (IPCC) to be about -0.2 Watts per square meter (Figure 1), therefore acting as a global cooling mechanism. This measurement, however, has a significant level of uncertainty. There is a large uncertainty in indirect effects by aerosols in general. As of 2001, the IPCC³⁸ had not given an estimated value for the indirect aerosol effects on climate forcing, but had only reported an error bar which reports an estimated uncertainty range of ~ 0 to -2 Watts per square meter. Unfortunately, the current level of scientific

understanding for both the direct and especially the indirect aerosol effect on climate forcing has a low level of scientific understanding. Questions such as how biomass burning aerosols affect the Earth's radiation budget through indirect effects are pressing. Knowledge of the significance of this effect on the Earth's climate will help drive both governmental policy and atmospheric modeling predictions.

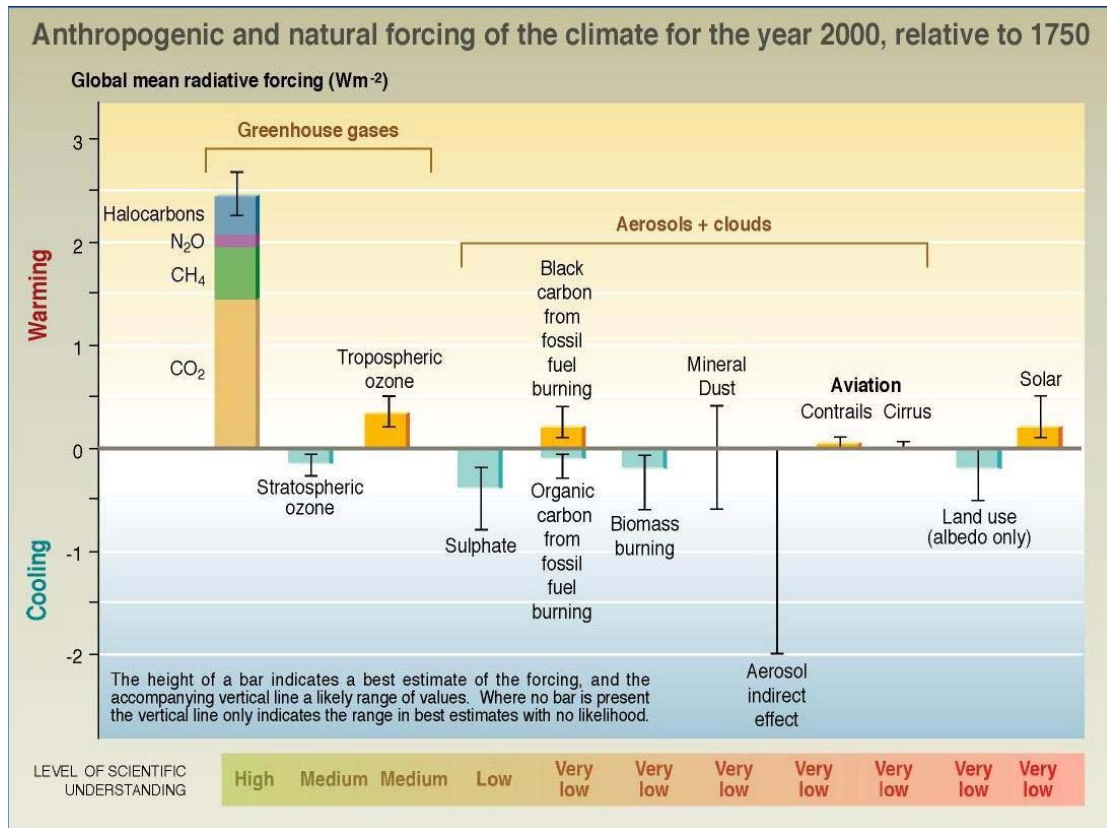


Figure 1-1 Estimated radiative forcing of atmospheric components, IPCC, 2001.³⁸

1.2.4. Cloud Condensation Properties of Biomass Burning Aerosols

Biomass burning particles are generally good cloud condensation nuclei (CCN) provided that there is a sufficient updraft velocity in the vicinity of the fire. Enhanced

densities of CCN lead to an increase in Earth's albedo through cloud formation.^{6, 39} Although organic compounds are often found to dominate up to ~90 % of the total aerosol mass in biomass burning aerosols,^{40, 41} it is not yet understood how either the organic or inorganic composition of these aerosols affect cloud formation. Biomass burning aerosols are typically known as cloud formers, although there are exceptions. Anomalous behavior in the cloud-forming properties of biomass burning aerosols has been observed. In Amazon fires, cloud-inhibiting phenomena have been observed by biomass burning aerosols through remote sensing measurements.⁷ Other physical effects, such as the Twomey effect,^{15, 16} which increases cloud droplet concentrations and therefore cloud albedo, are proposed as processes which cause this phenomenon. However, little is known about the chemistry within these aerosols and how the compounds affect the physical properties of these aerosols, especially how they affect the aerosols capacity as CCN.

1.3. Carbonaceous Aerosol Formed from Biomass Burning

1.3.1. Introduction

Carbon-containing aerosols (carbonaceous) have received significant attention over the past 10-15 years as their impact on human health, climate change, and atmospheric chemistry has come into view. Carbonaceous aerosols can exist in two general forms: organic carbon (OC) or elemental carbon (EC). OC refers to molecular hydrocarbons that are often functionalized with oxygen, nitrogen, sulfur and/or other

elements. OC possesses a wide range of physical and chemical properties as a result of the great variety of structures that can exist, including oligomeric and polymeric forms. The exact definition of an oligomer is currently a matter of debate, but it generally is accepted to be a molecule consisting of between 2 and 100 monomers. A polymer generally refers to a molecule with an undefined, and usually large, number of monomers. EC refers to carbon that is graphitic in nature and generally associated with soot.

A third category, black carbon (BC) refers to carbonaceous aerosols that absorb visible radiation significantly. This is a useful definition since the absorption properties of particles are of primary importance in assessing the direct climate forcing of aerosols. Though BC is predominately composed of elemental carbon (i.e., black soot), polyaromatic hydrocarbons, which are categorized as OC, are usually associated with soot particles and are also very strong absorbers of visible radiation. For this discussion, organic aerosol (OA) will describe atmospheric aerosols that have a significant OC (> 30 %) component.

A substantial portion (~20-50%) of the total atmospheric fine particulate matter is contains carbon and is emitted in significant amounts from both anthropogenic and natural sources.²⁵ Anthropogenic sources of OA are almost entirely the result of combustion processes such as biomass burning and can be either primary (POA) or secondary (SOA) in nature. Anthropogenic OA have been the cause for serious concern about the health effects of PM in urban areas, where PAHs and nitro-PAHs have been associated with fine PM from combustion sources, including vehicular

emissions and biomass burning. Though, technically, biomass burning, a large source of primary and secondary organic aerosols, can occur as a result of natural processes (e.g., lightning-induced forest fires), it is generally categorized as an anthropogenic contributor to OA.

OC contained in biomass burning aerosols is a complex mixture of hundreds or maybe thousands of different compounds. Some of the different classes of compounds that have been identified in biomass burning aerosols include: n-alkanes, polyaromatic hydrocarbons (PAHs), aromatic carbonyls, methoxyphenols, n-alkanoic acids, n-alkanedioic acids, n-alkeneoic acids, resin acids (e.g., abietic acid), mono- and di- saccharides, anhydrosaccharides, phytosterols, and amino acids.^{42,43} Across this diverse set of compounds, physical and chemical properties can vary substantially, controlling the role and fate of organic aerosols in the atmosphere. These properties can affect their gas-to-aerosol partitioning, water uptake, and light scattering and absorption.

1.3.2. Water Soluble Organic Compounds in Biomass Burning Aerosols

A few early field studies reported finding water-soluble compounds enriched in smoke aerosols. Interest in the water-soluble components of this type of aerosol increased when Novakav and Corrigan³⁹ reported that the burning of cellulose produced aerosols composed of nearly 100% water-soluble organic compounds (WSOC). The interest in these compounds was enhanced by studies indicating that WSOCs in aerosols could have a significant effect on their CCN nucleating

activity.⁴⁴⁻⁴⁷ Further, the high concentrations of WSOCs in smoke aerosol suggests that they may play important roles in the chemistry of cloud droplets which are nucleated by smoke aerosol.

Within the past decade, a strong research interest has developed in characterizing a class of WSOCs found in aerosols known as humic-like substances (HULIS).^{48, 49} The term HULIS originates from the apparent resemblance of this compound class to the macromolecular humic and fulvic acids found in terrestrial and aquatic environments. HULIS is a class of macromolecular compounds that has been measured in fogwater, aerosols, and cloudwater.⁵⁰⁻⁵³ Studies of HULIS are motivated by its potentially strong effects on aerosol properties such as hygroscopicity, their ability to nucleate cloud formation, and light absorption.^{48, 54} Also, in light of humic acids roles in the solubilization, sorption, complexation, and transport of organic and inorganic species in the biosphere, it is anticipated that HULIS may play a similar role in the atmosphere.

1.3.3. Organic Tracers for Biomass Burning Aerosols

Biomass burning aerosols vary between fires depending on moisture, fuel type, type of fire (smoldering and/or flaming), wind direction, and a variety of other meteorological variables. As these air parcels mix and age, optical, physical and CCN properties can change significantly. Even more difficult is assessing the effects of a combination of burning sources. Mixing of biomass burning aerosols with other natural and anthropogenic pollution sources forms hazes, which can affect the

atmosphere from a local, regional, seasonal, and a global scale.⁵⁵ In assessing these aerosol properties, chemical tracers are useful as fingerprints in identifying variables such as point sources, fuel types, aerosol parcel age, etc. Chemical markers have been identified for the combustion and pyrolysis of residential wood-smoke.⁵⁶ The use of terpenoid and lipid tracers has been applied to the characterization of biomass burning aerosols in Amazonia, Brazil³⁴, Oregon⁵⁷, China⁵⁸, and Southern California.⁵⁹ Retene, a thermal alteration product of terpenoids such as abietic acid in conifer wood, has been found in aerosols in Norway and Oregon. It has also been found to a limited extent in Los Angeles, California, and China. Retene is not measurable in aerosols collected in Nigeria or Amazonia, Brazil as conifers are not a fuel source in these areas. Since retene is a unique product of conifer wood burning, it is not always found in significant concentrations for it to be used as a tracer.

Not all wood-burning sources have been fully characterized for tracer composition in aerosols. There is a need to have molecular markers that are specific to point and regional sources, unique to foliage burning, atmospherically stable and exist in high concentrations. This information will help investigators to estimate its atmospheric stability and therefore quality as a marker for biomass burning aerosol parcels. Such markers and their atmospheric reaction products may be able to provide not only source information, but aerosol parcel age.³⁵ To understand the potential of biomass burning aerosols markers such as levoglucosan, laboratory and field studies must be performed to understand its chemical reactivity.

1.3.4. Levoglucosan

Levoglucosan (1,6-anhydro- β -D-glucopyranose), an anhydrosugar, is a common component of biomass burning aerosols that has been measured at relatively high concentrations in biomass burning aerosols (Figure 1-2). Also, it is a unique product of cellulose combustion giving it the special quality of being a marker for foliar fuel combustion.³⁵ Cellulose is the common structural element that dominates the mass of foliar fuels and is the major precursor to the production of levoglucosan. Due to its high concentrations in the biosphere, its combustion and pyrolysis products have been thoroughly studied due to their potential impact on atmospheric chemistry.³⁵

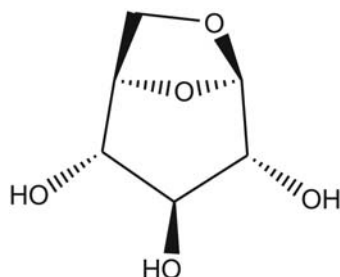


Figure 1-2 Structure of levoglucosan (1,6-anhydro- β -D-glucopyranose)

The combustion conditions of the foliar fuel (wood) are important in the amounts of levoglucosan which are produced in the aerosol-phase. During the initial stages of wood combustion, the wood starts to dehydrate, hydrolyze, oxidize, and pyrolyze, forming combustible volatile organic compounds, tarry substances, and highly reactive carbonaceous char.⁶⁰ Char is defined as the solid material left over in a combustion process after light gases and tar have been released from the foliar fuel.

Tar is the viscous liquid emitted from wood during carbonization at high temperatures under anoxic conditions. The composition of tar is complex and is commonly stated to contain water, diterpenes, oxygenated benzenes, resin acids (e.g., abietic and pimaric isomers, $C_{19}H_{29}COOH$), and fatty acid methyl esters.^{61, 62} At the ignition temperatures ($<300\text{ }^{\circ}C$) of the volatile organic compounds, gas-phase combustion begins and is visible as a flame. Resinous compounds and thermal decomposition products of cellulose, hemi-cellulose and lignan are stripped and undergo partial and complete combustion in the flaming zone. During flaming combustion, this process continues until the volatile combustible flux drops below a critical threshold where flaming ends. At this point, a process known as smoldering begins where the temperature is high enough ($>300\text{ }^{\circ}C$) for the continued propagation of char formation. During smoldering, bond cleavage of wood components produces tarry anhydrosaccharides as well as a variety of other gas- and aerosol-phase products.⁶³ . This process includes a gas-solid phase reaction between oxygen and the remaining reactive char which emits large amounts of incompletely oxidized pyrolysis products into the atmosphere. Many of these compounds, when emitted into the atmosphere, are found in the particulate phase because of their low vapor pressures. Major products of the smoldering-phase are levoglucosan (1,6-anhydro- β -D-glucopyranose) and its furanose isomer which are found in the fine aerosol size mode.³⁵ It is during the smoldering-phase where high aerosol-phase concentrations of levoglucosan are formed.

Due to its high water solubility and low vapor pressure, levoglucosan is a

common component of smoke aerosols, which are known to be hygroscopic at a young age.³⁰ Because levoglucosan is a unique product of foliar fuel combustion, it is currently considered a viable molecular tracer for biomass burning in urban and rural airsheds and sediments.⁶⁴ The atmospheric importance of these chemical processes relies on the conditions that levoglucosan is chemically stable on an atmospherically relevant time-scale and that viable concentrations of the relevant reactive species and levoglucosan are present in the biomass burning aerosol. Biomass burning aerosols may satisfy these conditions as anhydrosaccharides have been found to be a dominant class (e.g., ~ 61% of carbonaceous material by mass) within these types of aerosols. In some biomass burning aerosol measurements, levoglucosan has been found to be by far the dominant anhydrosaccharide and has been measured to be between 87-91% of the anhydrosaccharide fraction.³⁰

In the field of atmospheric science, broad questions concerning the use of levoglucosan as a biomass burning species/tracer include 1) what are the atmospheric chemical sinks/mechanisms for levoglucosan, 2) what products are formed from common reactive species, 3) what is the significance of these pathways under atmospheric conditions, 4) will identified chemical products of levoglucosan be unique to biomass burning, 5) can these products give information on a aerosol parcel's age and/or regional or point source, 6) what is the atmospheric lifetime of levoglucosan, and 7) how do these products affect the atmospheric physical and optical properties of the aerosols (e.g., CCN, etc.). This dissertation focuses on questions 1 and 2 which address the fundamental chemical reactions of the model

compound, levoglucosan, under simulated atmospheric conditions (i.e. $\bullet\text{OH}$ and H^+).

2. Levoglucosan Proxy Experimental Methodology

2.1. Model Reaction System

2.1.1. Introduction

In considering the question above, biomass burning aerosol proxy experiments were developed in the laboratory to understand chemical sinks and products of levoglucosan in aqueous reaction systems. An aqueous reaction system was chosen since biomass burning aerosols have been found to be highly aqueous. Levoglucosan was chosen as the model compound for this system since it often dominates the aerosol mass³⁰ and has been used as a tracer for biomass burning aerosol parcels.³⁵ Also, chemical mechanisms identified may be general for other reactive organic species in biomass burning aerosols, providing more information about the chemistry in this type of aerosol. Since levoglucosan is found mainly in fine mode aerosols, which generally have an atmospheric residence time of about 3-5 days, the experimental design was setup to measure the reactions of levoglucosan for up to 7 days. All studies in this dissertation used similar methods for the general experimental design and sample analysis. This section describes the common techniques used to investigate the levoglucosan proxy systems. Further details will be given in the chapters for the individual studies where new or augmented experimental design or sampling methods are used.

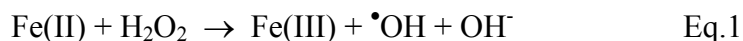
2.1.2. General Experimental Setup

Reactions were run in bulk solution on a 1 liter scale in 1.5-liter pyrex beakers at room temperature. Reactions were also performed in water as smoke aerosols are known to be largely aqueous. Since biomass burning aerosols often have a strong propensity to act as CCN, aqueous systems are especially relevant.

2.1.3. Model Chemical Reaction Systems

Two environmentally relevant reactive species were targeted for these studies. Both H^+ and $\bullet\text{OH}$ are ubiquitous reactants found in the atmosphere. The pH of cloudwater ranges between 3 and 6^{65, 66} and fine mode aerosols are often even more acidic.⁶⁷⁻⁷⁰ The pH of the chemical reaction systems in this work were adjusted to 4.5 for all reactions.

The hydroxyl radical is one of the strongest atmospheric oxidants known.⁷¹ In the atmosphere, it is considered as the most important oxidative species as it is a sink for most organic species. For these studies, $\bullet\text{OH}$ was produced *in-situ* in the bulk solution using the Fenton reaction.⁷² In the Fenton reaction, free $\bullet\text{OH}$ radicals are formed by the reaction of Fe(II) and hydrogen peroxide (H_2O_2) in aqueous acidic solution (Equation 1).



It is known that although about ~80% of $\bullet\text{OH}$ in atmospheric aerosols come from the

gas-phase, significant amounts of the $\bullet\text{OH}$ are produced within the aerosol, where one of the routes is through the Fenton reaction.⁶⁵

2.2. Development of Analytical Methodology

2.2.1. Proxy Reaction Conditions

The general protocol used for sampling from these reactions was to take 250 mL- aliquots of the solution for time points 0.5, 1, 3, 5, and 7 days. Since the reactions were in aqueous solution, the sample aliquots were lyophilized (freeze-dried) under vacuum at low temperature until dry. This served not only to remove water but to concentrate the reaction products for analysis.

2.2.2. Time-of-Flight Mass Spectrometry

Time-of-flight mass spectrometry (TOF-MS) was the main analysis method used for the research presented here. As discussed below, different techniques were used to ionize the analyte using this type of mass spectrometric analysis. The ionization of the analyte is a key step as a mass spectrometer works on the principle of accelerating a charged molecule in an electric field. Ions with the same charge will have the same kinetic energy but the velocity of the ion will depend on its mass-to-charge (m/z) ratio. In TOF-mass spectrometry, the time that it takes for a specific ion to reach a detector, with a known flight distance, will depend on the accelerating voltage, and the m/z of the ion. Heavier ions will have slower speeds. Once the time of the ion

flight is measured, conversion to the m/z domain is done mathematically, where the time-of-flight is proportional to the square root of the ion's mass to charge ratio (m/z).⁷³

2.2.3. Matrix-Assisted Laser Desorption and Ionization Time-of-Flight Mass Spectrometry

For these studies, matrix-assisted laser desorption and ionization time-of-flight mass spectrometry (MALDI-TOF-MS) was used as the primary analytical method for the analysis of the dried reaction products (Figures 2-1, 2-2). MALDI-TOF-MS is a good analytical tool for the soft-ionization of organic molecules and is most often used for high molecular weight compounds such as polypeptides or proteins.⁷⁴ Because of the unique ionization process, data interpretation is often straight-forward because the molecular ion (M) signal predominates. The general mechanism of ionization with this method constitutes combining the analyte with a solution containing matrix molecules. The matrix is usually a benzylic species that absorbs UV radiation and has a low vapor pressure. The instrument uses a pulsed nitrogen laser that emits at 337 nm. The analyte is combined in a solution containing the matrix. Often, an ionizing species such as an acid as a proton source (H^+) or alkali earth metal are added to form a positive charge on the analyte. A solvent is chosen that is compatible with the analyte and matrix as both need to be dissolved to give the best results.

A few microliters of this solution is spotted on a stainless steel sample plate and

dried either in the open air or, for these studies, under reduced pressure. The purpose of this step is to co-crystallize analyte with the matrix. Once in the mass spectrometer, the UV laser is pulsed on the sample spot. The laser energy is absorbed mostly by the matrix where the laser energy is changed to kinetic and vibrational energy (Figure 2-1). This energy is then transferred to the analyte, allowing for desorption of the sample into the gas-phase. Also, it should be noted that cationization from the solid-phase has been considered as an additionally viable route.⁷⁴

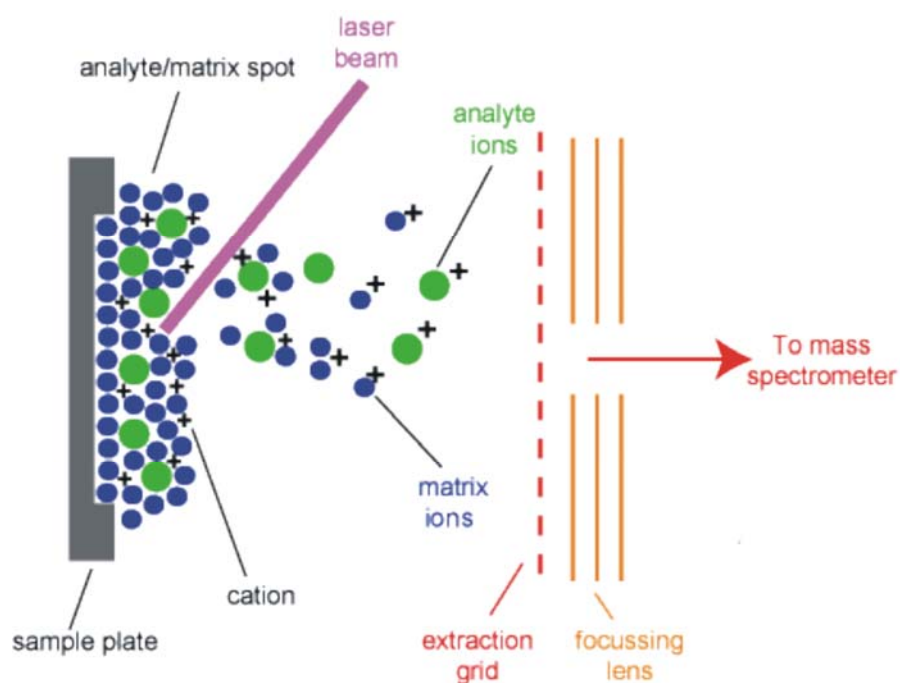


Figure 2-1 Diagram of MALDI process

Here, the analyte can be ionized through many chemical routes. Protonation ($[M+H]^+$) is a common route where the proton can come from the added acid or directly from the matrix molecules, which are also acidic. Addition of alkali metals,

such as sodium chloride, is another route to cationization of the analyte. The ideal cationization method depends primarily on the molecular structure of the analyte and is chosen to match this molecular character.

Successful measurement of reaction products in the levoglucosan system was achieved by using 2,5-dihydroxybenzoic acid (DHB) in an aqueous solution using sodium chloride as a cationization agent. Sodium cationized adducts of the molecular ion peaks were observed for both the acid-catalyzed and Fenton chemical reaction products. In general, for both systems, compounds within a class of glucose-type oligosaccharides were observed. Many studies have shown successful cationization using this MALDI sample preparation methodology for the cationization of oligosaccharides.⁷⁵⁻⁷⁷

2.2.4. MALDI-TOF-MS Sample Preparation and Instrument Settings

The samples were prepared for MALDI-TOF-MS by adding ~1 µg of analyte to 5 µL of deionized water. Precisely 1 µL of this solution was mixed with 9 µL of a matrix solution containing 10 mg/mL DHB and 1 mg/mL NaCl. 1x, 10x, and 100x dilutions were made. The 10x solution almost always gave the best signals. All measurements were made in positive ion, reflectron mode (Figure 2-2).

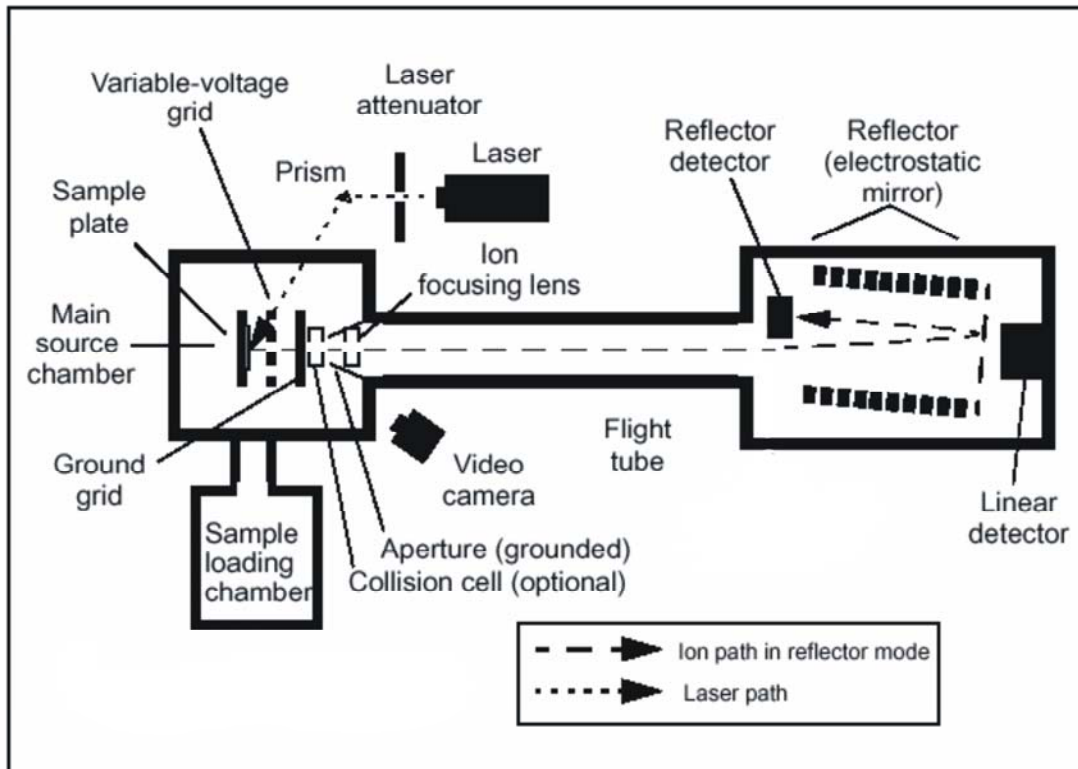


Figure 2-2 MALDI-TOF-MS schematic

Other variables critical to the optimization of the ion signals were laser energy, grid voltage, and the delayed extraction. The laser energy was optimized empirically and adjusted in the MALDI-TOF-MS software as a relatively arbitrary number. The grid voltage is the potential applied to the extraction grid which accelerates the ions toward the detector. This value was empirically optimized to 75%. Delayed extraction was a very important variable for obtaining high-resolution signals with a good signal-to-noise. After the ions enter the gas-phase, there is a time delay before the grid voltage is applied, accelerating the ions into the instrument. It has been shown that the momentum of ions of the same mass can vary significantly between ~200 –

1000 m/z. Also, ions with different molecular weights will have vastly different initial velocities. The time delay allows for ions with different velocities to move different distances from the extraction grids. At an optimum time, the extraction pulse is applied and ions further from the extraction grid will experience a different potential than, for example, a heavier ion that is closer to the grids. This allows for time focusing, increasing the likelihood that ions of the same mass will impact on the detector within a narrow time window, increasing mass resolution and signal intensity.⁷⁸ The optimized delayed extraction time used for these levoglucosan studies was 200 nanoseconds. This delay-time was determined empirically (c.f. Appendix 1).

All measurements were made in reflectron mode. A reflectron is an electrostatic lens which, by using an electrical potential sign (+/-) that matches the analyte's charge, allows for greater mass resolution and signal intensity. The field reverses the ions' initial direction of travel in the ion flight-tube by ~180 degrees, increasing their flight distance. If two ions with the same m/z approach the reflectron with different kinetic energies, the one with greater kinetic energy will penetrate deeper into the electrostatic area, increasing the flight path length compared to the ion with lower kinetic energy. A reflectron improves mass resolution by assuring that ions of the same m/z but with different kinetic energies arrive at the detector at the same time.

2.2.5. Laser Desorption and Ionization Time-of-Flight Mass Spectrometry

Laser Desorption and Ionization Time-of-Flight Mass Spectrometry (LDI-TOF-MS) was used as a complimentary technique to the MALDI-TOF-MS experiments.

Specifically, it provided unique data in the hydroxyl radical study. This uses the same instrument as the MALDI-TOF but the analyte is not co-crystallized with a matrix. Rather, powdered carbon was suspended in water and spotted on the MALDI sample plate and dried under vacuum. This was repeated until there was an even layer of dried carbon on the sample well. Next, $\sim 1 \mu\text{g}$ of analyte was dissolved in $5 \mu\text{L}$ of 1 mg/mL sodium chloride in deionized water. About $3 \mu\text{L}$ of this solution was spotted on top of the carbon and dried under vacuum. The sample plate was introduced into the MALDI-TOF instrument as before and the same instrument variables, except for laser energy, were used. To form ions, the laser is pulsed on the sample spot. The carbon is heated by the laser, and the analyte desorbs into the gas-phase. Also, the laser energy could be absorbed by the analyte if the absorption cross-section for the UV wavelength was optimal. Once sampled by the pulsed laser, the analytes were cationized by sodium.⁷⁹ The laser energy used was significantly higher than that used for the MALDI-TOF-MS experiments.

2.2.6. Electrospray Ionization Mass Spectrometry

Electrospray ionization mass spectrometry (ESI-MS) is an analytical technique where ion formation in the vacuum is accomplished by pushing the analyte, which is dissolved in a volatile solvent, through a high voltage capillary needle. Once through the needle, the sample is aerosolized and may possess multiple charges. As the aerosols travel in a nitrogen stream, the charged aerosols evaporate, reducing its size. As the charged aerosols get smaller and the charges are forced closer together, they

undergo Coulombic fission, breaking into smaller particles and evaporating until only the analyte is left. The analyte accommodates a charge (positive or negative) that comes from either the fission process or through the addition of added cationizing agents such as acids (+), alkali earth metals (+), or halogens (-).

The possibility for ionization artifacts from MALDI-TOF-MS exists due to non-covalent interactions. The ESI-mass spectra supported solution-phase chemistry rather than ionization artifacts during the MALDI process. This is discussed in Section 3.

2.2.7. Attenuated Total Reflectance Fourier-Transform Infrared Spectroscopy

Attenuated total reflectance Fourier-transform infrared spectroscopy (ATR-FTIR) provided supporting data for the proposed mechanisms in both the acid-catalyzed and hydroxyl radical studies. In this method, solid or liquid samples can be measured directly without further sample preparation. ATR uses a property of internal reflectance called an evanescent wave. An infrared beam is passed through an ATR crystal where multiple internal reflections create this evanescent wave that extends a few micrometers (μm) into the sample and finally into a detector. The crystal is typically made of materials such as germanium and zinc selenide which, to produce this effect, must have a much higher refractive index than sample being studied.⁸⁰ Dried samples were directly pressed onto the ATR crystal and spectra were measured between 4500 and 200 cm^{-1} using 32 scans, and 4-cm^{-1} resolution.

3. Water Soluble Oligomer Formation from Acid-Catalyzed Reactions of Levoglucosan in Proxies of Atmospheric Aqueous Aerosols⁸¹

3.1. Introduction

Because of its high reactivity, the hydroxyl radical is known to be the most important atmospheric oxidant as it governs the oxidation and removal of most trace gases⁸² as well as various organic species in cloudwater.⁶⁵ Within aqueous aerosols, the Fenton reactions may generate significant amounts of hydroxyl radicals through the reaction of hydrogen peroxide with Fe(II) under acidic conditions.⁶⁵ Here, an aqueous levoglucosan reaction system is studied to assess fundamental chemical pathways that may occur in aqueous biomass burning aerosols.

To be an effective marker for long-range transport, levoglucosan must be chemically stable on an atmospherically relevant time-scale compared with its loss from aerosol deposition to the landscape. To date, chemical processes that may remove levoglucosan from smoke aerosol remain unknown; therefore, the absence of measurable levoglucosan in an aerosol parcel should not necessarily negate apportionment of the aerosol to a biomass burning source. It is therefore the focus of this study to understand the chemical transformations of levoglucosan under atmospherically relevant conditions to better evaluate levoglucosan as a useful marker to characterize biomass burning aerosols. In cases where there are significant chemical removal pathways of levoglucosan, reaction products are generated that, it

is suggested here, may serve as secondary tracers for the aerosol parcel. Even in cases where levoglucosan is measured, the secondary tracers may provide additional information regarding the age of the aerosol parcel, its source and the atmospheric processing it has undergone. This laboratory study serves to elucidate upon chemical loss mechanisms for levoglucosan as well as to identify potential secondary tracers within simulated biomass burning aerosols.

Oligomerization via acid-catalyzed processes, including aldol condensation and reaction through the dehydration of hemi-acetal functionalities, has been observed previously in laboratory studies on secondary organic aerosol formation;⁸³⁻⁸⁵ therefore, it is hypothesized here that, in addition to hydroxyl radical reactions, acid-catalyzed oligomerization may also be a significant removal pathway for levoglucosan in atmospheric aqueous aerosols. Also, removal of atmospheric levoglucosan by acid-catalyzed oligomerization may be facilitated by the naturally acidic pH of atmospheric aqueous aerosols. In this study, matrix assisted laser desorption ionization (MALDI) time-of-flight (TOF) mass spectrometry (MS) and attenuated total reflectance (ATR) Fourier transform infrared (FTIR) spectroscopy were used to measure the reactivity of levoglucosan and identify molecular products in solutions designed to serve as proxies for atmospheric aqueous aerosols,⁸⁶ providing a qualitative description of possible atmospheric aerosol processes leading to the chemical removal of levoglucosan.

3.2. Experimental

3.2.1. Experimental Design

All reagents were used as supplied by the manufacturer. Initial reagent concentrations were the same for all experiments: levoglucosan (10^{-3} M) (99%, Alfa Aesar), hydrogen peroxide (10^{-4} M) (30% in water, Acros), anhydrous ferric chloride hexahydrate (5×10^{-6} M) (99%, Fisher), and sulfuric acid (to bring the solution pH to 4.5) (96.1%, Mallinckrodt). The concentration of hydrogen peroxide was based on experimental measurements in cloudwater.⁸⁷ The iron concentration was based on both experimental⁸⁸ and model studies⁶⁵ of cloudwater. The pH of cloud droplets ranges from 4 to 6; 4.5 is taken as a typical value.⁶⁵ Also, in general, fine-mode aerosols are known to be acidic.⁷⁰

Reactions were performed on a one-liter scale in 18 M Ω m water (Milli-Q, Model Gradient A10, TOC <5 ppb) at room temperature. All reactions were performed in the dark. Where the chemical experiment used Fenton chemistry (Reactions A, D, Table 3-1), the reaction was initiated by adding hydrogen peroxide. Reactions B, C and E (Table 3-1) were initiated by the addition of levoglucosan. Aliquots of 250.0 mL, sampled from each reaction on days 0.5, 1, 3, and 7, were frozen and lyophilized prior to analysis by MALDI-TOF-MS or ATR-FTIR.

3.2.2. Sample Preparation for Analytical Analysis

Lyophilized samples were dissolved in deionized water and 1 μ L of this solution

was combined with 9 μL of the matrix and cationizing agent. The water soluble reaction products were measured with MALDI-TOF-MS using a matrix of 10 mg/mL 2,5 di-hydroxybenzoic acid (DHB, 99%, Alfa Aesar) in deionized water and 1 mg/mL sodium chloride as the cationizing agent. Aliquots of 2 μL were spotted on a standard stainless steel MALDI sample plate (Applied Biosystems) and the chemical components co-crystallized by drying in a vacuum dessicator. Positive ion MALDI-TOF-MS was performed in reflectron mode with a 337 nm laser (Applied Biosystems Voyager-DE Pro). The MALDI-TOF mass spectra for 1000 laser shots (500 shots per well) were averaged for each measurement. As a supporting analytical method, Electrospray ionization mass spectrometry (ESI-MS) of reaction B (Table 3-1), day 1 was measured using a Finnigan-MATT TSQ-70. The sample was dissolved in 50/50 acetonitrile/water with 1 mg/L sodium acetate before injection into the mass spectrometer. ATR-FTIR spectra of dry lyophilized reaction products were measured using a Thermo-Nicolet IR200 series spectrometer using 4 cm^{-1} resolution and 32 scans.

3.3. Results and Discussion

3.3.1. Experimental Description and Background Control Experiments

Reactions A, B, and C, were run to investigate the bulk aqueous phase chemistry of levoglucosan with common reactants found in cloudwater (Table 3-1). Reaction A was designed to investigate the chemistry of levoglucosan with reactants (H^+ , H_2O_2 ,

Fe²⁺) that produce the hydroxyl radical through the Fenton reaction. In order to identify specific chemical formation mechanisms, variations of these reactants from Reaction A were tested using reactions B (H⁺) and C (Fe³⁺, H⁺). Reactions D and E were run as negative controls (i.e., no significant chemical reaction was expected). Oligomers were observed under all experimental reaction conditions except reactions D and E. The measured MALDI-TOF spectra were assumed to be for the water-soluble products from the simulated cloud water because co-crystallization of the analytes with the aqueous matrix solution was required for the generation of significant MALDI-TOF signals.

Reaction	Levoglucosan	Fe ³⁺	H ₂ O ₂	H ₂ SO ₄
A	X	X	X	X
B	X			X
C	X	X		X
D		X	X	X
E	X	X		

Table 3-1 Summary of the five experimental conditions used to investigate the aqueous-phase chemistry of levoglucosan in bulk. Reactant concentrations: Levoglucosan: 1x10⁻³ M, FeCl₃ • 6H₂O: 5x10⁻⁶ M, H₂O₂: 1x10⁻⁴ M, H₂SO₄: pH = 4.5.

3.3.2. The Fenton Reaction

For Reaction A (Fenton chemistry), two distinct oligomeric product classes were measured depending on the time of reaction: water-soluble (Figures 3-1,a-d) and

diethyl ether-soluble products. As the reactions progressed beyond the first day, up to 7 days, the intensities of the water-soluble MALDI-TOF mass peaks decreased with time. Generation of the measured water-soluble oligomeric products is described here by acid-catalyzed processes, such as hydration, hemi-acetal/acetal formation, aldol condensation and polymerization⁸³⁻⁸⁵.

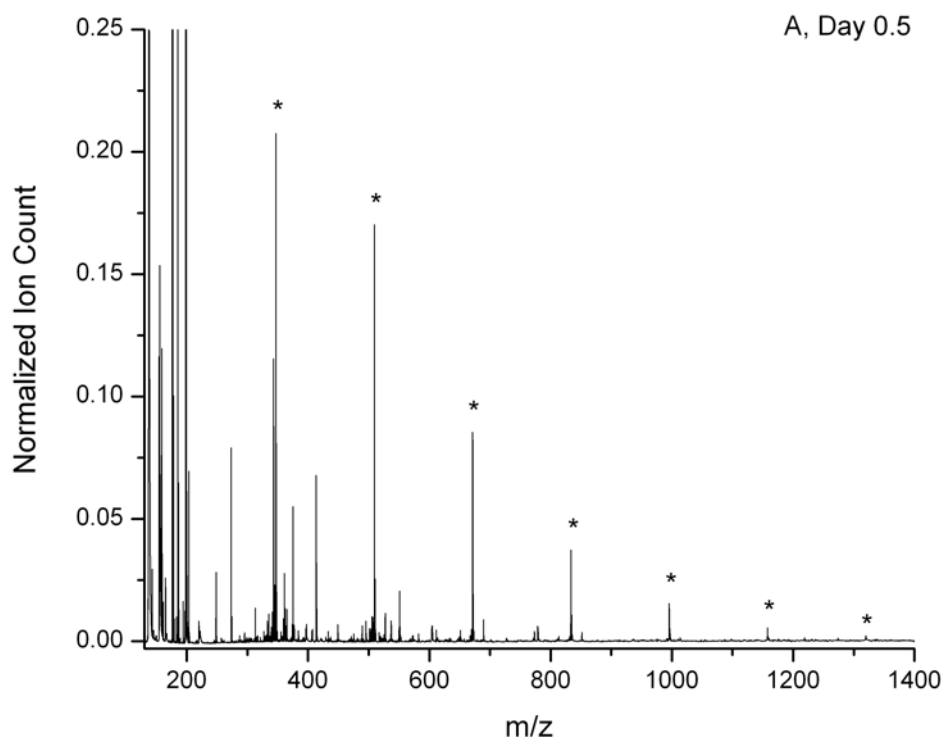


Figure 3-1a MALDI-TOF-MS of Reaction A (levoglucosan, H₂O₂, H₂SO₄, Fe³⁺), day 0.5, using DHB/NaCl matrix in positive ion, reflectron mode. Spectra are normalized to the 185 Da (levoglucosan + Na⁺) peak. (* - indicates relevant product peaks)

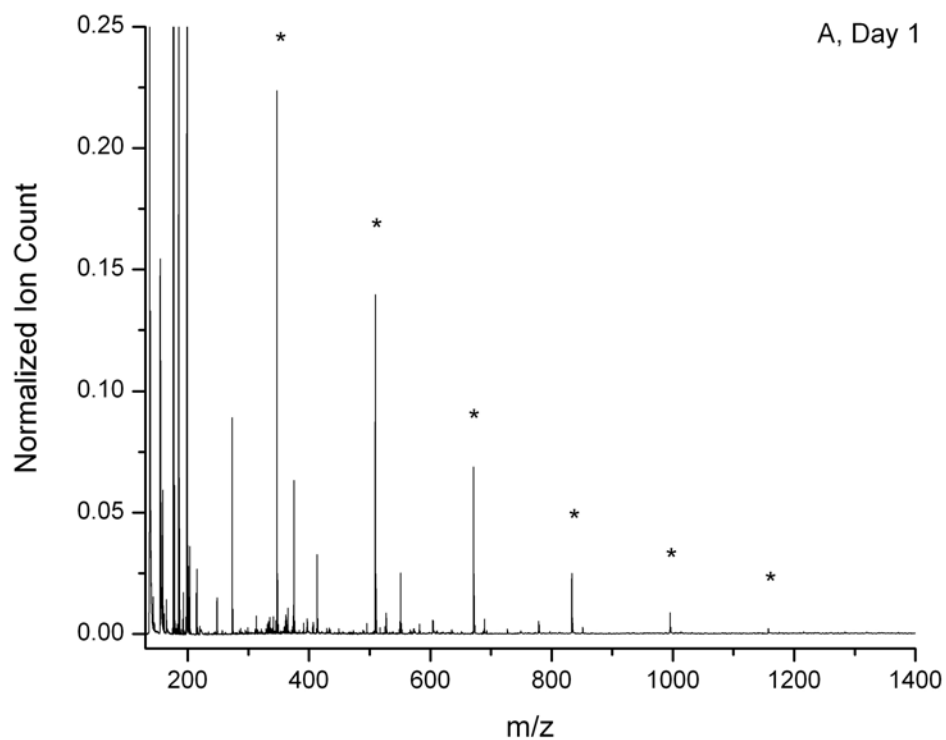


Figure 3-1b MALDI-TOF-MS of Reaction A (levoglucosan, H_2O_2 , H_2SO_4 , Fe^{3+}), day 1, using DHB/NaCl matrix in positive ion, reflectron mode. Spectra are normalized to the 185 Da (levoglucosan + Na^+) peak. (* - indicates relevant product peaks)

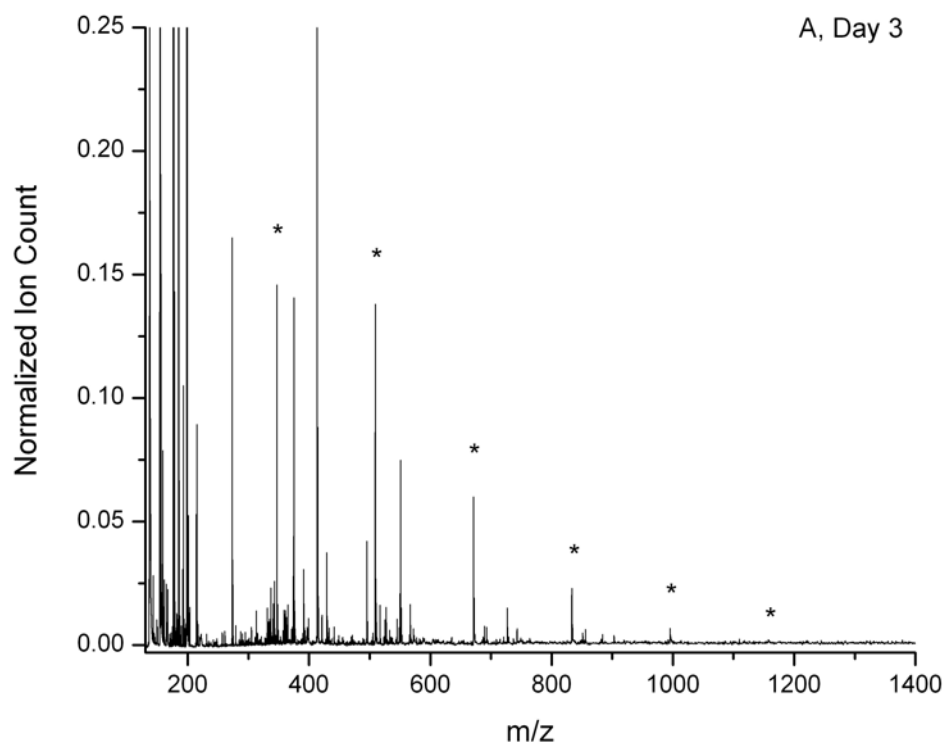


Figure 3-1c MALDI-TOF-MS of Reaction A (levoglucosan, H_2O_2 , H_2SO_4 , Fe^{3+}), day 3, using DHB/NaCl matrix in positive ion, reflectron mode. Spectra are normalized to the 185 Da (levoglucosan + Na^+) peak. (* - indicates relevant product peaks)

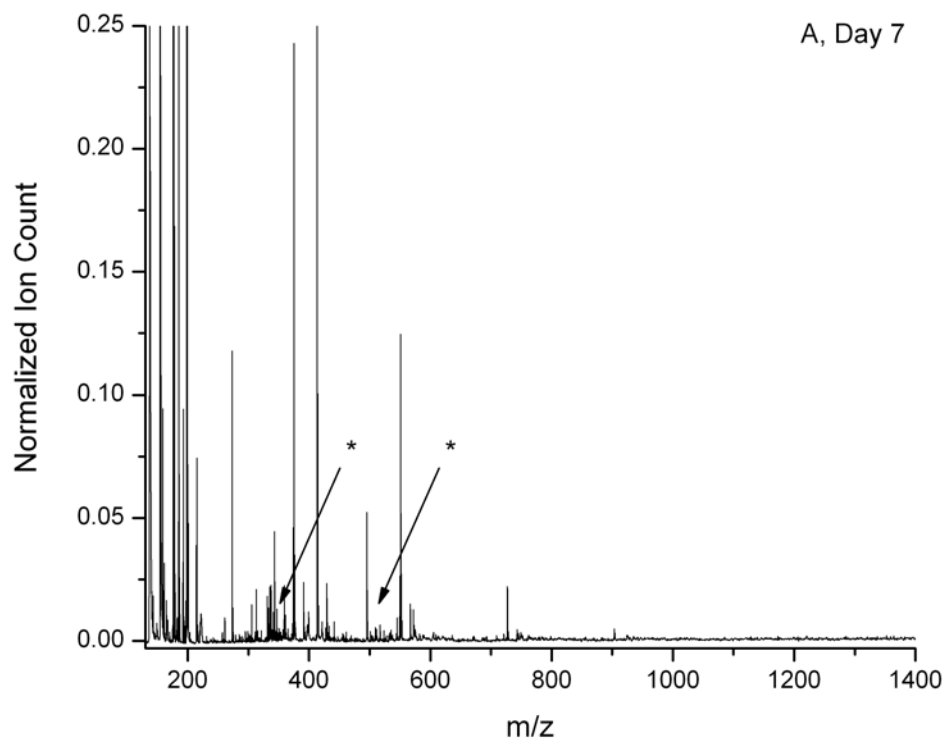


Figure 3-1d MALDI-TOF-MS of Reaction A (levoglucosan, H_2O_2 , H_2SO_4 , Fe^{3+}), day 7, using DHB/NaCl matrix in positive ion, reflectron mode. Spectra are normalized to the 185 Da (levoglucosan + Na^+) peak. (* - indicates relevant product peaks)

3.3.3. Identification of Chemical Mechanism

Oligomerization is a common feature observed for Reactions A, B and C. Although the deionized water used in these experiments contained <5 ppb total dissolved organic compounds, Reaction D was necessary to account for any background oligomerization of these innate organics. Reaction E, on the other hand, was run to account for the possibility that hydrated levoglucosan clusters could form

during sample preparation and/or the MALDI-TOF-MS measurement. An additional test for this potential artifact was performed by measuring levoglucosan dissolved in only deionized water at a number of concentrations (10^{-3} , 10^{-4} , 10^{-5} M). The MALDI-TOF spectra of these control experiments did not show any significant oligomer ion signals.

As a comparative method to test for instrumental artifacts, Electrospray ionization mass spectrometry (ESI-MS) was used to measure a dry sample from day 1 (Figure 3-2, full y-axis scale not shown). The results of this measurement show the same mass patterns from the oligomer products ($[M+Na]^+$) discussed below supporting the case that the MALDI-TOF-MS spectra were not due to artifact formation from the MALDI ionization process.

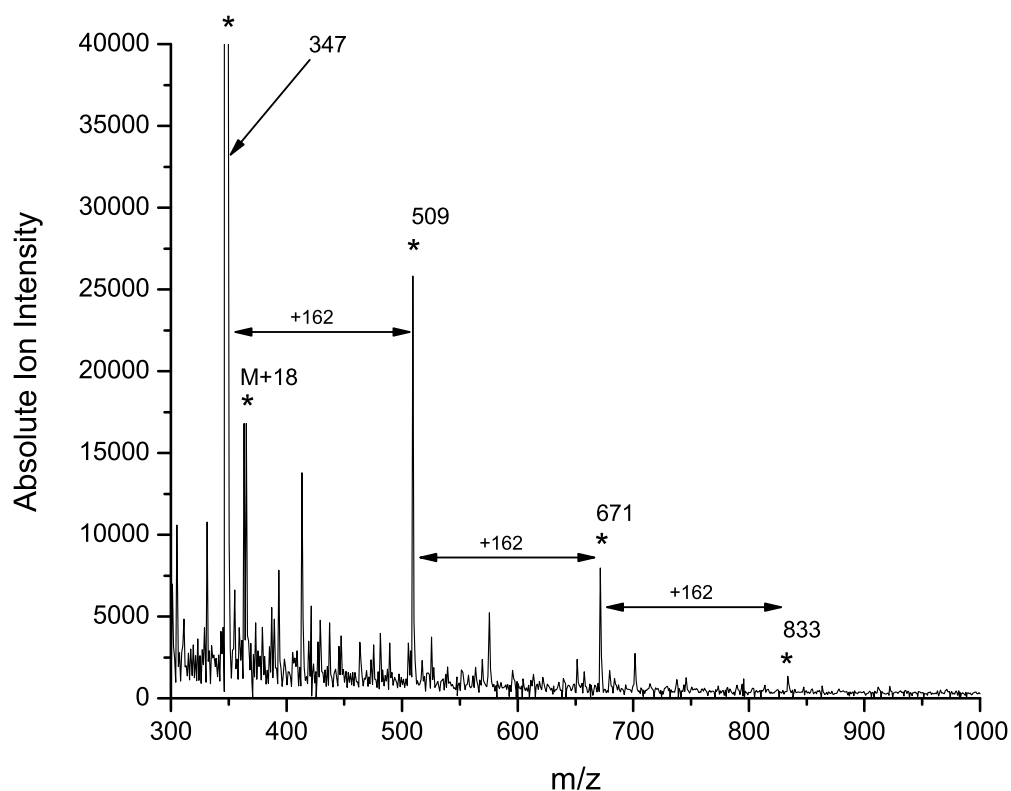


Figure 3-2 Electrospray ionization mass spectrometry (ESI-MS) of the dried day 1 sample for reaction B. (*- indicates relevant product peaks)

Reaction B (Figure 3-3) was designed to study the reactivity of levoglucosan (162 u) with respect to acid-catalyzed oligomerization. Sodium adduct peaks of repeating mass units of 162 u were measured up to $x = 9$ (1458 u). Also, significant, but less intense $[x\text{-mer} + 18]^+$ m/z ion signals were measured under all reaction conditions involving levoglucosan and sulfuric acid (Reactions A, B, and C). Mass spectra measured for Reaction A (Figures 3-1,a-d), which was devised to study the potential

for $\bullet\text{OH}$ -radical initiated oligomerization by the Fenton reaction, were essentially identical to those measured for reactions B and C. This leads us to believe that the hydroxyl radical mechanism is not an important route to the observed oligomerization products under these experimental conditions. Due to the high oxidative strength and relatively unselective attack of the hydroxyl radical, one would predict a continuum of product masses from the reaction between this oxidant and levoglucosan. However, the relative simplicity of the MALDI-TOF mass spectra for Reaction A lends further support to our hypothesis that Fenton-type chemistry is not a significant source of the measured water-soluble oligomers. Based on these observations, the observed products are attributed to an acid-catalyzed mechanism.

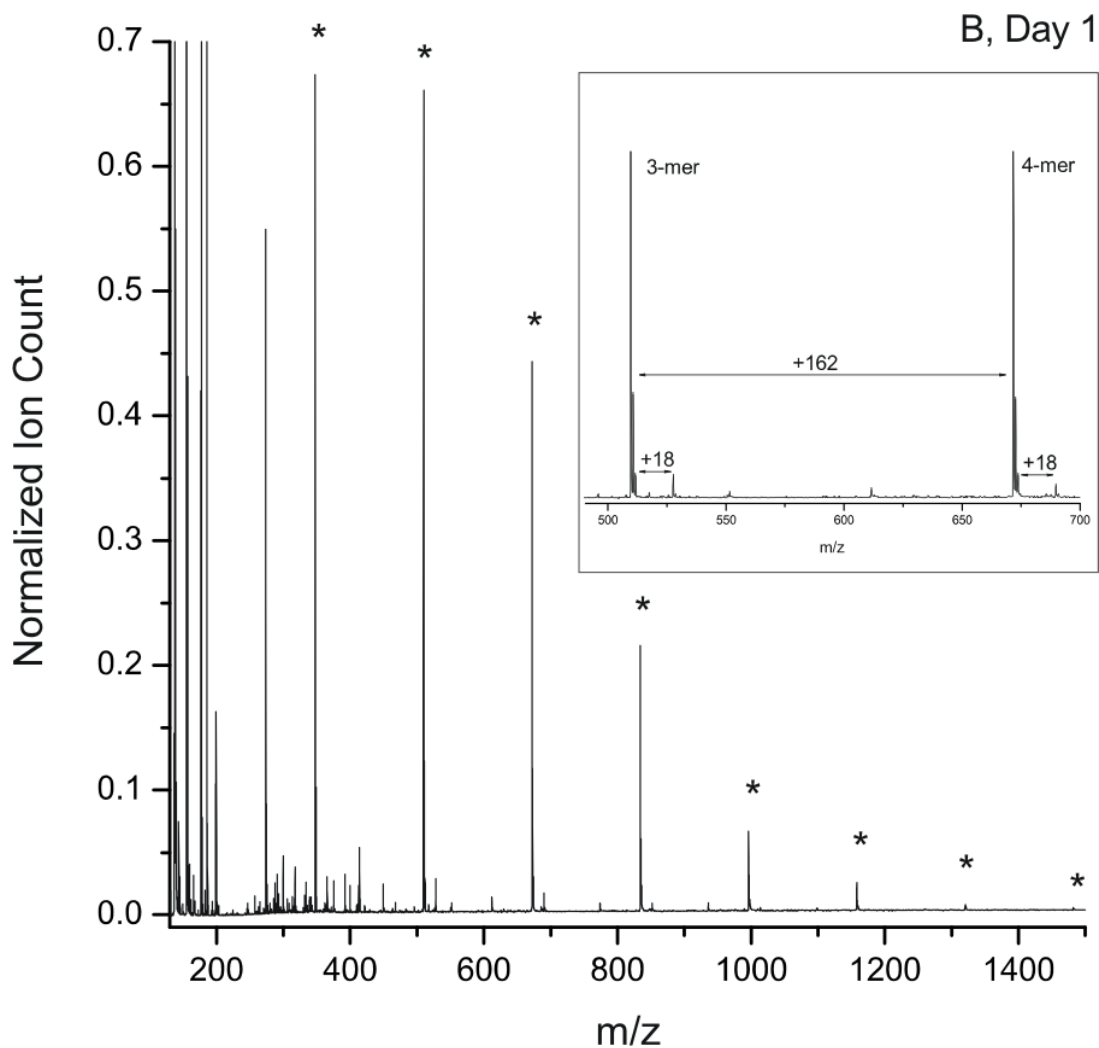


Figure 3-3 MALDI-TOF-MS of Reaction B (levoglucosan, H₂SO₄), day 1 using DHB/NaCl matrix in positive ion, reflectron mode. Spectrum is normalized to the 185 Da (levoglucosan + Na⁺) peak. (* - indicates relevant product peaks).

3.3.4. Potential Role of Iron in Reaction Systems

Reaction C was setup to better understand the potential role, if any, of iron in an acidic reaction system. For reactions B and C, ion signals were observed for all oligomer products (up to $x = 9$) throughout the duration of the reaction (i.e., 7 days).

Additionally, contrary to Reaction B, Reactions A and C produced an intractable white solid that appeared after a reaction time of 3 days. This fibrous solid was not soluble in a variety of common organic solvents (for example, ethyl acetate, methanol, dichloromethane, tetrahydrofuran and hexanes). We hypothesize that Fe^{3+} , which is present in Reactions A and C but not B, may be acting as a coagulant,⁸⁹ providing another mechanism for sequestration of organic carbon and loss of levoglucosan in our reaction systems. Analogous to our experimental systems involving Fe^{3+} , it is suggested here that Fe^{3+} is involved in the loss of organic carbon in aqueous atmospheric aerosols created from biomass burning. Although the experimental concentrations of iron were based on cloudwater measurements, significant amounts of iron have also been measured in newly-formed biomass burning aerosols.⁹⁰

3.3.5. Proposed Chemical Mechanism for Oligomers Pattern

In accord with the results reported above, a rational mechanism is proposed here, that results in the loss of levoglucosan from aqueous aerosols in the atmosphere and the prediction of two classes of oligomer products: (x-mer) and (x-mer+18). This proposed mechanism (Scheme 3-1) is in line with recently proposed acid-catalyzed processes shown to synthesize saccharide polymers from pyranose moieties⁹¹ and produce oligomers in secondary organic aerosols.⁸³⁻⁸⁵ In the proposed mechanism, any of the alcohol moieties of levoglucosan could act as nucleophiles, producing a range of product isomers. In fact, one predicted isomer, trehalose (MW = 342 u), has

been measured in biomass burning aerosol and was attributed to the biogenic source of the sugar;^{30, 92} however, it is possible that trehalose is also produced by compound III after further processing by reactions 1 and 2 (Figure 3-4). An ion signal was measured at 365 m/z for Reactions A, B and C, corresponding to the sodiated adduct ion of a product with the molecular weight of trehalose. In addition to nucleophilic attack by levoglucosan, water, which is in large excess, may also act as the nucleophile, hydrating levoglucosan to glucose.^{90,93-95} Addition of glucose, or conversion of levoglucosan by reactions 1 and 2 (Scheme 3-4) on the oligomer chain results in chemical products with weights 18 u greater than the x-mers (i.e., [x-mer + 18]⁺).

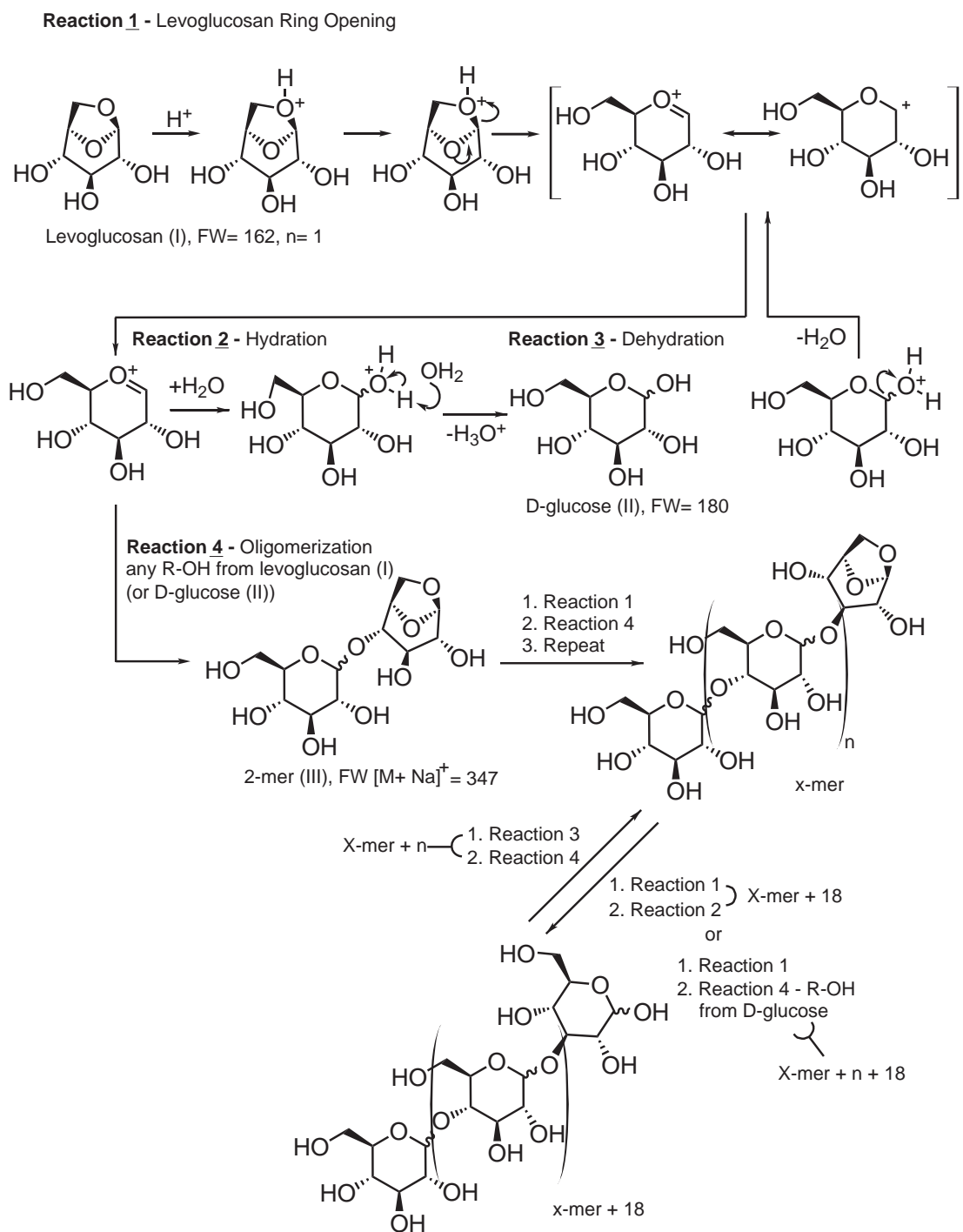


Figure 3-4 Proposed acid-catalyzed mechanism for the oligomerization of levoglucosan (I).

3.3.6. Oligomer Polydispersity and Reaction Kinetic Analysis

In both Reactions A and B, oligomerization was observed at the first measurement time point (0.5 days) for repeating mass units up to $x = 9$. The polydispersity (D) of these reaction products was calculated⁹⁶ to be between 1 and 2, indicating that they possess relatively narrow oligomer distributions. In all other aspects, the two chemical systems behaved differently. In Reaction A, simulating cloud water, the intensities of the $[x\text{-mer}]^+$ series peaks generally decreased with reaction time, to the point that very weak ion signals remained only for the $x = 2$ and 3 oligomers by day 7 (Figure 3-5).

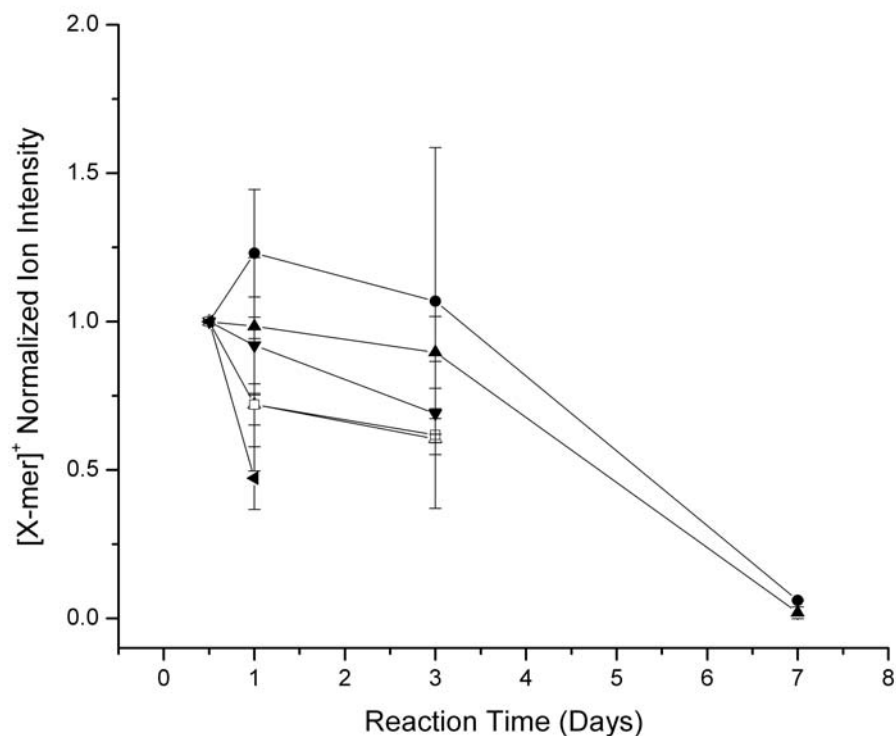


Figure 3-5 Mass peak intensity data normalized to day 0.5 for the $[x\text{-mer}]^+$ products for Reaction A. (●) 2-mer; (▲) 3-mer; (▼) 4-mer; (△) 5-mer; (□) 6-mer; (◄) 7-mer. Lines are drawn to aid the eye. Error bars represent 1 standard deviation on 1000 laser shots.

Analogous trends were observed for the $[x\text{-mer} + 18]^+$ products. The observed trends in the mass spectra are supported by both the number (M_n) and weight averaged (M_w) molar mass distributions for the $[x\text{-mer}]^+$ and $[x\text{-mer}+18]^+$ peaks from reaction A (Figures 3-6a,b). These values were calculated by standard methods.⁹⁶ Both plots show M_n and M_w following a similar trend between days 0.5 to 3. Beyond day three, these values for both plots decrease and converge, indicating the loss of

higher order oligomers for both the $[x\text{-mer}]^+$ and $[x\text{-mer}+18]^+$ peaks, which parallels the observations. Further, while the predominant oligomer formation pathway for Reaction A is proposed to proceed through an acid-catalyzed process, the decline of the water soluble oligomeric products (Figures 3-1,a-d) may be due to their consumption by reaction with Fenton reactants, such as the hydroxyl radical or hydrogen peroxide, leading to products that are relatively water-insoluble.

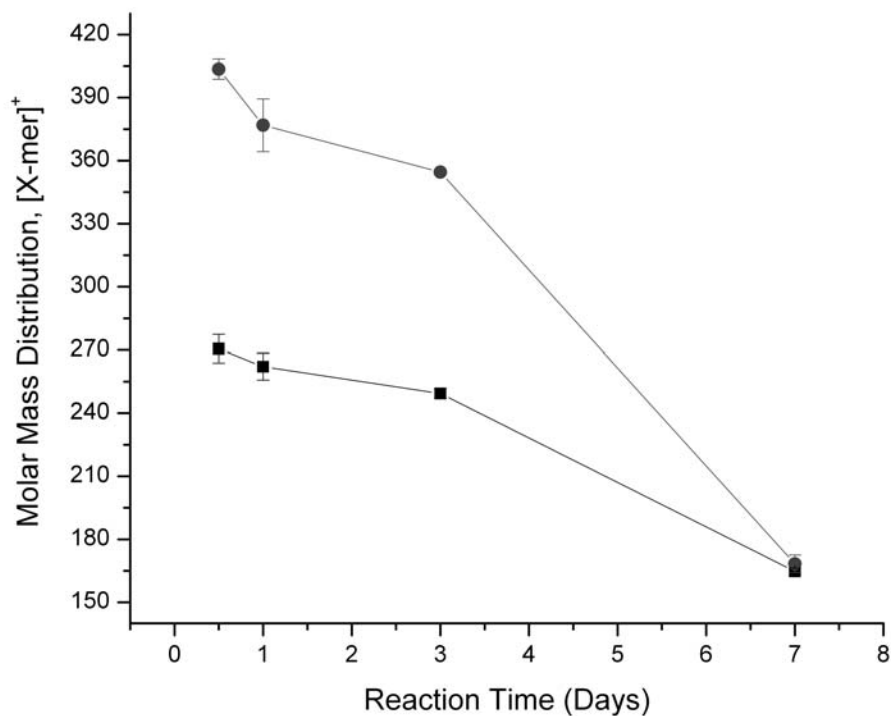


Figure 3-6a Number (Mn) and weight (Mw) averaged molar mass distributions for the $[x\text{-mer}]^+$ mass peaks from reaction A. (■) Mn, (●) Mw. Error bars represent 1 standard deviation on 1000 laser shots.

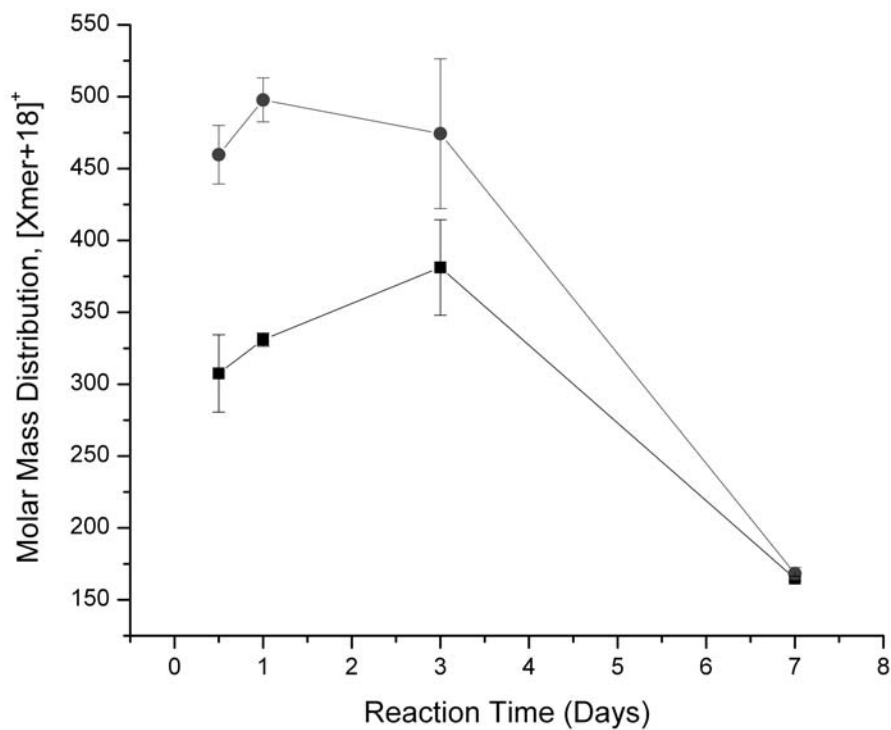


Figure 3-6b Number (Mn) and weight (Mw) averaged molar mass distributions for the $[x\text{-mer}+18]^+$ mass peaks from reaction A. (■) Mn, (●) Mw. Error bars represent 1 standard deviation on 1000 laser shots.

In reaction B, on the other hand, the relative intensities of the $[x\text{-mer}]^+$ series peaks increased initially on day 1 and then decreased by day 7 (Figure 3-7a). Also, the temporal increase of the $[x\text{-mer} + 18]^+$ series in Reaction B (Figure 3-7b) was different from Reaction A, where a general decrease in oligomer ion intensity was observed as a function of reaction time.

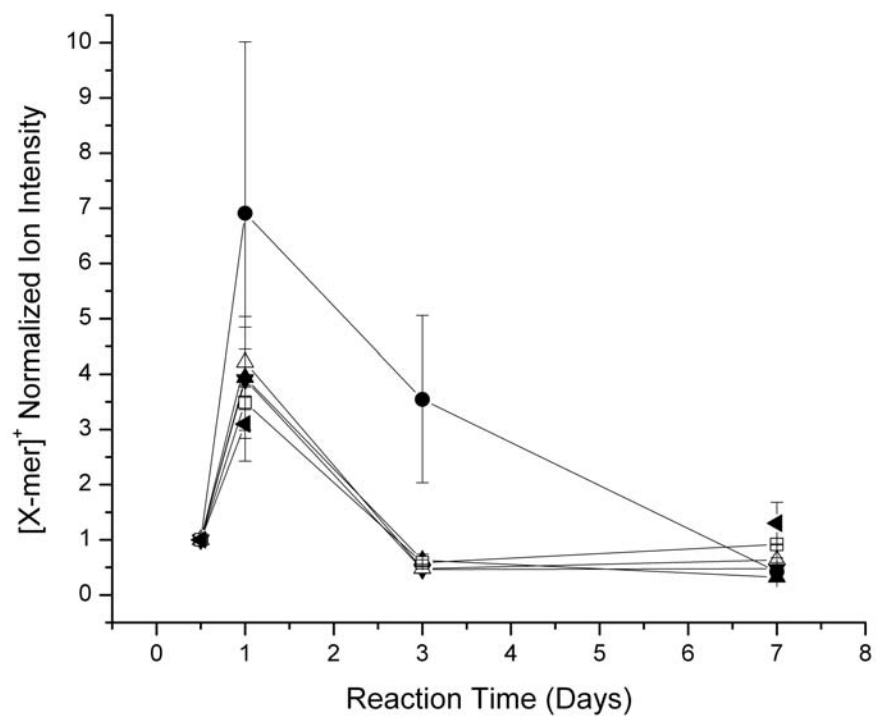


Figure 3-7a Mass peak intensity data normalized to day 0.5 for the $[x\text{-mer}]^+$ products for Reaction B. (■) 1-mer; (●) 2-mer; (▲) 3-mer; (▼) 4-mer; (△) 5-mer; (□) 6-mer, (◄) 7-mer. Lines are drawn to aid the eye. Error bars represent 1 standard deviation on 1000 laser shots.

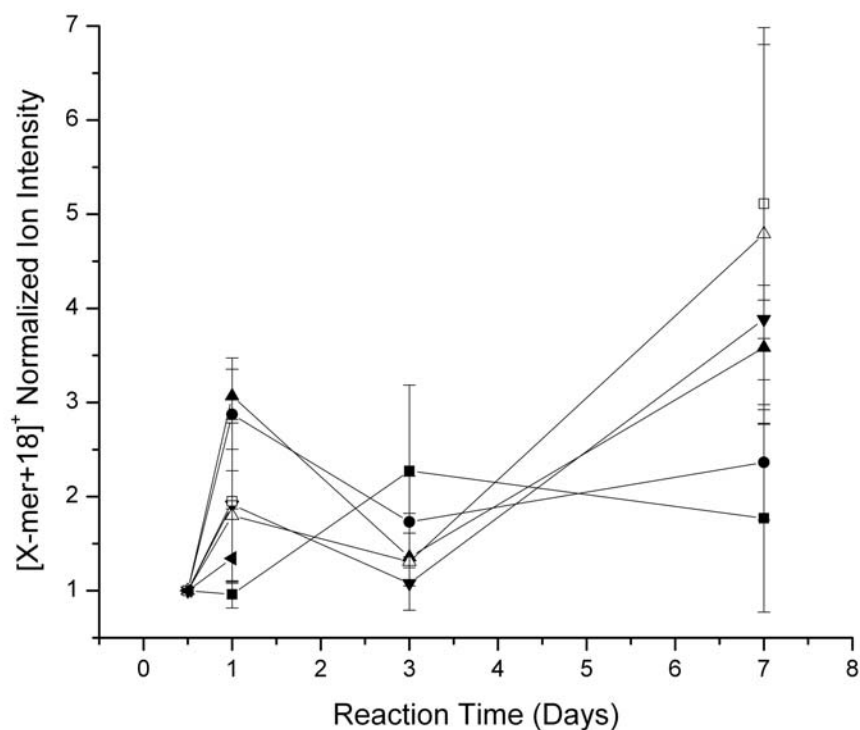


Figure 3-7b Mass peak intensity data normalized to day 0.5 for the $[x\text{-mer} + 18]^+$ products for Reaction B. (■)1-mer; (●) 2-mer; (▲) 3-mer; (▼) 4-mer; (△) 5-mer; (◻) 6-mer, (◄) 7-mer. Lines are drawn to aid the eye. Error bars represent 1 standard deviation on 1000 laser shots.

In Reaction B, the higher order (3-, 4-, 5-, 6-mer) ion signals for the $[x\text{-mer} + 18]^+$ series increased as a function of reaction time. Interestingly, contrary to Reaction A, both the $[x\text{-mer}]^+$ and $[x\text{-mer}+18]^+$ mass peaks showed an increase in their intensities for higher-order oligomers with time, which is supported by calculations of M_n and M_w values (Figures 3-8a, b). After day 3, an increase in M_w compared to M_n for both the $[x\text{-mer}]^+$ and $[x\text{-mer}+18]^+$ peaks support an increase in the importance of the

higher order oligomers for this time point. This trend is especially significant in the M_n and M_w plots for the $[x\text{-mer}]^+$ peaks (Figure 3-8a), where M_w increases considerably by day 7, whereas M_n decreases slightly. For Reaction B, two competing processes are proposed: (1) addition of a hydrated levoglucosan (i.e. glucose) to the oligomers and (2) nucleophilic attack by levoglucosan (reaction 4) at the carbocation created through the five-membered ring opening of oligomerized levoglucosan (reaction 1) to form the next higher order x-mer. We attribute the observed $[x\text{-mer}]^+$ and $[x\text{-mer}+18]^+$ peak trends to the possibility that, before day 0.5, nucleophilic attack by levoglucosan (reaction 4) at this carbocation to form the next higher order x-mer is a fast step compared to the reversible addition of water, which is in large excess, or addition of glucose to this same carbocation.⁹⁷ After day 0.5, the production rate of the higher order $[x\text{-mer}]^+$ peaks in reaction B decreased compared to the hydration of the oligomers ($[x\text{-mer} + 18]^+$). Acid-catalyzed reactions, such as the glycosidic ether bond formation discussed here, are known to be reversible processes.⁹⁷ An equilibrium process, such as is known for many acid catalyzed reactions, may explain the initial increase and subsequent decrease in production rate of the $[x\text{-mer}]^+$ compared to the $[x\text{-mer} + 18]^+$ peaks for Reaction B.

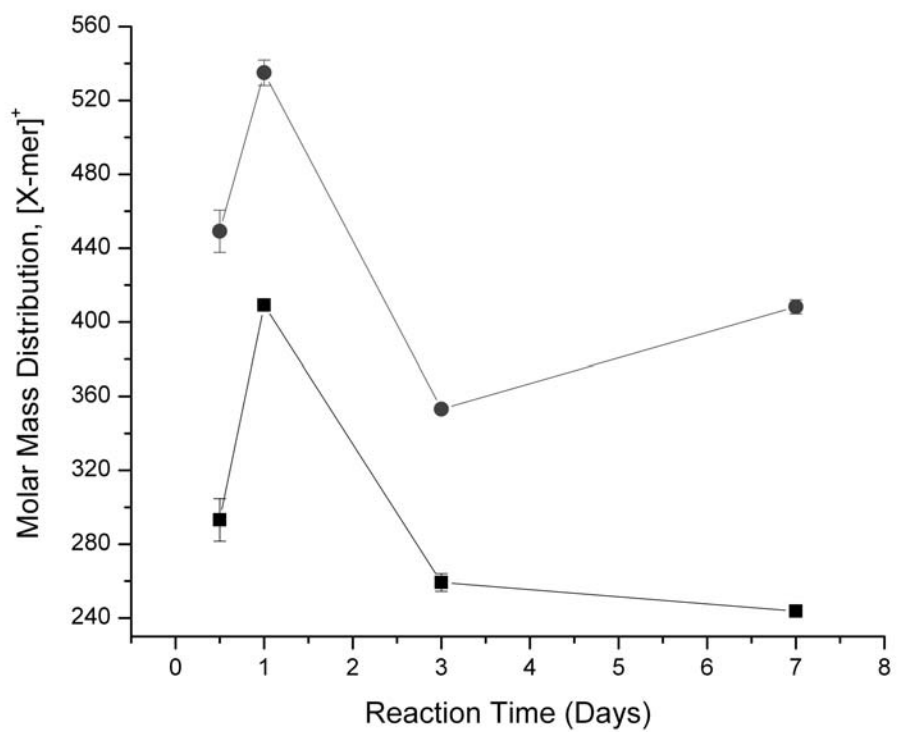


Figure 3-8a Number (Mn) and weight (Mw) averaged molar mass distributions for the [x-mer]⁺ mass peaks from Reaction B. (■) Mn, (●) Mw. Error bars represent 1 standard deviation on 1000 laser shots.

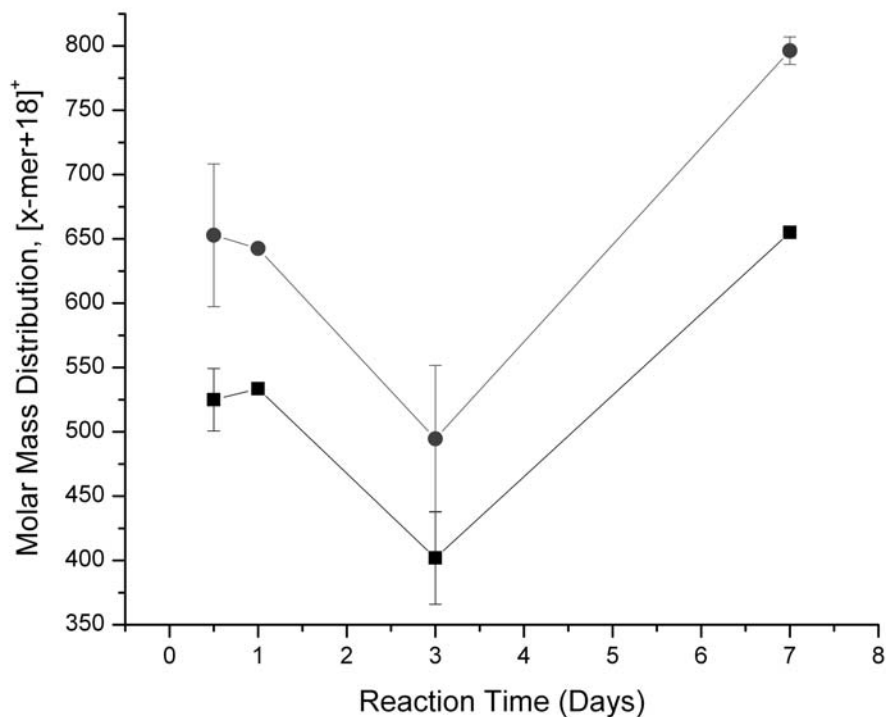


Figure 3-8b Number (Mn) and weight (Mw) averaged molar mass distributions for the $[x\text{-mer}+18]^+$ mass peaks from Reaction B. (■) Mn, (●) Mw. Error bars represent 1 standard deviation on 1000 laser shots.

3.3.7. ATR-FTIR Supporting Data for Saccharidic Oligomer Formation

The acid-catalyzed oligomerization of levoglucosan is further supported by the ATR-FTIR spectra of the lyophilized products from Reactions A and B (Figure 3-9), which showed broad peaks at $\sim 1710\text{-}1570\text{ cm}^{-1}$, possibly due to a bridging C-O-C functionality between saccharide units. An analogous spectral feature was observed for the reference compounds cellulose and α -cyclodextrin, which also contain the sugar-bridging C-O-C functionality, but not for unreacted levoglucosan and α -D-

glucose, which lack this functionality.

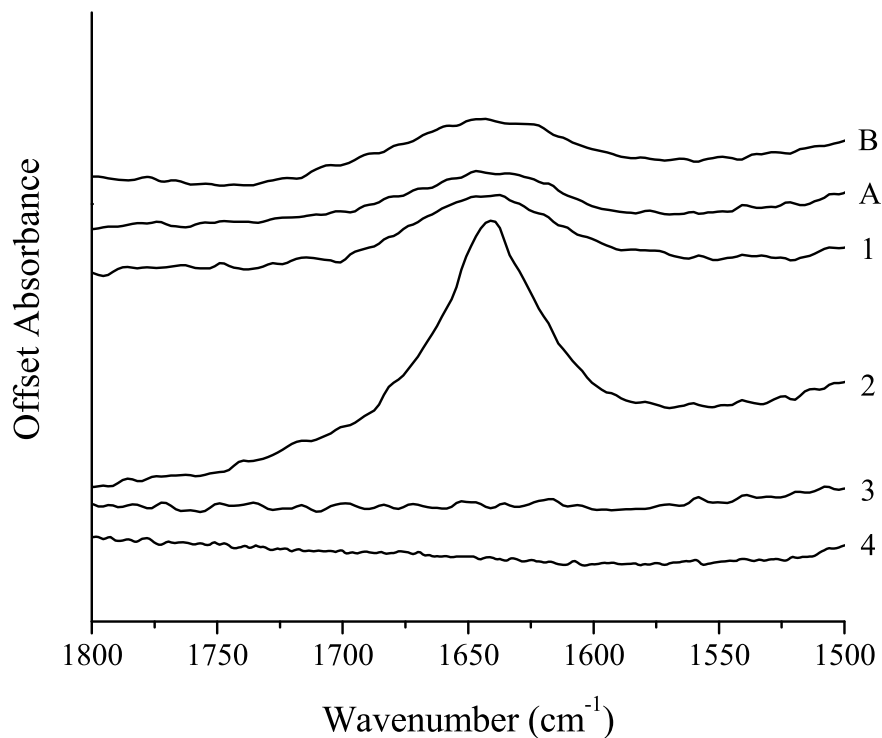


Figure 3-9 ATR-FTIR spectra of dry, lyophilized chemical products from (A) Reaction A and (B) Reaction B, in addition to the reference compounds (1) cellulose, (2) α -cyclodextrin, (3) levoglucosan and (4) α -D-glucose.

3.4. Conclusions

These laboratory experiments presented a simple model for the reactions of levoglucosan in bulk solutions using common chemical conditions found in cloudwater or aqueous aerosols. As in previous studies using proxies to study atmospheric chemical systems, it is expected that these bulk reactions in the laboratory mimic those occurring in the aerosol phase in the atmosphere (for

example, ref. 10). Clearly, in reality this relatively simple picture would be complicated by the complex mixture of organic and inorganic compounds found in atmospheric aerosols. By the mechanism (Figure 3-4) proposed here, the increase in the oligomer chain length by addition of levoglucosan depends on the condition that significant concentrations of this species are present compared to other potentially reactive species. Biomass burning aerosols, which are known to be hygroscopic, may satisfy this condition due to the high mass concentrations of levoglucosan often measured in these types of aerosols^{35,92}.

Water soluble oligomer concentrations in Reaction A were shown to decrease as a function of time (from 0.5 to 7 days), possibly as a result of reaction with the hydroxyl radical being produced through the Fenton reaction. Therefore, chemical processes such as acid-catalyzed polymerization and hydroxyl radical reactions could explain, in part, the absence of levoglucosan in analyzed aerosols known to originate from biomass burning. Based on the proposed mechanism, it follows that the products discussed here are highly polar, which would increase their ability to take on water. Support for their water-solubility has been through the experimental observation during the MALDI sample preparation. These reactions could have significant effects on the lifetime of these oligomer products, the water solubility of the aged aerosols, and the aerosols capacity as CCN.

Finally, the chemical products identified in this work may be useful as secondary tracers for measurements of the long-distance transport of biomass burning aerosols. A useful chemical tracer must have significant concentrations and be chemically

stable for the measurement time-period. It is proposed here that the high concentration of levoglucosan found in biomass burning aerosols may contribute to the potential of significant amounts of these oligomeric products existing as a stable component of biomass burning aerosols. The presence of these products in real atmospheric aerosols may allow their use as secondary tracers for biomass burning aerosol parcels. Such secondary chemical tracers are potentially important to advance our understanding of aerosol source, transport and processing in the atmosphere, which ultimately will add to the growing knowledge of how these types of aerosols affect global climate.

4. Oligomerization of Levoglucosan by Fenton Chemistry in Proxies of Biomass Burning Aerosols⁹⁸

4.1. Introduction

For this study, the chemistry of levoglucosan oxidized by *in-situ* derived $\cdot\text{OH}$, produced from an aqueous Fenton chemical system (Fe^{2+} , H_2O_2 , H^+), was investigated in bulk solution serving as a proxy for aqueous biomass burning aerosols. The primary focus of this investigation was to evaluate the importance of $\cdot\text{OH}$ -radical processing of anhydrosaccharides in the formation of HULIS in aqueous systems, as well as to identify specific chemical products that may provide information for both tracer⁵⁹ and cloud-condensation nucleation studies.⁹⁹ In this investigation, increasing the hydrogen peroxide concentration in the Fenton system relative to our previous acid-catalyzed oligomerization study⁸¹ enhanced $\cdot\text{OH}$ production. Chemical products were identified by matrix-assisted (MA) and matrix-free laser desorption-ionization (LDI) time-of-flight mass spectrometry (TOF-MS). Attenuated total reflectance (ATR) Fourier transform infrared (FTIR) spectroscopy was used to support our mass spectrometric results.

4.2. Experimental Design

4.2.1. Biomass Burning Aerosol Proxy Reactions

Reactions were run in aqueous solution containing levoglucosan (10^{-3} M) (99%, Alfa Aesar), hydrogen peroxide (10^{-3} M) (30% in water, Acros), anhydrous ferric chloride hexahydrate (5×10^{-6} M) (99%, Fisher), and sulfuric acid (96.1%, Mallinckrodt) (to bring the solution pH to 4.5). All reagents were used as supplied by the manufacturer. The concentration of hydrogen peroxide for this experiment was based on measurements from hydrated aerosols (e.g., cloudwater, fogwater).^{87, 100-103} Iron concentrations were used which correspond to model⁶⁵ and experimental⁸⁸ cloudwater studies although relevant amounts of iron are also found in aerosols.¹⁰⁴ Since biomass burning aerosols are known have a strong aqueous and sulfate component¹⁰⁵, the pH of a water solution was adjusted to 4.5 using sulfuric acid. This pH value was based on field measurements of hydrated aerosol.^{65, 106} In general, fine-mode aerosols are known to be acidic.⁷⁰

4.2.2. Sample Preparation and Analysis

Reactions, initiated by the addition of hydrogen peroxide, were performed on a one-liter scale in 18-MOhm water (Milli-Q, Model Gradient A10, TOC <5 ppb) at room temperature, unstirred and in the dark. Aliquots of 250.0 mL were sampled from each reaction on days 1, 3, and 7. These aliquots were frozen and lyophilized in preparation for mass spectral and ATR-FTIR analysis.

The reaction products, which are likely to have a high water-soluble character due to the sample preparation process, were measured with MALDI-TOF-MS and LDI-TOF-MS. The MALDI-TOF-MS sample preparation used a matrix of 10 mg/mL 2,5 dihydroxybenzoic acid (DHB, 99%, Alfa Aesar) in water and either 1 mg/mL sodium chloride or 2 mg/mL lithium chloride as the cationizing agent. About 1 μg of the dried products of the lyophilized samples were redissolved in 2 μL of deionized water and 2 μL of this solution was combined with 8 μL of the matrix and cationizing agent. Matrix/analyte dilutions of 1x, 10x, and 100x, were used. The 10x dilution gave the highest quality mass spectrometric data. A 10x dilution corresponds to a mass concentration of about 0.05 g/L and a total mass of 1×10^{-6} grams spotted on the MALDI sample plate. Aliquots of 1 μL were spotted on a standard stainless steel MALDI sample plate (Applied Biosystems) and the chemical components co-crystallized by drying in a vacuum desiccator. Positive ion MALDI-TOF-MS was performed in reflectron mode with a 337 nm laser source (Applied Biosystems Voyager-DE Pro). The ion signal was optimized by rastering the laser around the sample spot while monitoring the ion signal.

LDI-TOF-MS was performed with the same instrument, using a carbon powder substrate. For these measurements, carbon powder was produced from solid graphite (Ultra Carbon Corporation, ultra "F" purity) using a mortar and pestle. The carbon powder was suspended in water and ~ 5 μL of this suspension was spotted onto a stainless steel MALDI plate and dried in a vacuum desiccator to produce an even coat of dry carbon powder. Dried analyte samples were redissolved in 2 μL of a solution

of 1mg/mL sodium chloride in water and spotted on top of the dried carbon and redried in a vacuum desiccator. In all cases, the reported mass spectra represent the average of 1000 laser shots. ATR-FTIR spectra of dry lyophilized reaction products were measured using a Thermo-Nicolet IR200 Series spectrometer using 4 cm⁻¹ resolution and 32 scans.

4.3. Results and Discussion

4.3.1. •OH Production by the Fenton Reaction

This work builds on our previous investigation of the water soluble products formed from the acid-catalyzed oligomerization of levoglucosan in this same Fenton system.⁸¹ Re-analysis of the MALDI-TOF mass spectra using Na⁺ cationization presented in this preceding study revealed mass peaks that implied •OH saccharide chemistry, where the OH• were generated *in-situ* from the Fenton reaction. For this study, MALDI-TOF-MS using both sodium and lithium, individually, for cationization of the analyte were used as the primary analysis method. Supporting information was provided by LDI-TOF-MS using sodium cationization and ATR-FTIR.

It has been shown that under polluted air conditions about 80% of the OH• flux for aqueous aerosols comes from the gas phase.⁶⁵ Also, it is known that Fenton-type reactions within aqueous aerosols produce a significant amount of •OH.^{65, 107} In the absence of the dominant gas-phase sources of •OH, the experimental conditions used

in our previous study, we believe, represent a low-end limit for the $\cdot\text{OH}$ flux within the aerosol proxy system. Therefore, the formal concentration of hydrogen peroxide in this study was increased an order of magnitude to 1×10^{-3} M in order to enhance *in-situ* production of the $\cdot\text{OH}$ within the levoglucosan reaction system. Although the Fenton system was used as a source of $\cdot\text{OH}$ in these studies, there are many other sources of $\cdot\text{OH}$, both from the gas- and aerosol-phases that are reactive within a biomass burning aerosol. The experimental conditions used here are designed to produce a flux of $\cdot\text{OH}$ within a reasonable environmentally relevant range to allow observation of fundamental chemical processes using the available analytical instrumentation.

4.3.2. $\cdot\text{OH}$ Reactions of Levoglucosan

MALDI-TOF mass spectra of the reaction products of levoglucosan (Cmpd I, 4-3) in a Fenton chemical system were measured after reaction times of 1, 3, and 7 days. The spectra (Figures 4-1a-c) show oligomerization of levoglucosan to form water-soluble products, with masses for the single- mass unit continuum distribution occurring up to ~ 2000 u on day 3 (Figure 4-1b, full mass signal scale not shown). All mass spectra have been normalized to the sodiated ($[\text{M}+\text{Na}]^+$, 185 u) (Figures 4-1a-c) or, when applicable, the lithiated ($[\text{M}+\text{Li}]^+$, 169 u) levoglucosan ion signal. For day 1, the single-mass unit continuum mass distribution shows comparatively low relative ion intensity, ending ~ 500 u (Figure 4-1a).

The MALDI-TOF mass spectrum of day 3 products (Figure 4-1b) exhibits a distinct, relatively higher ion intensity single-mass unit continuum mass distribution compared to day 1. For day 3, a periodic spacing of 162 u, the molecular weight of levoglucosan, implies a chemical model involving incorporation of this saccharide in the HULIS structure. On day 7, the continuum mass series appears less periodic than on day 3 and ends ~1200 u (Figure 4-1c). The continuum of single-mass unit ion signals seen for all sampled time points is consistent with a $\bullet\text{OH}$ mechanism, highlighting its strong oxidizing capacity coupled with its known unselective hydrogen abstraction from organic substrates.^{82, 108}

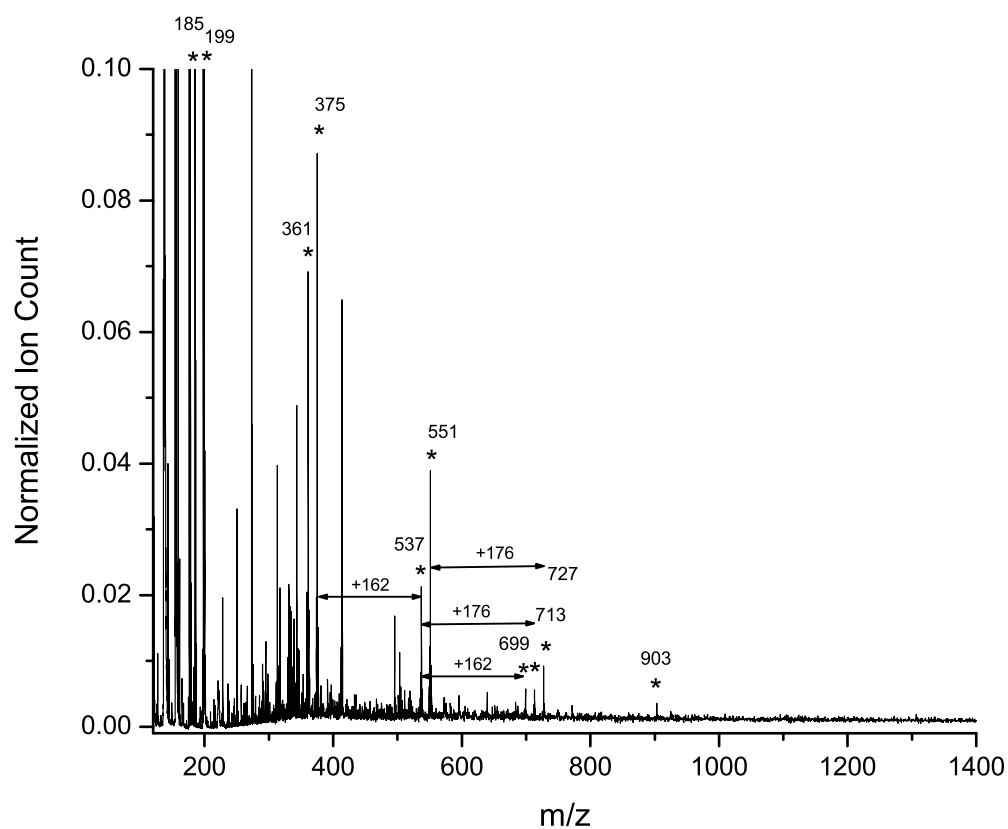


Figure 4-1a MALDI-TOF mass spectra of the sodiated products from the reaction of levoglucosan in the Fenton system; day 1, 1×10^{-3} M H_2O_2 using DHB/NaCl matrix in positive ion, reflectron mode. Spectrum is normalized to the 185 u (levoglucosan + Na^+) ion peak. (* - indicates emphasized oligomer mass peak pattern)

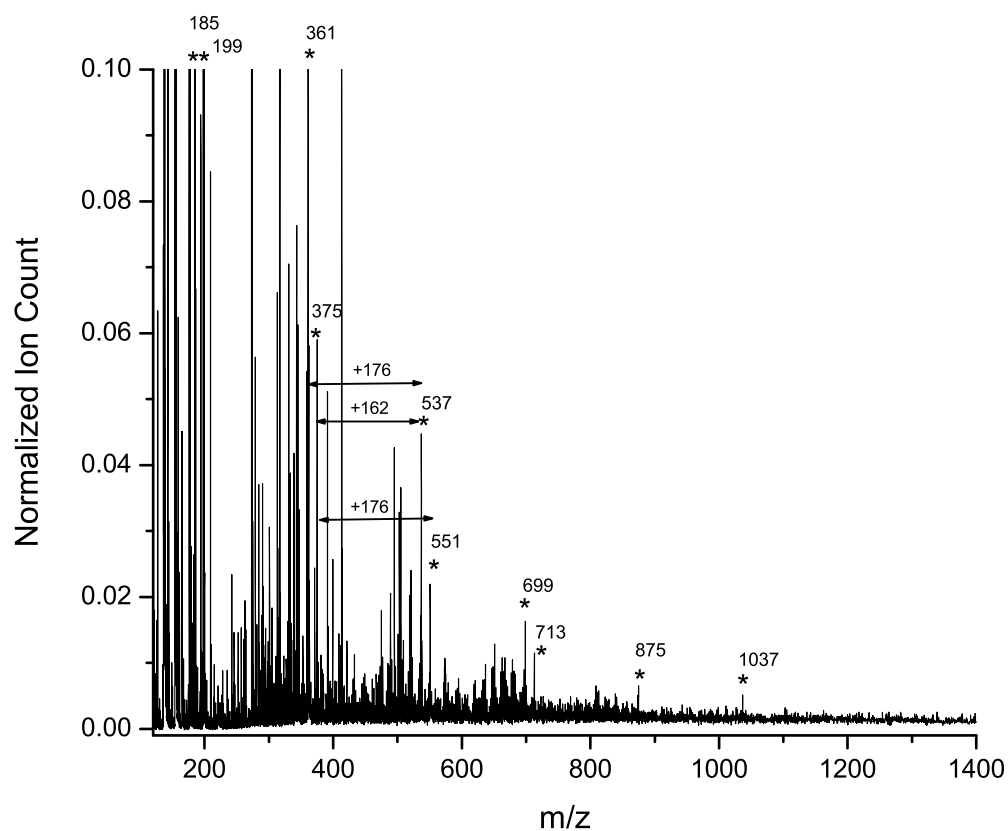


Figure 4-1b MALDI-TOF mass spectra of the sodiated products from the reaction of levoglucosan in the Fenton system; day 3, 1×10^{-3} M H_2O_2 using DHB/NaCl matrix in positive ion, reflectron mode. Spectrum is normalized to the 185 u (levoglucosan + Na^+) ion peak. (* - indicates emphasized oligomer mass peak pattern)

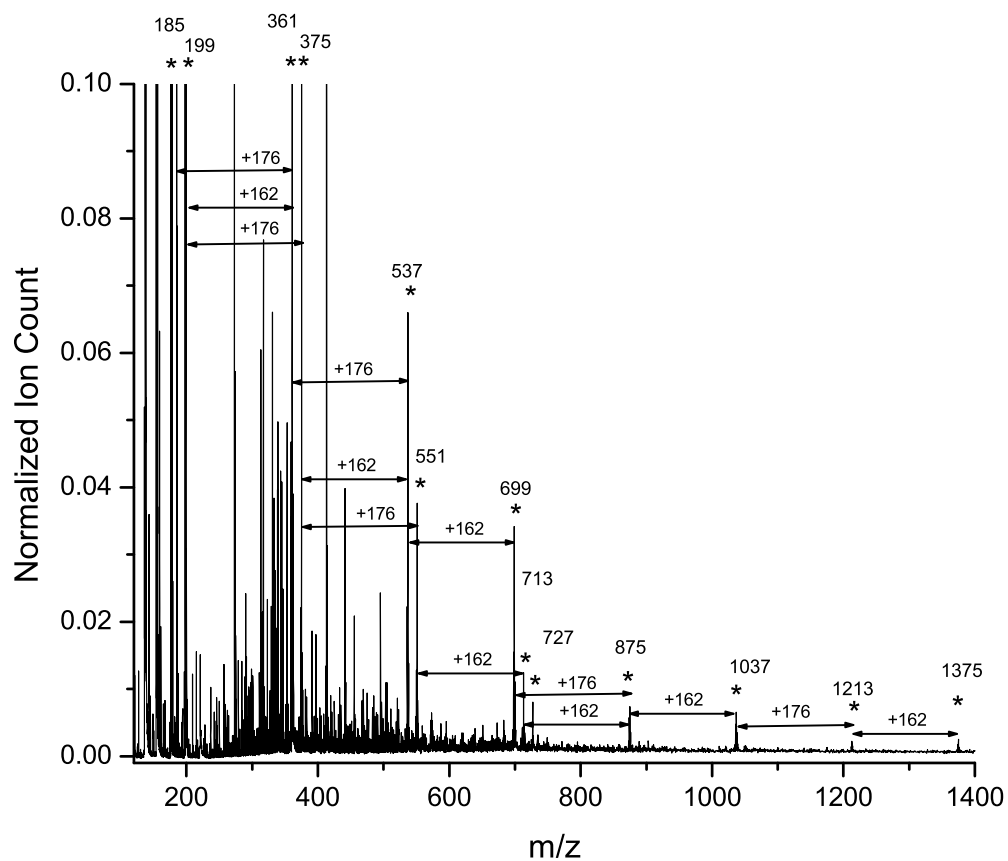


Figure 4-1c MALDI-TOF mass spectra of the sodiated products from the reaction of levoglucosan in the Fenton system; day 7, 1×10^{-3} M H_2O_2 using DHB/NaCl matrix in positive ion, reflectron mode. Spectrum is normalized to the 185 u (levoglucosan + Na^+) ion peak. (* - indicates emphasized oligomer mass peak pattern)

The LDI-TOF mass spectrum of the day 3 products (Figure 4-2) is much simpler than that recorded using MALDI-TOF-MS. Most notable, are the sodiated mass clusters observed in the regions 343-365 u and 503-509 u (Figure 4-2). In the mass

range 343-365 u, the first cluster is between 343-347 u, with the dominant ion peaks separated by 2 u. The second cluster in this region is observed at 357-365 u. In our previous study, the mass 347 u (Cmpd Ia, Figure 4-3) was assigned to the sodiated adduct of the acid-catalyzed levoglucosan dimer.⁸¹ The loss of 2 u in this Fenton system from 347 u to form a product with the mass 345 u is consistent with hydrogen abstraction by $\cdot\text{OH}$ on any alcoholic carbon of either levoglucosan or its dimer to produce a carbon-centered radical. Further reaction of this radical with oxygen will produce a peroxy radical in aqueous solution,¹⁰⁹ which can decompose to form a ketone (glucosone) (Cmpd Ib, Figure 4-3) with loss of a hydroperoxy radical.

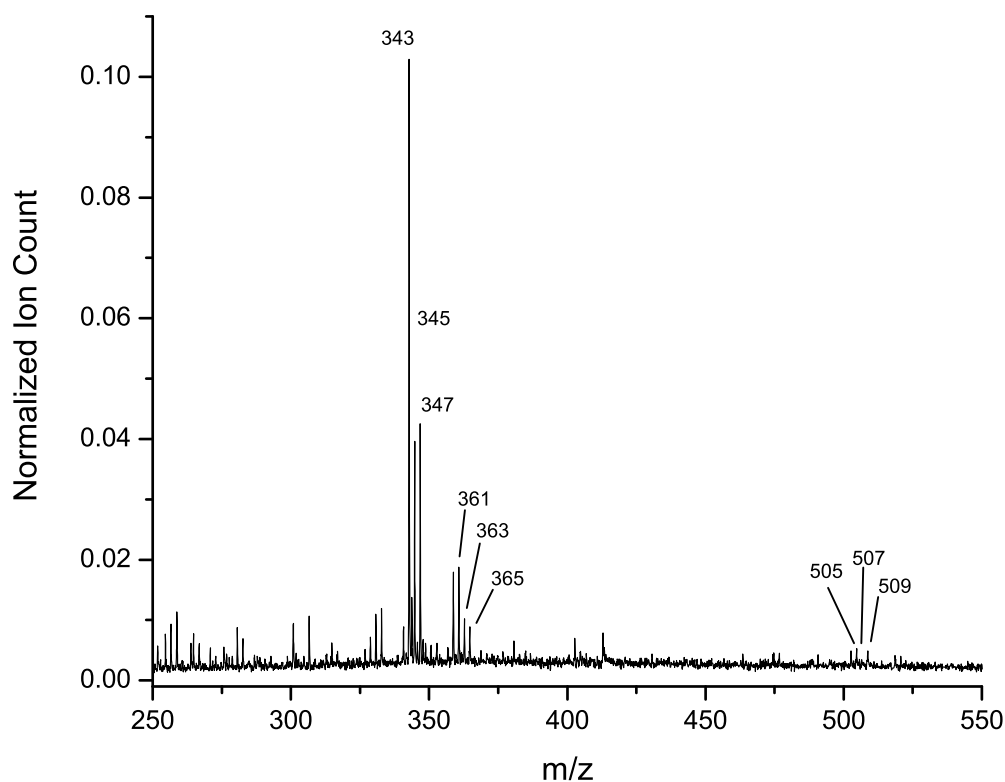


Figure 4-2 LDI-TOF mass spectra of the sodiated products from the reaction of levoglucosan in the Fenton system; day 3, using DHB/NaCl matrix in positive ion, reflectron mode. The spectrum is normalized to the 185 u (levoglucosan + Na⁺) ion peak.

This chemistry, which uses glucose, has been previously observed for saccharides under similar Fenton conditions.¹¹⁰ A glucosone-forming mechanism is proposed based on the reaction of this acid-catalyzed dimer (Cmpd Ia, Figure 4-3). The same mechanism can be applied to the 361-365 u mass cluster, where 365 u corresponds to the sodiated acid-catalyzed hydrated dimer (+18 u) observed previously.⁸¹

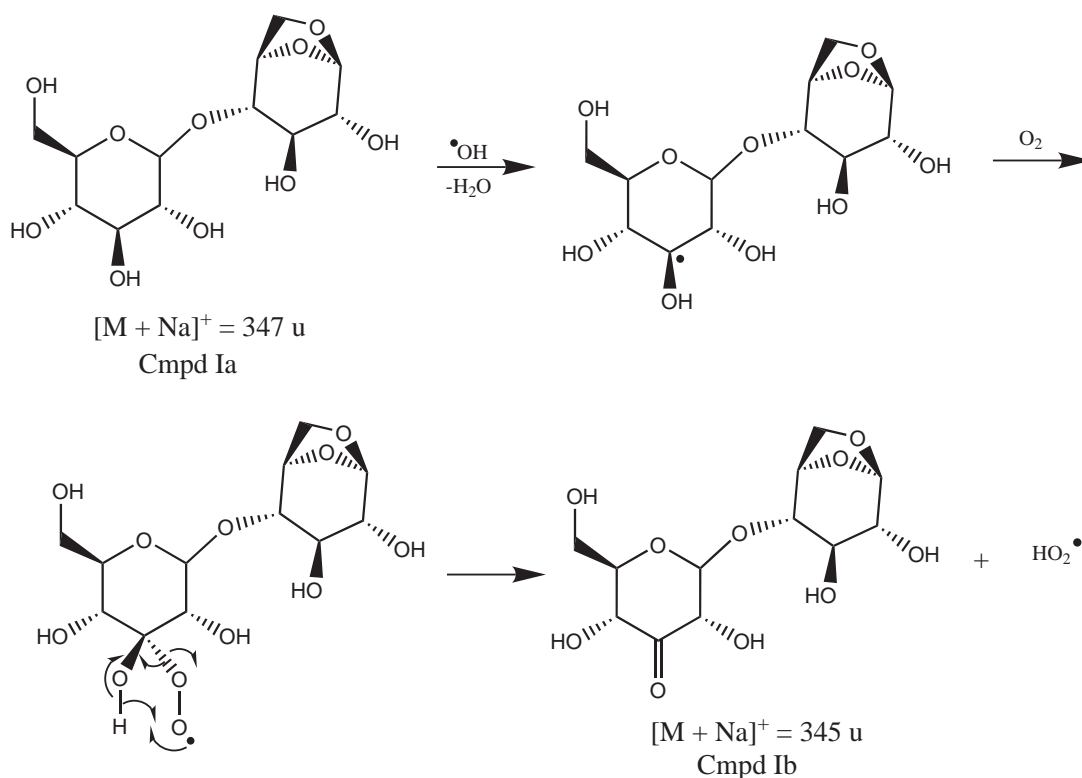


Figure 4-3 Proposed mechanism for the formation of a glucosone by reaction of a disaccharide with $\cdot\text{OH}$.

Alternatively, Criegee rearrangement of a hydroperoxide formed on the carbon-centered radicals described above can cause a ring expansion with creation of a lactone,^{111, 112} increasing the mass by 14 u (e.g., 347 u + 14 u = 361 u, Figure 4-2). This process is discussed further below (Figure 4-4). The mass range 503-509 u can be rationalized analogously based on the glucosone and Criegee chemistry acting on the acid-catalyzed trimer of levoglucosan⁸¹ (i.e. $[M + Na]^+ = 509 \text{ u}$). These same mass clusters are also observed with significant relative ion signal intensity within the continuum mass distribution of the MALDI-TOF mass spectra for all time points, albeit on a more complex mass spectral baseline. Oligomerization up to the 3-mer, 5-

mer, and 5-mer on days 1, 3, and 7, respectively, was observed by MALDI-TOF-MS. Background reactions (not shown) containing all reagents except hydrogen peroxide as a Fenton-initiator, did not show a significant background for the single-mass unit continuum products. Also, these levoglucosan solutions have been previously tested⁸¹ with individual and combinations of the reagents used and did not show an appreciable background. Further, for this study, a test was performed for reaction of levoglucosan with H₂O₂ at pH = 4.5 which also did not show a background interference.

4.3.3. Oligomerization Mass Patterns: MALDI-TOF-MS

Overlaid on the MALDI-TOF single-mass unit continuum mass distribution are higher intensity ion signals of two oligomeric series with repeating units of either +162 u (levoglucosan (Cmpd I)) or +176 u originating from the base peaks 185 u (levoglucosan + Na⁺) and 199 u (Cmpd II, Figure 4-4, [176 + Na]⁺) (Figures 4-1a-c). On days 1, 3, and 7, these series terminate at 903 u, 1037 u, and 1375 u, respectively. The formation of the 199 u ([176 + Na]⁺, Cmpd II) ion signal can be rationalized by reaction of levoglucosan through a [•]OH-initiated Criegee rearrangement (Figure 4-4), to form the lactone with ring expansion (i.e., 2,5-Dihydroxy-3,8,9-trioxabicyclo[4.2.1]nonan-4-one). This chemistry has been previously observed for saccharides and polysaccharides in a Fenton system and has been adapted here for levoglucosan.^{111, 112}

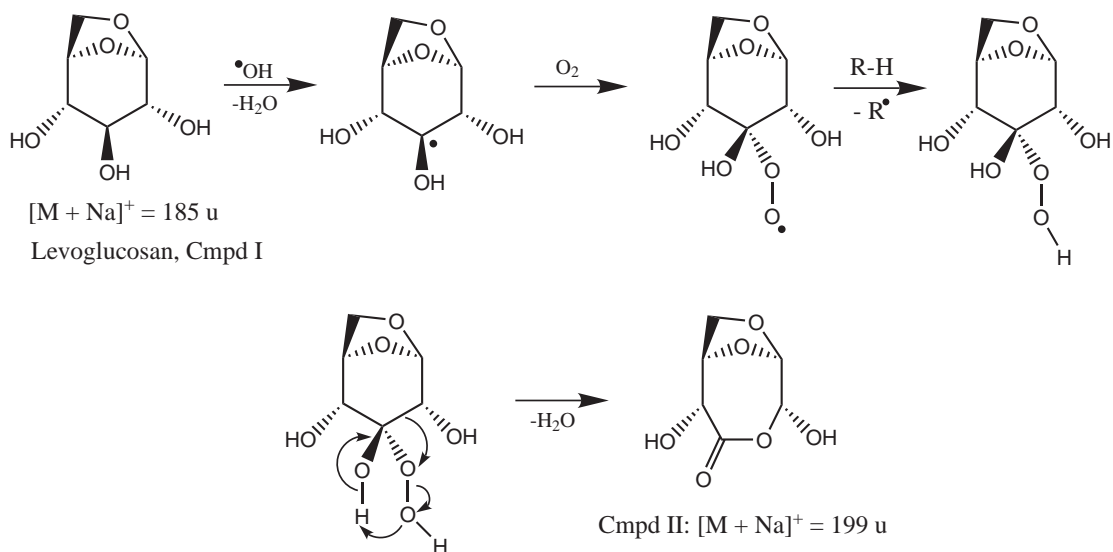


Figure 4-4 Proposed mechanism for the formation of a ring-expanded lactone from levoglucosan (Cmpd II) by hydroperoxyl formation initiated by $\cdot\text{OH}$ followed by a Criegee rearrangement.

Oligomerization of the lactone product (Cmpd II) is then hypothesized to proceed via an acid-catalyzed transesterification reaction with any ROH, likely from levoglucosan or compound II, to produce compounds IIIa and IIIb (Figure 4-5).

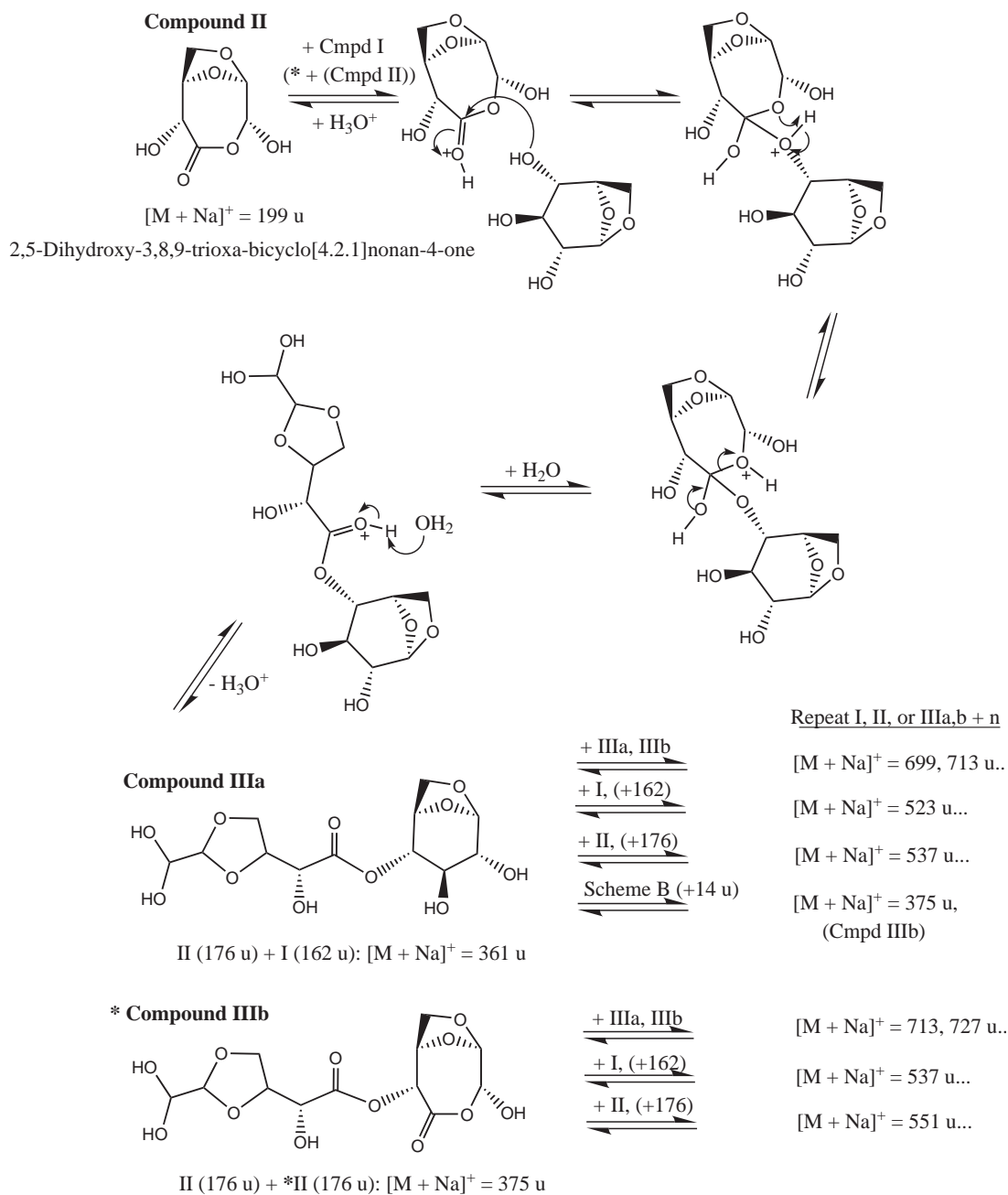


Figure 4-5 Proposed mechanism for the formation of ester-containing oligomeric products from the Fenton system through the acid-catalyzed transesterification reactions of levoglucosan and the monomeric Criegee lactone product (Cmpd II, Scheme 3-2).

If levoglucosan initially adds to compound II to produce compound IIIa, further reaction of this oligomerized levoglucosan moiety by the Criegee route (Figure 4-4) will produce compound IIIb (Figure 4-5). Also possible is addition of levoglucosan to IIIa via acid-catalyzed cationic ring-opening⁸¹ to produce an increase in mass of +162 u. Compound IIIb can be formed directly by homo-dimerization of compound II. In the cases where nucleophilic ROH attack occurs through transesterification at the lactone site in compound II or a higher-order oligomeric aliphatic ester, a propagating mechanism may begin, leading to the formation of polyesters (e.g., Cmpd IIIb).

4.3.4. MALDI-TOF-MS Matrix Background

The combination of DHB matrix and sodium cationization agent was selected because of its sensitivity to oligosaccharides and lower molecular weight analytes (<10,000 u).⁷⁶ However, when sampling only the DHB/NaCl matrix background, ion signals are observed at 199, 375, 551, and 727 u, which are all separated by 176 u (i.e., [DHB - H + Na]⁺). The ion peaks 176 and 177 u (i.e., [DHB + Na]⁺) are also observed in this background spectra. It should be noted that the formation of inclusion products of gas-phase matrix DHB species and analyte has been observed previously,^{75, 113} and potentially results in an overestimation of the molecular weight of the oligomer distributions. Such background inclusion products may confound identification of the proposed products since, for the transesterification process described above, the formation of a ring-expanded lactone from levoglucosan (Cmpd II, Figure 4-3), is the key species that allows this chemistry to propagate, appearing at

199 u. The background mass peak series (i.e. 199, 375, 551 u...) could then pose a direct interference with the proposed transesterification process where production of the sodiated lactone (199 u) would be followed by a propagating reaction with ROH from this same lactone product to produce a product series (+176 u) starting with the 2-mer (199 u + 176 u = 375 u). Another possible solution-phase process where the matrix background may interfere arises from Fenton chemistry where reaction of a transesterified levoglucosan (Cmpd IIIa, Figure 4-5) reacts with an $\cdot\text{OH}$ through the Criegee route (Figure 4-4) adding +14 u to generate compound II. Such a process would create a product with a mass of 375 u, identical to one of the possible DHB inclusion products. The production of the next higher order Fenton product which overlaps the 551 u matrix interference product proceeds by further oligomerization of the 375 u product with levoglucosan through transesterification followed by the Criegee rearrangement (375 u + 162 u + 14 u = 551 u).

4.3.5. Studies Supporting Solution-Phase Chemistry

The normalized ion signal for the non-background sodiated 537 u mass peak (Figures 4-1a-c) may arise either from inclusion of levoglucosan with the 375 u matrix background species and/or reaction through the Criegee/transesterification reactions of levoglucosan (Figures 4-4 and 4-5). In order to elucidate the extent of the Fenton/levoglucosan chemical system compared with the matrix interference, the relative ion counts for this 537 u mass peak were measured for the following aqueous levoglucosan experiments: 1) acid-catalyzed (Reaction C),⁸¹ 2) Fenton using 1×10^{-4}

M H₂O₂ (Reaction A),⁸¹ and 3) Fenton using 1x10⁻³ M H₂O₂ (this study). The MALDI-TOF mass spectra for the 537 u normalized ion signal for each sampled time point are not significantly different for both reactions C and A,⁸¹ when compared to the data using 1x10⁻³ M H₂O₂ in this study. The results from the H₂O₂ concentration used in this study showed a ten-fold increase in the normalized ion count compared to reactions C and A (Figure 4-6). Under the higher H₂O₂ concentrations used in this study, from day 1 to 7, the normalized ion count for the 537 u ion signal increases by a factor of three (Figure 4-7). These results suggest that chemical reactions in solution, as opposed to ionization artifacts, are responsible for the increase in the 537 u product. One would expect little change if the signal originated from inclusion of matrix species with levoglucosan because the same sample preparation process was used for all experiments.

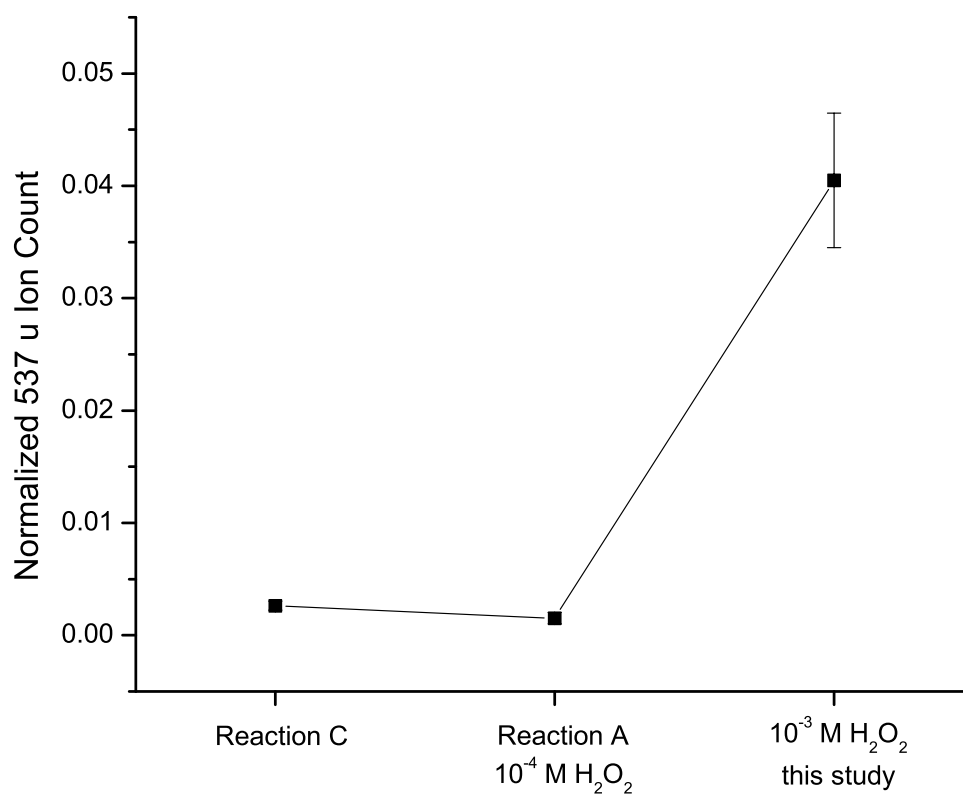


Figure 4-6 Comparison of the normalized 537 u mass peak ion signal. Error bars represent 1 standard deviation on 3000 laser shots (n=3).

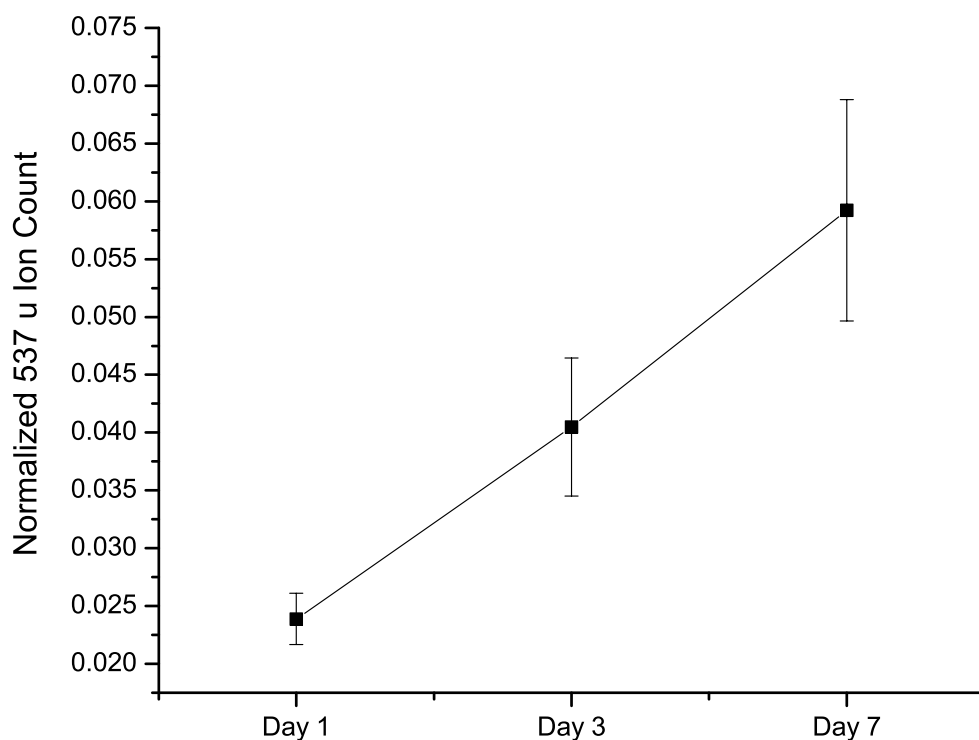


Figure 4-7 Comparison of the normalized 537 u ion signal for days 1, 3, and 7 using 10^{-3} M H_2O_2 . Error bars represent 1 standard deviation on 3000 laser shots ($n=3$).

Further support for the carbonyl-containing functionalities such as ketones, lactones, and esters discussed in this study is provided in the ATR-FTIR absorbance spectra of dried products. A carbonyl band ($\sim 1850\text{-}1650\text{ cm}^{-1}$) is visible and centered at $\sim 1740\text{ cm}^{-1}$, which is specifically indicative of ester and lactone functionalities¹¹⁴ (Figure 4-8). This band is not seen in the ATR-FTIR background spectrum of the dried products of the background solutions lacking the H_2O_2 initiator (Figure 4-8).

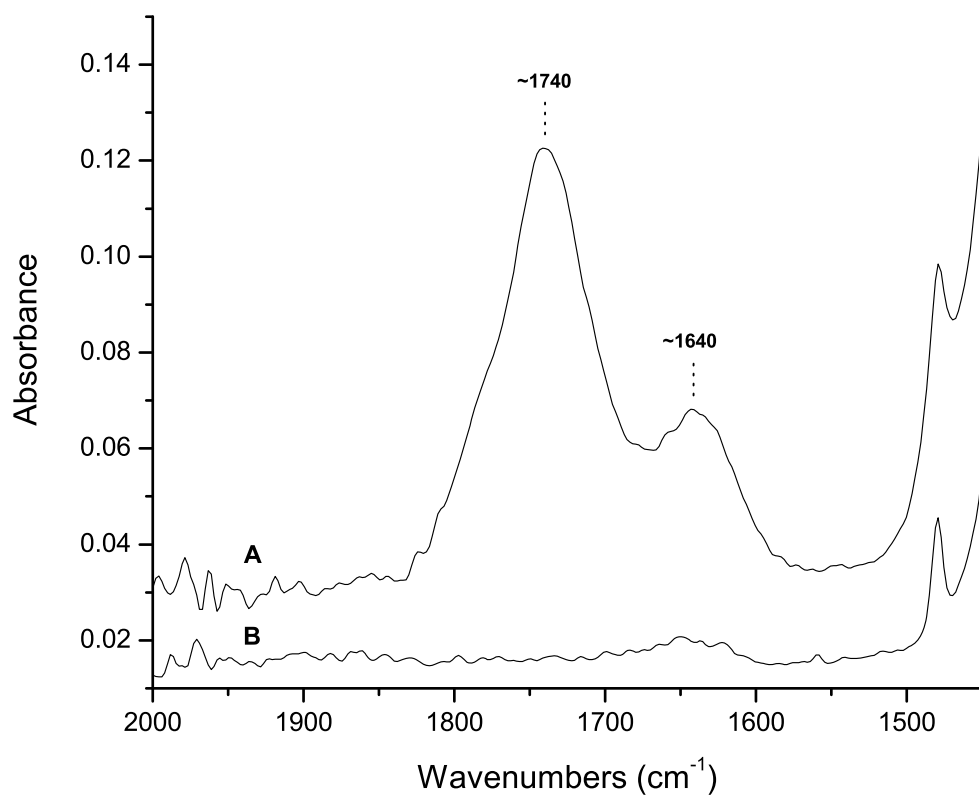


Figure 4-8 ATR-FTIR of the lyophilized, dried products of (A) the Fenton reaction of levoglucosan (10^{-3} M H_2O_2), day 3 and (B) the aqueous reaction of levoglucosan, H_2SO_4 , and Fe^{3+} in the absence of H_2O_2 on day 3.

4.3.6. MALDI-TOF-MS: Lithium Cationization

To minimize any potential artifact or interfering ion signals in the mass spectral data, various combinations of alternative chemical matrices and alkali salts (Na^+ , K^+ , Li^+) were used in the MALDI sample preparation. The use of Li as the cationizing agent with DHB matrix removes the previously discussed $[\text{DHB} - \text{H} + \text{Na}]^+$ (176 u)

interfering matrix species (Figures 4-1a-c) and has been used successfully for the efficient ionization of polyethers.¹¹⁵ Using this matrix solution, the MALDI-TOF mass spectrum of the Fenton reaction for day 7 (Figure 4-9) shows the predominant interfering matrix species as 137 u ($[\text{DHB} + \text{H} - \text{H}_2\text{O}]^+$), 160 u ($[\text{DHB} - \text{H} + \text{Li}]^+$), and 161 u ($[\text{DHB} + \text{Li}]^+$). Also seen in the analyte spectrum for day 7 is a polymer distribution repeating up to ~ 1000 u (Figure 4-9), with a distinct periodicity of 162 u (i.e., levoglucosan). A relatively simple mass spectrum is observed on day 7 using the DHB/LiCl matrix compared to the day 7 mass spectrum using the DHB/NaCl matrix (Figure 4-1c). Closer examination of each period, especially for the lower masses, reveals multiplet patterns where the mass differences are in the range of 12-16 u (Figure 4-9).

Of critical importance, is identification of the 176 u ($+ \text{Li}^+ = 183$ u) mass peak corresponding to the ring-expanded lactone (Cmpd II), which does not, in this lithiated case, have matrix or levoglucosan/matrix (Figure 4-9) background interferences. This later background test is discussed below. Application of Figure 4-5 to these MALDI-TOF mass patterns for both the sodiated and lithiated spectra shows the oligomerization of compound II with levoglucosan to form compound IIIa, which possesses the lithiated mass 345 u ($+ \text{Na}^+ = 361$ u) and overlaps the proposed first glucosone formed from the acid-catalyzed levoglucosan dimer described above (Figure 4-3). Further reaction with levoglucosan through transesterification yields the observed lithiated mass 507 u ($+ \text{Na}^+ = 523$ u). Also, the formation of compound IIIb from IIIa ($+ \text{Li}^+ = 345$ u, $+ \text{Na}^+ = 361$ u) (Figure 4-5) is measured by observation of

the lithiated 359 u mass peak. The alternating +176/+162 u mass series starting from both the lithiated levoglucosan (169 u) and compound II (183 u) base peaks increase in oligomer order until 535 u (Figure 4-9). Often, the +176/+162 u mass patterns fall next to a more intense mass peak, usually 2 u lower. This mass diversity may arise from the glucosone-forming reactions combined with the Criegee and transesterification chemistry discussed in this dissertation.

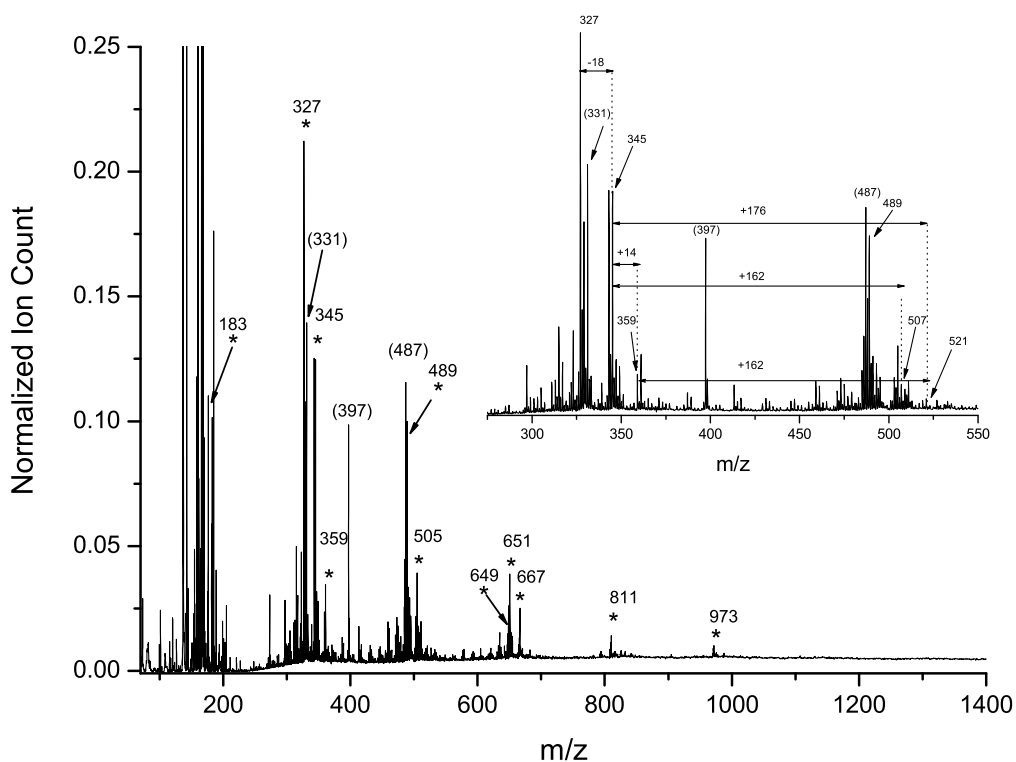


Figure 4-9 MALDI-TOF mass spectra of the sodiated products from the reaction of levoglucosan in the Fenton system; day 7, 1×10^{-3} M H_2O_2 using DHB/LiCl matrix in positive ion, reflectron mode. Spectrum is normalized to the 169 u (levoglucosan + Li^+) ion peak. Peak in parenthesis indicate significant mass peaks observed in the background measurements. (* - indicates emphasized oligomer

mass peak pattern)

A strong lithiated 327 u mass peak (Figure 4-9) is also observed, which is suggested to be formed through cyclization by a higher order oligomer, such as compound IIIa (+ Li = 345 u), through dehydration (-18 u) whereby any ROH on the compound completes the cyclization through a nucleophilic attack on the gem-diol endgroup carbon. As an example, we show this to occur with the alpha ketone ROH moiety to form a six-membered ring, where an ester connects the two cyclic moieties to form compound IIIc (Figure 4-10). Cyclization of this compound (IIIa) by other ROH functionalities is possible. We propose Figure 4-8 as the most likely representation because of the thermodynamically favored six-membered ring formation.

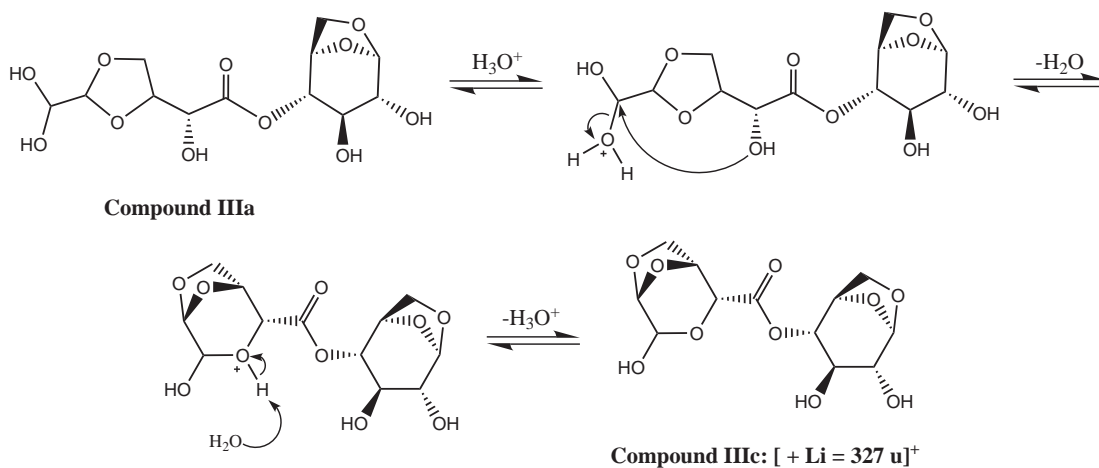


Figure 4-10 Proposed mechanism for the dehydration (-18 u) of compound IIIa through nucleophilic intramolecular cyclization by ROH with the terminal gem-diol carbon to produce compound IIIc (+Li = 327 u).

For this analysis, dehydration of the 2-mer product, lithiated 345 u, to produce the lithiated 327 u mass peak discussed above has a dominant role in the observed oligomerization series. An oligomer mass series is observed for day 7 (Figure 4-9) using the DHB/LiCl matrix which connects the lithiated 327 u base peak with the highest masses observed on this day (~973 u). From the lithiated 327 u mass peak, oligomerization of levoglucosan (+162 u) and +160 u is observed up to the lithiated 973 and 975 u mass peak (6-mer). This may occur through transesterification of levoglucosan and/or its first glucosone product (-2 u, Figure 4-3) by reaction with the proposed ester functionalities (Figure 4-4) or, alternatively, through acid-catalyzed oligomerization.⁸¹ The +160 u mass peak is likely due to a glucosone formation on any of the oligomer compounds with loss of 2 u (Figure 4-3) as discussed above. These assignments are based on the relatively intense ion signals (marked by *, Figure 4-9) measured in this MALDI-TOF mass spectrum for day 7 using the DHB/LiCl matrix solution.

As a further test for matrix inclusion products with this levoglucosan chemistry, samples of only levoglucosan were prepared and measured with MALDI-TOF-MS using the DHB/LiCl matrix solution in a wide range of concentrations (Figure 4-9, peaks in parentheses). This levoglucosan background measurement, as well as the DHB/LiCl matrix background measurements made in the absence of levoglucosan, do not interfere with either the 176 u (Cmpd II) peak or the resulting transesterification oligomer patterns seen in the MALDI-TOF mass spectra using the DHB/LiCl matrix solution, supporting the proposed Criegee and transesterification chemical

mechanisms. Also, using lithium as the matrix cationization agent simplifies the spectra significantly compared to sodium. Matrix/analyte inclusion formation for this system may be suppressed by the use of lithium, which, due to its small ionic radius compared to that of sodium and potassium, is less likely to chelate with the carboxylic/alcohol ligands in DHB during MALDI cationization.¹¹⁶ In addition, the simplified MALDI-TOF mass spectra using the DHB/LiCl matrix solution may also be a result of the selectivity of Li⁺ for certain compound classes.¹¹⁵

4.4. Conclusions

Aerosols emitted from biomass burning are multi-component admixtures^{35, 63} containing a variety of water soluble organic species,^{30, 42, 117, 118} hydrogen peroxide, iron, and other transition metals in an acidified aqueous medium; all necessary components for Fenton chemistry.¹⁰⁷ As noted previously, these aqueous levoglucosan proxy experiments were designed to discern which pathways and subsequent products that may predominate in complex, multi-component tropospheric aerosols. In this respect, oligomerization of levoglucosan appears as an important pathway in both Fenton (this study) and acid-catalyzed chemistry.⁸¹ Also possible, is that the proposed products are intermediates, which incorporate into new compounds through reactions with other species within aerosols by, for example, acid-catalyzed, [•]OH oxidation, or photo-oxidation processes, potentially forming HULIS.

Chemical products proposed here may aid the understanding of the atmospheric

processing of biomass burning aerosol parcels, possibly revealing information such as its age and source.³⁵ Identification of chemical products by proxy experiments are useful to guide analytical strategies in field investigations where chemical separations are critical for the measurement of a complex chemical matrix such as biomass burning aerosols. Further, the chemical processes identified in this work may participate in the formation of atmospheric HULIS, which may significantly alter the hygroscopicity^{42, 48, 119-122} of the aged biomass burning aerosol, affecting its ability to act as effective cloud condensation nuclei.^{5, 99} Increase in HULIS density with the aging of biomass burning aerosols has been shown previously and was attributed to an oxidative mechanism,¹²³ which is consistent with the $\cdot\text{OH}$ mechanism proposed in this study. Results reported here provide a direct chemical route by which levoglucosan is chemically processed by atmospheric reactants and possibly incorporated into chemical structures that represent HULIS. This is in agreement with studies that show a strong saccharide nature in HULIS.^{124, 125} The understanding of HULIS formation and the fundamental chemical processes occurring within biomass burning aerosols will further our knowledge of how these phenomena affect global climate.

5. Comprehensive Conclusions

5.1. Summary of Experimental Findings

Results of these laboratory investigations show fundamental chemical transformations of levoglucosan with both acid-catalyzed⁸¹ and oxidative (i.e. $\cdot\text{OH}$)⁹⁸ reactions under atmospherically relevant conditions. The main feature of the levoglucosan chemistry reported here is oligomerization to form high molecular weight (< 2000 m/z) products. Under acidic conditions (pH = 4.5), MALDI-TOF mass spectrometric measurements showed repeating mass patterns of +162 u, the molecular weight of levoglucosan. A rational mechanism was proposed showing the oligomerization of levoglucosan by acid-catalyzed cationic ring-opening of levoglucosan and nucleophilic attack of ROH from levoglucosan on the hemi-acetal carbon to produce pyranose oligomers (up to 9-mer) through the formation of glycosidic bonds. Because of the high degree of oxygenated functional groups, the predicted reaction products are highly polar and therefore, hydrophilic.

In the case of reaction with $\cdot\text{OH}$, a much more complicated oligomer series was observed, where the mass spectrometric data showed a single mass unit continuum up to ~ 2000 m/z. A mass intensity period of ~ 162 u in the spectral data indicated incorporation of levoglucosan into the oligomer structure. Despite the complicated baseline, a more intense oligomer series of +162/176 was discernable and increased in intensity and m/z with time. Mass spectral behavior for both the MALDI-TOF and

LDI-TOF mass spectrometric data was interpreted and fundamental $\cdot\text{OH}$ chemistry known to occur with saccharides in aqueous solution^{111, 126} was proposed to explain the mass patterns. Single mass unit continuum mass distributions with dominant -2 u patterns were measured and superimposed by the +162/+176 u oligomer series. The -2 u pattern was proposed to occur through glucosone formation by hydrogen abstraction by $\cdot\text{OH}$ from any alcoholic carbon to produce a carbon centered radical. After reaction of the carbon centered radical with O_2 , a rearrangement occurs creating a cyclic ketone. This latter oligomer pattern (i.e., +176) was attributed to a Criegee rearrangement (+14 u) of levoglucosan, initiated by $\cdot\text{OH}$, forming a lactone (176 u). Further acid-catalyzed reaction of any ROH from levoglucosan (+162 u) forms an ester through transesterification of the lactone functionality, whereupon propagation forms polyesters. Supporting data for the acid-catalyzed formation of the saccharidic C-O-C bridging functionality, and $\cdot\text{OH}$ initiated formation of ester and lactone functionalities was provided by ATR-FTIR spectroscopy.

5.2. General Implications of Experimental Results on Climate Science

Chemical processes such as acid-catalyzed oligomerization/polymerization and hydroxyl radical reactions could explain, in part, the absence of levoglucosan in analyzed aerosols known to originate from biomass burning.¹²⁷ These reaction products could have significant effects on the lifetime of these oligomer products, the water solubility of the aged aerosols, and the capacity of the aerosol to act as CCN.

Also, the chemical products identified in this work may be useful as secondary tracers for measurements of the long-distance transport of biomass burning aerosols. A useful chemical tracer must have significant concentrations and be chemically stable for the measurement time-period. It is proposed here that the high concentration of levoglucosan found in biomass burning aerosols may contribute to the potential of significant amounts of these oligomeric products existing as a stable component of biomass burning aerosols. Chemical products proposed here may aid the understanding of the atmospheric processing of biomass burning aerosol parcels, possibly revealing information such as its age and source.^{35, 81, 98} Also, identification of chemical products by proxy experiments are useful to guide analytical strategies in field investigations where chemical separations are critical for the measurement of a complex chemical matrix such as biomass burning aerosols.

5.2.1. Application of Experimental Results to Formation Mechanisms of Humic-Like Substances (HULIS)

Much attention in recent years has been directed to the ill-defined class of water soluble organic compounds found in atmospheric aerosols known as HULIS. The interest in HULIS is based on its high water solubility and light absorbing properties, which could affect an aerosol's potential as CCN and radiation balance of the Earth, respectively. There are many proposed mechanisms for the atmospheric formation of HULIS. Terrestrial lofting of soils¹²⁸, marine sources^{129, 130}, secondary organic aerosol formation,^{83, 131, 132} aqueous chemistry within hydrated aerosol or cloudwater¹³³, and

biomass burning processes^{30,118,134,135} are all proposed as potential sources of HULIS. Many sources and mechanisms for HULIS formation have been studied.⁴⁹ Terrestrial sources are considered a potentially minor source of HULIS because it is found mostly in fine mode aerosols. Many studies have shown seasonal variations in the amount of HULIS measured in real samples as well as descriptions of potential chemistry to form HULIS.¹²⁴ One study showed an increase in the aromatic composition of HULIS in autumn samples compared to summertime samples. This was attributed to the breakdown of lignin from the increased amount of wood burning during the cooler times of the year.¹³⁶ Also, studies have shown an aliphatic and polysaccharidic nature to HULIS.¹²⁵ Some suggested mechanisms for the formation of HULIS in biomass burning aerosols include, soil-derived humic matter lofted into the air due to the burning process, the combustion and subsequent chemical transformations of cellulose and lignan combustion products emitted directly in primary aerosols, and finally, condensation and chemical reactions of volatile low molecular weight combustion products in primary aerosols.¹¹⁸

The chemical processes identified in this dissertation may participate in the formation of atmospheric HULIS in primary biomass burning aerosols and/or their aged entities. In alignment with Gelenscer's mechanism,⁸⁶ it is proposed here that the acid-catalyzed oligomerization of levoglucosan may contribute to the secondary formation of the saccharide chemical character of HULIS within aqueous aerosols created from biomass burning. Also, an increase in HULIS density with the aging of biomass burning aerosols has been shown previously and was attributed to an

oxidative mechanism,¹²³ which is consistent with the $\cdot\text{OH}$ mechanism presented in this study. These results provide a direct chemical route by which levoglucosan is chemically processed by atmospheric reactants and possibly incorporated into chemical structures that represent HULIS.

5.2.2. Broad Scientific Implications of Chemical Research in Biomass Burning Aerosols

The understanding of fundamental chemical processes that produce chemical products within biomass burning aerosols may provide important information that can aid investigators understand how biomass aerosol processes affect global climate. Especially important is identification of real atmospheric chemical products which may change aerosol hygroscopicity (CCN) and be used as a secondary tracer for biomass burning aerosol parcels. The fundamental chemical mechanisms that influence HULIS formation will aid understanding of HULIS's potential affect on the CCN capacity and light-absorbing properties of biomass burning aerosols. Such information is important to advance our understanding of biomass burning aerosol source, transport, and processing in the atmosphere, which ultimately will add to the growing knowledge of how these types of aerosols affect global climate.

5.3. Suggested Research Directions

Limitations exist when interpreting laboratory proxy experimental data to real biomass burning aerosols which are complex admixtures under dynamic chemical and physical conditions. Therefore, further experimentation is necessary to improve understanding of the chemical behavior of levoglucosan in biomass burning aerosols. Here, a few basic experiments are proposed.

First, the effect of a range of acidic pH on the reactions of levoglucosan should be investigated to understand how these acid-catalyzed processes, which are often reversible, affect removal of levoglucosan from an aqueous system. Monitoring of the chemical products formed as well as their concentrations will give new information on the effect of pH on levoglucosan in this system. Direct and quantitative monitoring of levoglucosan concentration by high performance liquid chromatography (HPLC) or gas chromatography (GC) is pertinent in understanding its reaction kinetics. This information will be important in addressing the atmospheric stability of levoglucosan and therefore its usefulness as a molecular tracer for biomass burning aerosols.

Another suggestion given here is to generate these model levoglucosan aerosols in a Teflon bag using conditions similar in this dissertation or additional reactants such as simulated sunlight or NO_x to measure products in the *aerosol*-phase rather than bulk solution, on a time-scale of minutes to hours. Analysis of the chemical system may be done by 1) collection of fine mode aerosols on glass fiber filters and subsequent detection by MALDI mass spectrometry after a filter extraction method

has been applied, or 2) in-situ measurements by real-time aerosol instruments such as photo-electron capture and resonance aerosol mass spectrometry (PERCI-AMS).

Most speciation studies of the organic composition of biomass burning aerosols have focused on relatively simple, lower molecular weight compounds using conventional analytical methodologies.^{29, 30, 118} High molecular weight, water soluble products such as those proposed in this study should help guide the development of analytical methodologies for field measurement campaigns to target real aerosol-phase organic compounds that represent the experimentally identified chemical products or products in the general product class. Where chemical speciation is possible, this direction could increase the chances of identifying oligomeric products that may exist in significant concentrations in real biomass burning aerosol samples.

6. Appendix A

6.1. Development and Optimization of the MALDI-TOF-MS Methodology

Major challenges existed when analyzing the acid-catalyzed and Fenton reactions of levoglucosan discussed in Section 3. The products were hypothesized to be high molecular weight (>300 u) chemical products with a saccharidic character. The extent to which levoglucosan reacted under these conditions was initially unknown. It was possible that the reactions did not form product concentrations necessary for observation by MALDI-TOF-MS. Another possibility is that a different class of products had formed that were not compatible with the different experimental MALDI sample preparation methods. The experimental MALDI sample preparation conditions that were successful in identifying the hypothesized chemical products were based on research that showed favorable ionization of oligosaccharide compounds using DHB as a MALDI matrix with sodium as a cationizing agent.

Ideally for MALDI, the solvent, analyte, matrix and cationization agent should be co-soluble. Under these conditions, this sample solution was spotted within a sample well on the stainless steel MALDI plate. This solution was dried under reduced pressure. By having all the components soluble in the chosen solvent, the analyte, matrix compound, and cationization agent should co-crystallize during the drying process. It has been shown in MALDI that, when these constituents co-crystallize, that ionization is enhanced.

Initial attempts to identify the chemical products used DHB and tetrafluoroacetic acid as a proton source for positive ionization. Addition of an acid to the

analyte/matrix solution is a common method to enhance proton attachment/ionization of a variety of analytes for detection of positive ions. Sodium chloride was also used for cationization.

Many solvents were tried using these conditions. Methanol, ethanol, diethyl ether, ethyl acetate and acetone were used individually to dissolve the reaction products, DHB, and tetrafluoroacetic acid. For each sample, 10 mg of DHB was dissolved in 1 mL of each of the individual solvents. 1 mg/mL of tetrafluoroacetic acid was used for cationization. DHB was found to have limited solubility in the less polar solvents (i.e., ethanol, diethyl ether, ethyl acetate). Evidence of this was observed when the DHB solid was visible after five or more minutes of shaking the solution in the eppendorf tube. For the concentration used, DHB was completely soluble in methanol and acetone after vigorous shaking. Levoglucosan reaction product mass signals were not observed using these conditions. Different matrix compounds, such as α -Cyano-4-hydroxycinnamic acid (CHCA) and sinapic acid (SA), were also tried using the discussed solvents and cationization agents without success.

As discussed in the main dissertation (c.f., chapter 3, 4), meaningful results were identified using 10 mg/mL DHB, and 1 mg/mL sodium chloride in water. Dissolving the reaction products in Milli-Q water was necessary to observe the MALDI mass signals. If the DHB and sodium chloride were dissolved with the reaction products in any other solvent, the mass signals due to these reaction products were not measured.

Optimization of the MALDI matrix conditions were done empirically. As stated in the main dissertation, the 10x diluted samples gave the best results and therefore this

dilution was used to optimize the mass signals. The effects of sodium chloride concentration were studied by varying the amount of sodium chloride by 0.5 mg/mL between 0.5 and 2 mg/mL. Using the acid-catalyzed products of levoglucosan (Reaction B), the mass signal was optimized using 1 mg/mL sodium chloride. Mass signal suppression was observed above 1 mg/mL sodium chloride. Using the optimized conditions, the observed mass signal intensity of the acid-catalyzed 2-mer mass signal (Reaction B) was approximately 20,000 units.

A similar procedure was used to optimize the DHB concentration using 1 mg/mL sodium chloride in water. By varying the DHB concentration by 5 mg/mL, between 1 and 20 mg/mL, optimized results were observed using 10 mg/mL DHB. Again, mass signal suppression was observed above this DHB concentration.

The reaction product amounts that were sampled were kept as consistent as possible by visually scooping the dried powder out of the round bottom flasks after extensive scraping and mixing. The same amount of reaction products were approximated by visual inspection and its size was on the order of the size of a 1 microliter drop spotted on a stainless steel plate. Once on the spatula, the sample was transferred to an eppendorf tube. In the tube, the sample was moved to the bottom by tapping the tube on a surface. One microliter of Milli-Q water was added to this sample as in the main dissertation (c.f. Chapter 3). After mixing 1 microliter of this solution in another eppendorf tube with 10 mg/mL DHB and 1 mg/mL sodium chloride, 10x and 100x dilution were made. By sampling the 1x, 10x, and 100x dilutions of the reaction products in the MALDI-TOF-mass spectrometer, it was empirically determined that

the 10x diluted samples, no matter what the reaction conditions were, always gave the best mass signals.

7. References

1. Finlayson-Pitts, B. J., and J. N. Pitts Jr., *Chemistry of the Upper and Lower Atmosphere: Theory, Experiments, and Applications*. Elsevier: New York, 2000.
2. Seinfeld, J. H.; Pandis, S. N., *Atmospheric Chemistry of Physics: From Air Pollution to Climate Change*. John Wiley and Sons, Inc.: New York, NY, 1998.
3. Hollander, W.; Dunkhorst, W.; Windt, H., Characterization of aerosol particles by their heterogeneous nucleation: Activity at low supersaturations with respect to water and various organic vapors. *AIP Conference Proceedings* **2000**, 534, (Nucleation and Atmospheric Aerosols 2000), 732-735.
4. Rissler, J.; Swietlicki, E.; Zhou, J.; Roberts, G.; Andreae, M. O.; Gatti, L. V.; Artaxo, P., Physical properties of the sub-micrometer aerosol over the Amazon rain forest during the wet-to-dry season transition - comparison of modeled and measured CCN concentrations. *Atmospheric Chemistry and Physics* **2004**, 4, (8), 2119-2143.
5. Lee, Y. S.; Collins, D. R.; Li, R. J.; Bowman, K. P.; Feingold, G., Expected impact of an aged biomass burning aerosol on cloud condensation nuclei and cloud droplet concentrations. *Journal of Geophysical Research-Atmospheres* **2006**, 111, (D22), D22204. doi:10.1029/2005JD006464
6. Roberts, G. C.; Nenes, A.; Seinfeld, J. H.; Andreae, M. O., Impact of biomass burning on cloud properties in the Amazon Basin. *Journal of Geophysical Research-Atmospheres* **2003**, 108, (D2), 4062. doi:10.1029/2001JD000985
7. Koren, I.; Kaufman, Y. J.; Remer, L. A.; Martins, J. V., Measurement of the effect of Amazon smoke on inhibition of cloud formation. *Science* **2004**, 303, (5662),

1342-1345.

8. Engardt, M.; Rodhe, H., A comparison between patterns of temperature trends and sulfate aerosol pollution. *Geophysical Research Letters* **1993**, 20, (2), 117.
9. Mitchell, J. F. B.; Johns, T. C.; Gregory, J. M.; Tett, S. F. B., Climate response to increasing levels of greenhouse gases and sulfate aerosols. *Nature* **1995**, 376, 501.
10. Santer, B. D.; Taylor, K. E.; Wigley, T. M. L.; Penner, J. E.; Jones, P. D.; Cubasch, U., Towards the detection and attribution of an anthropogenic effect on climate. *Climate Dynamics* **1995**, 12, (2), 77.
11. Santer, B. D.; Wigley, T. M. L.; Jones, P. D., Correlation methods in fingerprint detection studies. *Climate Dynamics* **1993**, 8, (6), 265.
12. Wigley, T. M. L.; Raper, S. C. B., Implications for climate and sea-level of revised IPCC emissions scenarios. *Nature* **1992**, 357, (6376), 293.
13. Charlson, R. J.; schwartz, S. E.; Hales, J. M.; Cess, R. D.; Coakley, J. A.; Hansen, J. E.; Hofmann, D. J., Climate forcing by anthropogenic aerosols. *Science* **1992**, 255, (5043), 423.
14. Ramanathan, V.; Crutzen, P. J.; Kiehl, J. T.; Rosenfeld, D., Atmosphere - Aerosols, climate, and the hydrological cycle. *Science* **2001**, 294, (5549), 2119-2124.
15. Chuang, C. C.; Penner, J. E.; Prospero, J. M.; Grant, K. E.; Rau, G. H.; Kawamoto, K., Cloud susceptibility and the first aerosol indirect forcing: Sensitivity to black carbon and aerosol concentrations. *Journal of Geophysical Research, [Atmospheres]* **2002**, 107, (D21), AAC10/1-AAC10/23.

16. Twomey, S., Aerosols, clouds and radiation. *Atmospheric Environment Part A-General Topics* **1991**, 25, (11), 2435.
17. Haywood, J.; Boucher, O., Estimates of the direct and indirect radiative forcing due to tropospheric aerosols: a review. *Reviews of Geophysics* **2000**, 38, (4), 513-543.
18. Andrea, M. O., *Biogeochemistry of Global Change: Radiatively Active Trace Gases*. Chapman and Hall: New York, 1993.
19. Penner, J. E.; Ghan, S. J.; Walton, J. J., *Global Biomass Burning: Atmospheric, Climatic, and Biospheric Implications*. MIT Press: Cambridge, Mass., 1991; p 432-438.
20. Andreae, M. O., Biomass burning: Its history, use, and distribution and its impact on environmental quality and global climate. In *Global Biomass Burning*, Levine, J. S., Ed. MIT Press: Cambridge, Mass., 1991; pp 3-21.
21. Sjostrom, E., *Wood Chemistry: Fundamentals and Application*. Academic Press: 1993.
22. Rowell, R., *Chemistry of Solid Wood*. American Chemical Society: Washington, D. C., 1984; p 489-529.
23. Reid, J. S.; Hobbs, P. V., Physical and optical properties of young smoke from individual biomass fires in Brazil. *Journal of Geophysical Research-Atmospheres* **1998**, 103, (D24), 32013-32030.
24. Kleeman, M. J.; Schauer, J. J.; Cass, G. R., Size and composition distribution of fine particulate matter emitted from wood burning, meat charbroiling, and

- cigarettes. *Environmental Science & Technology* **1999**, 33, (20), 3516-3523.
25. Kanakidou, M.; Seinfeld, J. H.; Pandis, S. N.; Barnes, I.; Dentener, F. J.; Facchini, M. C.; Van Dingenen, R.; Ervens, B.; Nenes, A.; Nielsen, C. J.; Swietlicki, E.; Putaud, J. P.; Balkanski, Y.; Fuzzi, S.; Horth, J.; Moortgat, G. K.; Winterhalter, R.; Myhre, C. E. L.; Tsigaridis, K.; Vignati, E.; Stephanou, E. G.; Wilson, J., Organic aerosol and global climate modeling: a review. *Atmospheric Chemistry and Physics* **2005**, 5, 1053-1123.
26. Pope, C. A. I.; Bates, D. V.; Raizenne, M. E., Health effects of particulate air pollution: time for reassessment? *Environmental Health Perspectives* **1995**, 103, (5), 103-110.
27. Englert, N., Fine particles and human health - a review of epidemiological studies. *Toxicology Letters* **2004**, 149, (1-3), 235-242.
28. Lighty, J. S.; Veranth, J. M.; Sarofim, A. F., Combustion aerosols: Factors governing their size and composition and implications to human health. *Journal of the Air & Waste Management Association* **2000**, 50, (9), 1565-1618.
29. Hays, M. D., Speciation of gas-phase and fine particle emissions from burning of foliar fuels. *Environmental Science & Technology* **2002**, 36, (11), 2281-2295.
30. Graham, B.; Mayol-Bracero, O. L.; Guyon, P.; Roberts, G. C.; Decesari, S.; Facchini, M. C.; Artaxo, P.; Maenhaut, W.; Koll, P.; Andreae, M. O., Water-soluble organic compounds in biomass burning aerosols over Amazonia 1. Characterization by NMR and GC-MS. *Journal of Geophysical Research-Atmospheres* **2002**, 107, (D20), LBA14/1-LBA14/16.

31. Jacobson, M. C.; Hansson, H. C.; Noone, K. J.; Charlson, R. J., Organic atmospheric aerosols: Review and state of the science. *Reviews of Geophysics* **2000**, 38, (2), 267-294.
32. Koll, P.; Borchers, G.; Metzger, J. O., Thermal-degradation of chitin and cellulose. *Journal of Analytical and Applied Pyrolysis* **1991**, 19, 119-129.
33. Koll, P.; Borchers, G.; Metzger, J. O., Preparative isolation of oligomers with a terminal anhydrosugar unit by thermal-degradation of chitin and cellulose. *Journal of Analytical and Applied Pyrolysis* **1990**, 17, (4), 319-327.
34. bin Abas, M. R.; Simoneit, B. R. T.; Elias, V.; Cabral, J. A.; Cardoso, J. N., Composition of higher molecular weight organic matter in smoke aerosol from biomass combustion in Amazonia. *Chemosphere* **1995**, 30, (5), 995-1015.
35. Simoneit, B. R. T.; Schauer, J. J.; Nolte, C. G.; Oros, D. R.; Elias, V. O.; Fraser, M. P.; Rogge, W. F.; Cass, G. R., Levoglucosan, a tracer for cellulose in biomass burning and atmospheric particles. *Atmospheric Environment* **1999**, 33, 173-182.
36. Fang, M.; Zheng, M.; Wang, F.; To, K. L.; Jaafar, A. B.; Tong, S. L., The solvent-extractable organic compounds in the Indonesia biomass burning aerosols - characterization studies. *Atmospheric Environment* **1999**, 33, (5), 783-795.
37. Narukawa, M.; Kawamura, K.; Takeuchi, N.; Nakajima, T., Distribution of dicarboxylic acids and carbon isotopic compositions in aerosols from 1997 Indonesian forest fires. *Geophysical Research Letters* **1999**, 26, (20), 3101-3104.
38. Watson, R. T., *Climate Change 2001: Synthesis Report*. Cambridge

University Press: Cambridge, 2001.

39. Novakov, T.; Corrigan, C. E., Cloud condensation nucleus activity of the organic component of biomass smoke particles. *Geophysical Research Letters* **1996**, 23, (16), 2141-2144.
40. Yamasoe, M. A.; Artaxo, P.; Miguel, A. H.; Allen, A. G., Chemical composition of aerosol particles from direct emissions of vegetation fires in the Amazon Basin: water-soluble species and trace elements. *Atmospheric Environment* **2000**, 34, (10), 1641-1653.
41. Andrea, M. O.; Merlet, P., Emission of trace gases and aerosols from biomass burning. *Global Biogeochemical Cycles* **2001**, 15, (4). doi: 10.1029/2000GB001382.
42. Chan, M. N.; Choi, M. Y.; Ng, N. L.; Chan, C. K., Hygroscopicity of water-soluble organic compounds in atmospheric aerosols: amino acids and biomass burning derived organic species. *Environmental Science and Technology* **2005**, 39, (6), 1555-1562.
43. Hays, M. D.; Geron, C. D.; Linna, K. J.; Smith, N. D.; Schauer, J. J., Speciation of gas-phase and fine particle emissions from burning of foliar fuels. *Environmental Science & Technology* **2002**, 36, (11), 2281-2295.
44. Cruz, C. N.; Pandis, S. N., A study of the ability of pure secondary organic aerosol to act as cloud condensation nuclei. *Atmospheric Environment* **1997**, 31, (15), 2205-2214.
45. Corrigan, C. E.; Novakov, T., Cloud condensation nucleus activity of organic compounds: a laboratory study. *Atmospheric Environment* **1999**, 33, (17), 2661-2668.

46. Facchini, M. C.; Mircea, M.; Fuzzi, S.; Charlson, R. J., Cloud albedo enhancement by surface-active organic solutes in growing droplets. *Nature (London)* **1999**, 401, (6750), 257-259.
47. Facchini, M. C.; Decesari, S.; Mirceaa, M.; Fuzzi, S.; Loglio, G., Surface tension of atmospheric wet aerosol and cloud/fog droplets in relation to their organic carbon content and chemical composition. *Atmospheric Environment* **2000**, 34, (28), 4853-4857.
48. Dinar, E.; Taraniuk, I.; Graber, E. R.; Katsman, S.; Moise, T.; Anttila, T.; Mentel, T. F.; Rudich, Y., Cloud Condensation Nuclei properties of model and atmospheric HULIS. *Atmospheric Chemistry and Physics* **2006**, 6, 2465-2481.
49. Graber, E. R.; Rudich, Y., Atmospheric HULIS: how humic-like are they? A comprehensive and critical review. *Atmospheric Chemistry and Physics Discussions* **2005**, 5, 9801-9860.
50. Feng, J. S.; Moller, D., Characterization of water-soluble macromolecular substances in cloud water. *Journal of Atmospheric Chemistry* **2004**, 48, (3), 217-233.
51. Kiss, G.; Tombacz, E.; Varga, B.; Alsberg, T.; Persson, L., Estimation of the average molecular weight of humic-like substances isolated from fine atmospheric aerosol. *Atmospheric Environment* **2003**, 37, (27), 3783-3794.
52. Cappiello, A.; De Simoni, E.; Fiorucci, C.; Mangani, F.; Palma, P.; Trufelli, H.; Decesari, S.; Facchini, M. C.; Fuzzi, S., Molecular characterization of the water-soluble organic compounds in fogwater by ESIMS/MS. *Environmental Science & Technology* **2003**, 37, (7), 1229-1240.

53. Krivacsy, Z.; Kiss, G.; Varga, B.; Galambos, I.; Sarvari, Z.; Gelencser, A.; Molnar, A.; Fuzzi, S.; Facchini, M. C.; Zappoli, S.; Andracchio, A.; Alsberg, T.; Hansson, H. C.; Persson, L., Study of humic-like substances in fog and interstitial aerosol by size-exclusion chromatography and capillary electrophoresis. *Atmospheric Environment* **2000**, 34, (25), 4273-4281.
54. Hoffer, A.; Gelencser, A.; Guyon, P.; Kiss, G.; Schmid, O.; Frank, G. P.; Artaxo, P.; Andreae, M. O., Optical properties of humic-like substances (HULIS) in biomass-burning aerosols. *Atmospheric Chemistry and Physics* **2006**, 6, 3563-3570.
55. Reid, J. S., A review of biomass burning emissions part II: intensive physical properties of biomass burning particles. *Atmospheric Chemistry and Physics* **2005**, 5, 799-825.
56. Hornig, J. F.; Soderberg, R. H.; Barefoot, A. C., III ; Galasyn, J. F., Wood smoke analysis: vaporization losses of PAH from filters and levoglucosan as a distinctive marker for wood smoke. In *Polynuclear Aromatic Hydrocarbons: Mechanisms, Methods, and Metabolism*, Cooke, M.; Dennis, A. J., Eds. Battelle Press: Columbus, 1985; pp 561-568.
57. Standley, L. J.; Simoneit, B. R. T., Resin diterpenoids as tracers for biomass combustion aerosols. *Journal of Atmospheric Chemistry* **1994**, 18, 1-15.
58. Zheng, M.; Wan, T. S. M.; Fang, M.; Wang, F., Characterization of the non-volatile organic compounds in the aerosols of Hong Kong- Identification, abundance and origin. *Atmospheric Environment* **1997**, 31, 227-237.
59. Schauer, J. J.; Rogge, W. F.; Hildemann, L. M.; Mazurek, M. A.; Cass, G. R.,

Source apportionment of airborne particulate matter using organic compounds as tracers. *Atmospheric Environment* **1996**, 30, (22), 3837-3855.

60. Shafizadeh, F., *The chemistry of pyrolysis and combustion*. American Chemical Society: Washington, D. C., 1984; p 489-529.

61. Egenberg, I. M.; Aasen, J. A. B.; Holtekjolen, A. K.; Lundanes, E., Characterisation of traditionally kiln produced pine tar by gas chromatography-mass spectrometry. *Journal of Analytical and Applied Pyrolysis* **2002**, 62, (1), 143-155.

62. Egenberg, I. M.; Holtekjolen, A. K.; Lundanes, E., Characterisation of naturally and artificially weathered pine tar coatings by visual assessment and gas chromatography-mass spectrometry. *Journal of Cultural Heritage* **2003**, 4, (3), 221-241.

63. Simoneit, B. R. T., Biomass burning- a review of organic tracers for smoke from incomplete combustion. *Applied Geochemistry* **2002**, 17, 129-162.

64. Elias, V. O., Simoneit, B. R. T., Cordeiro, R. C., and Turcq, B., Evaluating levoglucosan as an indicator of biomass burning in Carajas, Amazonia: A comparison to the charcoal record. *Geochimica et Cosmochimica Acta* **2001**, 65, (2), 267-272.

65. Herrmann, H.; Ervens, B.; Jacobi, H. W.; Wolke, R.; Nowacki, P.; Zellner, R., CAPRAM2.3: A chemical aqueous phase radical mechanism for tropospheric chemistry. *Journal of Atmospheric Chemistry* **2000**, 36, (3), 231-284.

66. Ervens, B.; George, C.; Williams, J. E.; Buxton, G. V.; Salmon, G. A.; Bydder, M.; Wilkinson, F.; Dentener, F.; Mirabel, P.; Wolke, R.; Herrmann, H., CAPRAM 2.4 (MODAC mechanism): an extended and condensed tropospheric

aqueous phase mechanism and its application. *Journal of Geophysical Research, [Atmospheres]* **2003**, 108, (D14), AAC12/1-AAC12/21.

67. Koutrakis, P.; Wolfson, J. M.; Spengler, J. D., An Improved Method for Measuring Aerosol Strong Acidity - Results from a 9-Month Study in St-Louis, Missouri and Kingston, Tennessee. *Atmospheric Environment* **1988**, 22, (1), 157-162.

68. Lipfert, F. W.; Wyzga, R. E., On the Spatial and Temporal Variability of Aerosol Acidity and Sulfate Concentration. *Journal of the Air & Waste Management Association* **1993**, 43, (4), 489-491.

69. Liu, L. J. S.; Burton, R.; Wilson, W. E.; Koutrakis, P., Comparison of aerosol acidity in urban and semirural environments. *Atmospheric Environment* **1996**, 30, (8), 1237-1245.

70. Ludwig, J.; Klemm, O., Acidity of Size-Fractionated Aerosol-Particles. *Water Air and Soil Pollution* **1990**, 49, (1-2), 35-50.

71. Atkinson, R.; Arey, J., Gas-phase tropospheric chemistry of biogenic volatile organic compounds: a review. *Atmospheric Environment* **2003**, 37, S197-S219.

72. Pignatello, J. J.; Oliveros, E.; MacKay, A., Advanced oxidation processes for organic contaminant destruction based on the Fenton reaction and related chemistry. *Critical Reviews in Environmental Science and Technology* **2006**, 36, (1), 1-84.

73. Stephens, W. E., A pulsed mass spectrometer with time dispersion. *Physical Review* **1946**, 69, 691.

74. Zenobi, R.; Knochenmuss, R., Ion formation in MALDI mass spectrometry. *Mass Spectrometry Reviews* **1998**, 17, (5), 337-366.

75. Harvey, D. J.; Rudd, P. M.; Bateman, R. H.; Bordoli, R. S.; Howes, K.; Hoyes, J. B.; Vickers, R. G., Examination of complex oligosaccharides by matrix-assisted laser-desorption ionization mass-spectrometry on time-of-flight and magnetic-sector instruments. *Organic Mass Spectrometry* **1994**, 29, (12), 753-766.
76. Hao, C. Y.; Ma, X. L.; Liu, Z. Q.; Ji, Y. P.; Liu, S. Y.; Liu, C. C.; Sun, Y. X.; Liu, J. Z., Matrix-assisted laser desorption/ionization mass spectral study of saccharides. *Chemical Journal of Chinese Universities-Chinese* **1998**, 19, (7), 1090-1094.
77. Mohr, M. D.; Bornsen, K. O.; Widmer, H. M., Matrix-Assisted Laser-Desorption Ionization Mass-Spectrometry - Improved Matrix for Oligosaccharides. *Rapid Communications in Mass Spectrometry* **1995**, 9, (9), 809-814.
78. Brown, R. S., Mass resolution improvement by incorporation of pulsed ion extraction in a matrix-assisted laser-desorption ionization linear time-of-flight mass spectrometer. *Analytical Chemistry* **1995**, 67, (13), 1998-2003.
79. Peterson, D. S., Matrix-free methods for laser desorption/ionization mass spectrometry. *Mass Spectrometry Reviews* **2007**, 26, (1), 19-34.
80. Workman, J. J., Review of process and non-invasive near-infrared and infrared spectroscopy: 1993-1999. *Applied Spectroscopy Reviews* **1999**, 34, (1-2), 1-89.
81. Holmes, B. J.; Petrucci, G. A., Water-soluble oligomer formation from acid-catalyzed reactions of levoglucosan in proxies of atmospheric aqueous aerosols. *Environmental Science & Technology* **2006**, 40, (16), 4983-4989.

82. Lelieveld, J.; Dentener, F. J., Hydroxyl radicals maintain the self-cleansing capacity of the troposphere. *Atmospheric Chemistry and Physics Discussions* **2004**, 4, 3699-3720.
83. Jang, M., Czoschke, N. M., Lee, S., Kamens, R. M., Heterogeneous atmospheric aerosol production by acid-catalyzed particle-phase reactions. *Science* **2002**, 298, 814-817.
84. Tolocka, M. P. J., M.; Ginter, J. M.; Cox, F. J.; Kames, R. M.; Johnston, M. V., Formation of Oligomers in Secondary Organic Aerosol. *Environmental Science and Technology* **2004**, 38, (5), 1428-1434.
85. Kalberer, M., Paulsen, D., Sax, M., et al., Identification of polymers as major components of atmospheric organic aerosols. *Science* **2004**, 303, 1659-1662.
86. Gelencser, A., et al., In-situ formation of light-absorbing organic matter in cloud water. *Journal of Atmospheric Chemistry* **2003**, 45, 25-33.
87. Kelly, T. J.; Daum, P. H.; Schwartz, S. E., Measurements of peroxides in cloudwater and rain. *Journal of Geophysical Research-Atmospheres* **1985**, 90, (D5), 7861-71.
88. Deutsch, F.; Hoffmann, P.; Ortner, H. M., Field experimental investigations on the Fe(II)- and Fe(III)-content in cloudwater samples. *Journal of Atmospheric Chemistry* **2001**, 40, (1), 87-105.
89. Kang, S.-F., Liao, C.- H., Chen, M.- C., Pre-oxidation and coagulation of textile wastewater by the Fenton process. *Chemosphere* **2002**, 46, 923-928.
90. Gao, S.; Hegg, D. A.; Hobbs, P. V.; Kirchstetter, T. W.; Magi, B. I.; Sadilek,

- M., Water-soluble organic components in aerosols associated with savanna fires in southern Africa: Identification, evolution, and distribution. *Journal of Geophysical Research-Atmospheres* **2003**, 108, (D13), 8491. doi:10.1029/2002JD002324
91. Kanazawa, A.; Suzuki, M., Solid-state polycondensation of natural aldopentoses and 6-deoxyaldohexoses. Facile preparation of highly branched polysaccharide. *Polymer* **2006**, 47, 176-183.
92. Simoneit, B. R. T.; Elias, V. O.; Kobayashi, M.; Kawamura, K.; Rushdi, A. I.; Medeiros, P. M.; Rogge, W. F.; Didyk, B. M., Sugars-dominant water-soluble organic compounds in soils and characterization as tracers in atmospheric particulate matter. *Environmental Science and Technology* **2004**, 38, (22), 5939-5949.
93. Shafizadeh, F.; Furneaux, R. H.; Cochran, T. G.; Scholl, J. P.; Sakai, Y., Production of levoglucosan and glucose from pyrolysis of cellulosic materials. *Journal of Applied Polymer Science* **1979**, 23, 3525-3539.
94. Shafizadeh, F., and Y. L. Fu, Pyrolysis of cellulose. *Carbohydrate Research* **1973**, 29, 113-122.
95. Shafizadeh, F., and Stevenson, T. T., Saccharification of douglas-fir wood by a combination of prehydrolysis and pyrolysis. *Journal of Applied Polymer Science* **1982**, 27, 4577-4585.
96. Montaudo, G.; Lattimer, R. P., *Mass Spectrometry of Polymers*. CRC Press: Boca Raton, 2002.
97. Solomons, T. W. G., Fryhle, C. B., *Organic Chemistry*. 8 ed.; John Wiley and Sons, Inc.: Hoboken, 2004; p 1083-1084.

98. Holmes, B. J.; Petrucci, G. A., Oligomerization of levoglucosan by Fenton chemistry in proxies of biomass burning aerosols *Journal of Atmospheric Chemistry* **2007**. doi: 10.1007/s10874-007-9084-8
99. Rosenorn, T.; Kiss, G.; Bilde, M., Cloud droplet activation of saccharides and levoglucosan particles. *Atmospheric Environment* **2006**, 40, (10), 1794-1802.
100. Daum, P. H., Observations of hydrogen peroxide and sulfur(IV) in air, cloudwater, and precipitation and their implications for the reactive scavenging of sulfur dioxide. *Atmospheric Research* **1990**, 25, (1-3), 89-102.
101. Weinstein-Lloyd, J.; Schwartz, S. E., Low-intensity radiolysis study of free-radical reactions in cloudwater: hydrogen peroxide production and destruction. *Environmental Science and Technology* **1991**, 25, (4), 791-800.
102. Arakaki, T.; Anastasio, C.; Shu, P. G.; Faust, B. C., Aqueous-phase photoproduction of hydrogen peroxide in authentic cloud waters: wavelength dependence, and the effects of filtration and freeze-thaw cycles. *Atmospheric Environment* **1995**, 29, (14), 1697-703.
103. Vione, D.; Maurino, V.; Minero, C.; Pelizzetti, E., The atmospheric chemistry of hydrogen peroxide: A review. *Annali Di Chimica* **2003**, 93, (4), 477-488.
104. Majestic, B. J.; Schauer, J. J.; Shafer, M. M.; Turner, J. R.; Fine, P. M.; Singh, M.; Sioutas, C., Development of a wet-chemical method for the speciation of iron in atmospheric aerosols. *Environmental Science & Technology* **2006**, 40, (7), 2346-2351.
105. Balasubramanian, R.; Victor, T.; Begum, R., Impact of biomass burning on

rainwater acidity and composition in Singapore. *Journal of Geophysical Research-Atmospheres* **1999**, 104, (D21), 26881-26890.

106. Calvert, J. G.; Lazrus, A.; Kok, G. L.; Heikes, B. G.; Walega, J. G.; Lind, J.; Cantrell, C. A., Chemical mechanisms of acid generation in the troposphere. *Nature* **1985**, 317, (6032), 27-35.

107. Deguillaume, L.; Leriche, M.; Chaurnerliac, N., Impact of radical versus non-radical pathway in the Fenton chemistry on the iron redox cycle in clouds. *Chemosphere* **2005**, 60, (5), 718-724.

108. Hoffer, A.; Kiss, G.; Blazso, M.; Gelencser, A., Chemical characterization of humic-like substances (HULIS) formed from a lignin-type precursor in model cloud water. *Geophysical Research Letters* **2004**, 31, (6), L06115. doi:10.1029/2003GL018962

109. Willson, R. L., The reaction of oxygen with radiation-induced free radicals in DNA and related compounds. *International Journal of Radiation Biology* **1970**, 17, (4), 349-358.

110. Schuchmann, M. N.; Sonntag, C. V., Radiation chemistry of carbohydrates. Part 14. Hydroxyl radical induced oxidation of D-glucose in oxygenated aqueous solutions. *Journal of the Chemical Society Perkin Transactions 2* **1977**, 1958-1963.

111. Manini, P.; La Pietra, P.; Panzella, L.; Napolitano, A.; d'Ischia, M., Glyoxal formation by Fenton-induced degradation of carbohydrates and related compounds. *Carbohydrate Research* **2006**, 341, (11), 1828-1833.

112. Schreiber, S. L.; Liew, W. F., Criegee rearrangement of alpha-alkoxy

hydroperoxides - A synthesis of esters and lactones that complements the Baeyer-Villiger oxidation of ketones. *Tetrahedron Letters* **1983**, 24, (23), 2363-2366.

113. Mele, A.; Malpezzi, L., Noncovalent association phenomena of 2,5-dihydroxybenzoic acid with cyclic and linear oligosaccharides. A matrix-assisted laser desorption/ionization time-of-flight mass spectrometric and x-ray crystallographic study. *Journal of the American Society for Mass Spectrometry* **2000**, 11, (3), 228-236.

114. Silverstein, R. M.; Bassler, G. C.; Morrill, T. C., *Spectrometric identification of organic compounds*. 5th ed.; John Wiley and Sons, Inc.: New York, 1991.

115. Wang, Y. Q.; Rashidzadeh, H.; Guo, B. C., Structural effects on polyether cationization by alkali metal ions in matrix-assisted laser desorption/ionization. *Journal of the American Society for Mass Spectrometry* **2000**, 11, (7), 639-643.

116. Keki, S.; Szilagy, L. S.; Deak, G.; Zsuga, M., Effects of different alkali metal ions on the cationization of poly(ethylene glycol)s in matrix-assisted laser desorption/ionization mass spectrometry: a new selectivity parameter. *Journal of Mass Spectrometry* **2002**, 37, (10), 1074-1080.

117. Mochida, M.; Kawamura, K., Hygroscopic properties of levoglucosan and related organic compounds characteristics to biomass burning aerosol particles. *Journal of Geophysical Research, [Atmospheres]* **2004**, 109, (D21), D21202/1-D21202/8.

118. Mayol-Bracero, O. L.; Guyon, P.; Graham, B.; Roberts, G.; Andreae, M. O.; Decesari, S.; Facchini, M. C.; Fuzzi, S.; Artaxo, P., Water-soluble organic

compounds in biomass burning aerosols over Amazonia 2. Apportionment of the chemical composition and importance of the polyacidic fraction. *Journal of Geophysical Research* **2002**, 107, (D20), 8091. doi:10.1029/2001JD000522

119. Padro, L. T.; Asa-Awuku, A.; Morrison, R.; Nenes, A., Inferring thermodynamic properties from CCN activation experiments: a) single-component and binary aerosols. *Atmospheric Chemistry and Physics Discussions* **2007**, 7, 3805–3836.

120. Badger, C. L.; George, I.; Griffiths, P. T.; Braban, C. F.; Cox, R. A.; Abbatt, J. P. D., Phase transitions and hygroscopic growth of aerosol particles containing humic acid and mixtures of humic acid and ammonium sulphate. *Atmospheric Chemistry and Physics* **2006**, 6, 755-768.

121. Dinar, E.; Taraniuk, I.; Graber, E. R.; Anttila, T.; Mentel, T. F.; Rudich, Y., Hygroscopic growth of atmospheric and model humic-like substances. *Journal of Geophysical Research-Atmospheres* **2007**, 112, (D5), D05211.

122. Chan, M. N.; Chan, C. K., Hygroscopic properties of two model humic-like substances and their mixtures with inorganics of atmospheric importance. *Environmental Science & Technology* **2003**, 37, (22), 5109-5115.

123. Dinar, E.; Mentel, T. F.; Rudich, Y., The density of humic acids and humic like substances (HULIS) from fresh and aged wood burning and pollution aerosol particles. *Atmospheric Chemistry and Physics* **2006**, 6, 5213-5224.

124. Graber, E. R.; Rudich, Y., Atmospheric HULIS: How humic-like are they? A comprehensive and critical review. *Atmospheric Chemistry and Physics* **2006**, 6, 729-

753.

125. Havers, N.; Burba, P.; Lambert, J.; Klockow, D., Spectroscopic characterization of humic-like substances in airborne particulate matter. *Journal of Atmospheric Chemistry* **1998**, 29, (1), 45-54.

126. Schuchmann, M. N.; Von Sonntag, C., Reactions of ozone with D-glucose in oxygenated aqueous solution - direct action and hydroxyl radical pathway. *Aqua (Oxford)* **1989**, 38, (5), 311-17.

127. Gao, S.; Hegg, D. A.; Hobbs, P. V.; Kirchstetter, T. W.; Magi, B. I.; Sadilek, M., Water-soluble organic components in aerosols associated with savanna fires in southern Africa: Identification, evolution and distribution. *J. Geophys. Res.* **2003**, 108, (D13), 8491.

128. Simoneit, B. R. T., Eolian particulates from oceanic and rural areas – their lipids fulvic and humic acids and residual carbon. In *Advances in Organic Geochemistry*, Douglas, A. G.; Maxwell, J. R., Eds. Pergamon Press: Oxford, 1980; pp 343-352.

129. Cavalli, F.; Facchini, M. C.; Decesari, S.; Mircea, M.; Emblico, L.; Fuzzi, S.; Ceburnis, D.; Yoon, Y. J.; O'Dowd, C. D.; Putaud, J. P.; Dell'Acqua, A., Advances in characterization of size-resolved organic matter in marine aerosol over the North Atlantic. *Journal of Geophysical Research-Atmospheres* **2004**, 109. doi:10.1029/2004JD005137

130. Cini, R.; Innocenti, N. D.; Loglio, G.; Oppo, C.; Orlandi, G.; Stortini, A. M.; Tesei, U.; Udisti, R., Air-sea exchange: Sea salt and organic micro components in

Antarctic snow. *International Journal of Environmental Analytical Chemistry* **1996**, 63, 15-27.

131. Gelencser, A.; Hoffer, A.; Krivacsy, Z.; Kiss, G.; Molnar, A.; Meszaros, E., On the possible origin of humic matter in fine continental aerosol. *Journal of Geophysical Research- Atmospheres* **2002**, 107, (D12), 4137. doi:10.1029/2001JD001299

132. Jang, M. C., B.; Chandramouli, B.; Kamens, R. M., Particle growth by acid-catalyzed heterogeneous reactions of organic carbonyls on preexisting aerosols. *Environmental Science & Technology* **2003**, 37, (17), 3828-3837.

133. Gelencser, A.; Hoffer, A.; Kiss, G.; Tombacz, E.; Kurdi, R.; Bencze, L., In-situ formation of light-absorbing organic matter in cloud water. *Journal of Atmospheric Chemistry* **2003**, 45, (1), 25-33.

134. Mukai, H., and Ambe, Y., Characterization of a humic acid-like brown substance in airborne particulate matter and tentative identification of its origin. *Atmospheric Environment* **1986**, 20, 813-819.

135. Zappoli, S. A., A.; Facchini, M. C.; et al., Inorganic, organic and macromolecular components of fine aerosol in different areas of Europe in relation to their water solubility. *Atmospheric Environment* **1999**, 33, 2733-2743.

136. Duarte, R.; Pio, C. A.; Duarte, A. C., Spectroscopic study of the water-soluble organic matter isolated from atmospheric aerosols collected under different atmospheric conditions. *Analytica Chimica Acta* **2005**, 530, 7-14.